



**Politecnico
di Torino**



**UNIVERSITÀ
DEGLI STUDI
DI TORINO**



ScuDo

Scuola di Dottorato - Doctoral School
WHAT YOU ARE, TAKES YOU FAR



Dipartimento Interateneo di Scienze, Progetto e Politiche del Territorio
Eccellenza MIUR 2018-2022

Doctoral Dissertation
Doctoral Program in Urban and Regional Development (34th Cycle)

Geothermal resources exploitation from disused hydrocarbon wells: simplified tools for a reuse strategies analysis

By

Martina Gizzi

Supervisors:

Prof. Lo Russo Stefano, Supervisor
Dott.ssa Taddia Glenda, Co-Supervisor

Doctoral Examination Committee:

Dott.ssa A. Manzella, Referee, *Istituto di Geoscienze e Georisorse di Pisa (CNR-IGG)*
Dott.ssa A.C. Violante, Referee, *Agenzia nazionale per le nuove tecnologie, l'energia e lo sviluppo economico sostenibile (ENEA)*
Prof.ssa L. Longoni, *Dipartimento di Ingegneria Civile e Ambientale, Politecnico di Milano*
Prof. P. Fabbri, *Dipartimento di Geoscienze, Università di Padova*
Prof. P. Dabove, *Dipartimento di Ingegneria dell'Ambiente, del Territorio e delle Infrastrutture, Politecnico di Torino*

Politecnico di Torino
06 May 2022

Declaration

I hereby declare that the contents and organization of this dissertation constitute my own original work and do not compromise in any way the rights of third parties, including those relating to the security of personal data.

Martina Gizzi
Turin, 06 May 2022

* This dissertation is presented in partial fulfillment of the requirements for **Ph.D. degree** in the Graduate School of Politecnico di Torino (ScuDo).

To my loving parents...

Acknowledgment

The Geotermia office of DIATI department has represented for me such a lively and stimulating workplace over the last three years. I would like to thank all the people and colleagues who supported me during the exciting adventure that was my PhD at the Politecnico di Torino.

My first acknowledgment goes to my supervisor Prof. Lo Russo for being always a precious guide, for having transmitted all his passion for geology, and for having followed and accompanied me in every phase of the research work, by correcting my mistakes and supporting my ideas.

A special thank goes to Prof. Glenda Taddia. She was always ready to listen to my technical and non-technical troubles. Thank you for being that reference which I can refer to at any time.

I cannot forget my parents, my brother Giovanni, and my boyfriend Stefano: thank you for the support that you have never stopped giving me.

Abstract

Clean energy production using sustainable resources has become one of the central topics of European and National development policy visions. Besides, the Italian Piano Nazionale Integrato per l'Energia e il Clima establishes the new national targets for 2030 on energy efficiency, renewable sources, and CO₂ emissions reduction. Energy companies' primary aim has become to provide new, more sustainable energy solutions, unlike those based on fossil fuels, and guarantee access to low-cost energy through technological development and environmental protection.

Recognized as equitably and environmentally sustainable, geothermal energy resources can ensure a renewable potentiality, establishing its importance for a new production model for the forthcoming future. Consequently, the need for developing new geothermal energy-related solutions has assumed increasing importance to cope with the energy demands. In the described process, the exploitation of deep geothermal energy resources derived from disused hydrocarbon wells in oilfields represents a considerable environmental energy solution. The hydrocarbon wells' technological reconversion can allow hypothesizing long-term scenarios for the exploitation of suspended wells near municipalities, even at the end of their production cycle to the benefit of end-users in the industrial, civil, and agriculture districts.

Since 1985, more than 8000 wells have been drilled for hydrocarbon extraction activities in Italy. In mature Italian oilfields, deep wells represent suitable candidate structures for geothermal heat exploitation, thus providing access to subsurface energy resources. Closed-loop geothermal technologies currently represent a more effective technological solution to harness deep geothermal energy resources in oilfields. Due to their proven advantages, in the proposed research work, the attention was centered on two different geothermal closed-loop-type technologies (U-tube and Coaxial WellBore Heat Exchangers). Heat exchange mechanisms in three different Italian oilfields (the Villafortuna-Trecate, Val d'Agri - Tempa Rossa and Gela fields) were reconstructed, employing simplified heat exchange models, implemented in both Python and Matlab programming languages. Differences in potentially extracted thermal energy were emphasized, both considering the

peculiar geological context and the selected system configuration. The results obtained demonstrated how the Coaxial WBHE technology performs better for each hydrocarbon well analysed. Even for variable inlet flow rate values, ever-higher output temperatures for the Coaxial configuration are recorded. The outflow temperatures of working fluid at the wellhead for both Coaxial and U-tube WBHEs in Villafortuna 1 and Trecate 4 hydrocarbon wells (Northwestern Italy) could be progressively used for some of several direct applications: greenhouse heating (100°C - 40°C), soil heating (60°C - 30°C), animal breeding, aquaculture and agricultural cultures (<30 °C). Coaxial or U-tube WBHEs' implementation in Tempa Rossa 1D and Gela 38 hydrocarbon wells is not energetically or economically worthwhile.

Simplified tools for a reuse strategies analysis, such as those presented in the proposed research work can guide the identification of case studies potentially suitable for the considered energy reconversion project.

Contents

1. Introduction.....	1
2. Geoscience and Decarbonisation	8
3. Hydrocarbons.....	15
3.1 Hydrocarbon occurrences in Italy.....	15
3.1.1 Oil and thermogenic gas in the Mesozoic carbonate substratum....	18
3.1.2 Thermogenic gas in the thrustured terrigenous Oligo-Miocene foredeep sedimentary wedges.....	23
3.1.3 Biogenic gas in the terrigenous Plio-Pleistocene foredeep wedges	23
3.2 Hydrocarbon wells in Italian petroleum systems	25
3.2.1 ViDEPI Project: petroleum exploration data in Italy.....	27
4. Geothermal Energy	31
4.1 Classification of geothermal energy resources	31
4.1.1 Direct and indirect uses of geothermal energy resources	36
4.1.2 Direct uses of geothermal energy resources in Italy	47
4.2 Geothermal energy in sedimentary basins.....	51
4.2.1 Geothermal energy in Italian hydrocarbon fields	53
4.2.2 Thermal properties of rocks in Italian hydrocarbon fields	57
4.2.3 Geothopica: The Italian National Geothermal Database	63
4.2.4 Rete Geotermica Italiana e Unione Geotermica Italiana	67
5. Materials and Methods.....	69
5.1 Background of geothermal resources utilization in oilfields.....	69
5.1.1 Closed-loop geothermal systems: Wellbore Heat Exchangers (WBHEs).....	77
5.2 Heat transfer process in wellbores in oilfields.....	80
5.3 Heat transfer in Coaxial WBHEs.....	83

5.3.1 Coaxial WBHE: coefficient of heat exchange between outer-pipe fluid and the wellbore exterior	84
5.3.2 Coaxial WBHE: coefficient of the heat exchange between the outer-pipe fluid and the inner pipe	86
5.3.3 Coaxial WBHE: current methodological developments.....	87
5.4 U-tube WBHE: thermal resistances model.....	92
5.5 Pressure losses	96
5.6 The Codes	97
5.6.1 WBHEs models assumptions.....	97
5.6.2 The Python Code	99
5.6.3 The Matlab Code	103
6. Results.....	106
6.1 Influence of ground's thermal properties	108
6.2 The Villafortuna–Trecate Field	111
6.2.1 Villafortuna 1 hydrocarbon well.....	112
6.2.2 Trecate 4 hydrocarbon well	120
6.3 The Val d'Agri-Tempa Rossa Field	127
6.3.1 Tempa Rossa 1D hydrocarbon well.....	127
6.4 The Gela Field	134
6.4.1 Gela 38 hydrocarbon well.....	134
7. Discussion.....	140
8. Conclusions and future research perspectives	148
9. References.....	153

List of Figures

Figure 1 Estimated Renewable Share of Total Final Energy Consumption, 2009 and 2019 (IEA, 2021).	10
Figure 2 Stratigraphic and geographic location of the Italian petroleum systems (Modified from Cazzini, 2018. Copyright Geological Society of London, 2018).17	
Figure 3 Spatial comparison between exploited hydrocarbon fields and natural gas seeps in Italy (Martinelli et al., 2021).....	18
Figure 4 Villafortuna –Trecate oil field: geological sections and major hydrocarbon occurrences (vertical exaggeration 2:1) (Bertello et al., 2010).	19
Figure 5 Gela oil field: geological sections and hydrocarbon occurrences (vertical exaggeration 2:1) (Bertello et al., 2010).....	21
Figure 6 Val d’Agri oil field: geological sections and significant hydrocarbon occurrences (vertical exaggeration 2:1) (Bertello et al., 2010).....	22
Figure 7 Tectono-stratigraphic cycles and hydrocarbon occurrences (from Bertello et al., 2010).	24
Figure 8 a. Oil production in EJ (Exajoule), Italy 1990-2020 b. Natural gas production in TJ-gross (Terajoule), Italy 1990-2020 (Data from IEA, 2020).....	26
Figure 9 Italian research permits and cultivation concessions (Data from WebGIS UNMIG. Ministero dello Sviluppo Economico).	28
Figure 10 Italian hydrocarbon wells location (Data from WebGIS UNMIG. Ministero dello Sviluppo Economico).....	29
Figure 11 Trecate 004 hydrocarbon well location (Data from WebGIS UNMIG. Ministero dello Sviluppo Economico).....	29
Figure 12 Seismic line of the CROP-11/b Atlas project (from VIDEPI Project UNMIG. Ministero dello Sviluppo Economico).	30
Figure 13 Seismic profile of the CROP-11/b Atlas project (from VIDEPI Project UNMIG. Ministero dello Sviluppo Economico).....	30
Figure 14 Simplified representation of the relationship between Earth’s structure and variation of the Geothermal Gradient (Online resource).	32
Figure 15 Map of heat flow measurement points (Davies, 2013).....	34

Figure 16 Geothermal energy overview (from GeoVision report by the U.S. DOE).....	37
Figure 17 Modified Lindal diagram (Gudmundsson et al., 1985; Operacz and Chowaniec, 2018).	39
Figure 18 Ground source heat pump (GSHP) system schematic diagram (from Moon et al., 2019).....	40
Figure 19 Growth curves for some crops (from Beall and Samuels, 1971)....	41
Figure 20 Worldwide installed direct-use geothermal capacity and annual utilization from 1995-2020 (from Lund & Toth, 2021).....	43
Figure 21 Heat generation from renewables and geothermal sources, Italy 2004-2020 (Data from IEA, 2020).....	49
Figure 22 Temperature valuea recorded in the Italian territory at a. 3000 depth (° C), b. 2000 depth (° C), c. 1000 depth (° C). Representations not to scale. (Modified from Inv. Ris. Geotermiche Italiane, 1986).....	50
Figure 23 Conceptualized basin sedimentary formations (modified from Onajite, 2014 - Seismic Data Analysis Techniques in Hydrocarbon Exploration).	52
Figure 24 Deep Geothermal Potential a. Regione Campania b. Regione Puglia (from VIGOR Project - online resources).....	56
Figure 25 Deep Geothermal Potential a. Regione Calabria b. Regione Sicilia (VIGOR Project from VIGOR Project - online resources).....	57
Figure 26 Geothopica webGIS – Italian hydrocarbon wells location (image above is not to scale).....	65
Figure 27 Geothopica webGIS – Hydrogeological Complexes of Italy - from the Atlas of Water Resources of the European Community (image above is not to scale).	65
Figure 28 Geothopica webGIS – Lito-stratigraphic profile and selected hydrocarbon well information.	66
Figure 29 Geothermal resource assessment: definition of influencing factors according to Muffler & Cataldi, 1978.	71
Figure 30 Extraction geothermal technologies: (a) producer-injector doublet (open-loop system), (b) wellbore heat exchanger single U-tube, (c) wellbore heat	

exchanger double U-tube, (d) coaxial wellbore heat exchanger (Raos et al., 2019).	76
Figure 31 Schematic representation of a U-tube heat exchanger (U-tube WBHE) geometry (Lo Russo et al., 2020).....	78
Figure 32 Schematic representation of a single Coaxial heat exchanger (Coaxial WBHE) geometry (Lo Russo et al., 2020).....	78
Figure 33 Thermal resistances definition steps: (a) borehole resistance, (b) parallel borehole resistances, (c) convective and conductive resistances and (d) final resistances configuration (reproduced from Ruiz-Calvo et al. 2015. Copyright Elsevier, 2014).	92
Figure 34 Geometrical model characteristics for calculating the equivalent diameter (reproduced from Ruiz-Calvo et al. 2015. Copyright Elsevier, 2014). ..	93
Figure 35 Python codes simplified research flowchart.	100
Figure 36 Developed Python Settings.py code structure.	101
Figure 37 Developed Python Coaxial.py model general structures.	102
Figure 38 Geological formations' thermal parameters definition section (Python Coaxial.py model structures).	102
Figure 39 Matlab codes simplified research flowchart.	103
Figure 40 Geological formations' thermal parameters definition section (MATLAB Coaxial model structures).	104
Figure 41 Developed MATLAB Coaxial model general structures (MATLAB Editor).	105
Figure 42 Thermal resistance over time with different specific heat values (pc rock - J/kg/K).	109
Figure 43 Thermal resistance over time with different ground density values (ρ – kg/m ³).	109
Figure 44 Thermal resistance over time with different conductivity values (λ – W/mK).	110
Figure 45 Thermal resistance over time with different thermal diffusivity (α).	110
Figure 46 Villafortuna 1 and Trecate 4 hydrocarbon wells location (Villafortuna-Trecate Oilfield, Western Po Plain).	111

Figure 47 Temperature data visualisation for the Villafortuna 1 hydrocarbon well: Depth (m); Temperature (°C).	113
Figure 48 Temperature profile associated with the Coaxial WBHE configuration considering site-specific stratigraphy (Villafortuna 1 hydrocarbon well).	116
Figure 49 Wellhead temperature as the flow rate value changes: Coaxial WBHE (Villafortuna 1 hydrocarbon well).	117
Figure 50 Heat Power as the flow rate value changes: Coaxial WBHE (Villafortuna 1 hydrocarbon well).	117
Figure 51 Temperature profile associated with the U-tube WBHE (b) configuration considering site-specific stratigraphy (Villafortuna 1 hydrocarbon well).	118
Figure 52 Wellhead temperature as the flow rate value changes: U-tube WBHE (Villafortuna 1 hydrocarbon well).	119
Figure 53 Heat Power as the flow rate value changes: U-tube WBHE (Villafortuna 1).	119
Figure 54 Temperature data visualisation for the Trecate4 hydrocarbon well: Depth (m); Temperature (°C).	121
Figure 55 Temperature profile associated with the coaxial WBHE configuration considering site-specific stratigraphy (Trecate4 hydrocarbon well).....	123
Figure 56 Wellhead temperature as the flow rate value changes: Coaxial WBHE (Trecate4 hydrocarbon well).....	124
Figure 57 Heat Power as the flow rate value changes: Coaxial WBHE (Trecate4 hydrocarbon well).	124
Figure 58 Temperature profile associated with the U-tube WBHE (b) configuration considering site-specific stratigraphy (Trecate4 hydrocarbon well).	125
Figure 59 Wellhead temperature as the flow rate value changes: U-tube WBHE (Trecate4 hydrocarbon well).....	125
Figure 60 Heat Power as the flow rate value changes: U-tube WBHE (Trecate4 hydrocarbon well).	126
Figure 61 Tempa Rossa 1D hydrocarbon well location (Tempa Rossa Field, Basilicata Region).....	127

Figure 62 Temperature data visualization for the Tempa Rossa 1D hydrocarbon well: Depth (m); Temperature (°C)	129
Figure 63 Temperature profile associated with the coaxial WBHE configuration considering site-specific stratigraphy (Tempa Rossa 1D hydrocarbon well).	131
Figure 64 Wellhead temperature as the flow rate value changes: Coaxial WBHE (Tempa Rossa 1D hydrocarbon well).	132
Figure 65 Temperature profile associated with the U-tube WBHE (b) configuration considering site-specific stratigraphy (Tempa Rossa 1D hydrocarbon well).	132
Figure 66 Wellhead temperature as the flow rate value changes: U-tube WBHE (Tempa Rossa 1D hydrocarbon well).	133
Figure 67 Gela 38 hydrocarbon well location (Gela Field, Sicily Region)...	134
Figure 68 Temperature data visualization for the Gela 38 hydrocarbon well: Depth (m); Temperature (°C)	136
Figure 69 Temperature profile associated with the coaxial WBHE configuration considering site-specific stratigraphy (Gela 38 hydrocarbon well).	138
Figure 70 Wellhead temperature as the flow rate value changes: Coaxial WBHE (Gela 38 hydrocarbon well).	138
Figure 71 Temperature profile associated with the U-tube WBHE (b) configuration considering site-specific stratigraphy (Gela 38 hydrocarbon well).	139
Figure 72 Wellhead temperature as the flow rate value changes: U-tube WBHE (Gela 38 hydrocarbon well).	139

List of Tables

Table 1 Geothermal energy resources classifications (Muffler & Cataldi, 1978)	33
Table 2 Summary of direct-use data worldwide by region and continent, 2019 (Modified from Lund & Toth, 2021)	43
Table 3 The geological unit selected considering the four different Italian region (VIGOR Project).....	59
Table 4 Thermal conductivity values ($Wm^{-1}K^{-1}$) of the main geological units derived by direct measurements on samples (dry condition).	60
Table 5 Comparison between thermal conductivity values ($Wm^{-1}K^{-1}$) measured in dry and wet conditions and derived by literature.....	60
Table 6 Laboratory results of physical properties from Pasquale et al., 2011.	62
Table 7 Various forced convection correlations for circular tubes (Bergman et al. 2011)	82
Table 8 Coaxial WBHE–geometric parameters.	84
Table 9 Coaxial WBHE tube sizing in Alimonti and Soldo, 2016 – ID: internal diameter, OD: external diameter.....	92
Table 10 U-tube WBHE - Geometric parameters	95
Table 11 Villafortuna 1 hydrocarbon well (Villafortuna Trecate Oilfield, Western Po Plain) - technical data available on VIDEPI project website	112
Table 12 Villafortuna 1 hydrocarbon well - lithostratigraphic profile.....	113
Table 13 Trecate 4 hydrocarbon well (Villafortuna-Trecate Oilfield, Western Po Plain) - technical data available on VIDEPI project website	120
Table 14 Trecate4 hydrocarbon well - lithostratigraphic profile	121
Table 15 Tempa Rossa 1D hydrocarbon well (Tempa Rossa Field, Basilicata Region) - technical data available on VIDEPI project website	128
Table 16 Tempa Rossa 1D hydrocarbon well - lithostratigraphic profile.....	128

Table 17 Gela 38 hydrocarbon well (Gela Field, Sicily Region) - technical data available on VIDEPI project website.....	135
Table 18 Gela 38 hydrocarbon well - lithostratigraphic profile.....	135
Table 19 Recorded working fluid temperatures in Villafortuna 1, Trecate 4, Tempa Rossa 1D, Gela 38 hydrocarbon wells.....	144
Table 20 Additional abbreviation of parameters.....	152

Chapter 1

Introduction

Since the 1970s, researchers have studied the direct relationship between physical urban characteristics and energy systems. The resulting systemic-critical framework of the connection between energy and physical-functional organization has outlined the relevance of including increasingly new energy-related strategies in spatial planning policies. However, this theoretical awareness seems not yet to find an equivalent practical application in day-life national governance and management. It is generally accepted that, in the sustainability and global challenges framework, metropolitan areas are the front-runners, with their decisive role to be the core of a new sustainable energy transition process. This role turns out to be recognized by the high presence of energy efficiency topics in the European Urban Agenda (European Commission, 2019). However, a holistic and integrated approach to comprehending energy efficiency, urban and regional planning is far from being completed.

The current energy paradigm, strongly relying on fossil fuels, turns out not to be more sustainable. The limits of this type of energy system, in terms of air pollutant emissions and resource depletion, have taken on more and more evidence over the last few decades. For more than a century, it took advantage of fossil fuels to generate most of the energy required to propel transportation, power businesses, energy generation, cooling, and heating buildings. Consequently, an energy production strategy based on

fossil fuels has caused an enormous impact on humanity and the environment. In addition, due to the end of oil and gas extraction activities, a large number of wells are decommissioned and dismissed every year, frequently causing significant adverse environmental consequences and economic losses. The potential to further increase energy consumption related to the expected contribution provided by the fast-developing countries and, in the future, by the less fast-developing countries could also determine severe and unrecoverable effects if a radical transition is not undertaken in time.

Energy production by means of affordable and renewable energy resources has become one of the central topics of European and National development policy visions: medium-long term objectives concerning the decarbonization of the European Energy Systems are corroborated in the 2020 Climate and Energy Package, and the following 2030 climate and energy framework. Besides, the Italian Piano Nazionale Integrato per l'Energia e il Clima establishes the new national targets for 2030 on energy efficiency, renewable sources, and the reduction of CO₂ emissions. It also fixes the targets for energy security, interconnections, the single energy market and competitiveness, sustainable development, and mobility, outlining the measures that will be implemented to ensure their achievement (Ministero dello Sviluppo Economico et al., 2019).

The overall efforts to be done in order to achieve full decarbonisation by 2050 were reported in the document entitled "Strategia Italiana di lungo termine sulla riduzione delle emissioni dei gas a effetto serra" (Ministero dello Sviluppo Economico, 2021). The described long-term national strategy identifies possible paths to reach a condition of climate neutrality in the country to 2050, in which the residual greenhouse gas emissions are offset by the absorption of CO₂ e from the possible use of forms of geological storage and reuse of CO₂. In Italy, 70% of residual CO₂ emissions by 2050 derives from energy uses. The transport sector is the first in emissions, covering about 30% of the total (agricultural vehicles included). In contrast, the industrial sector drops significantly, weighing, in terms of emissions, about 25% of the total, with dynamics well distributed between the energy and non-energy sectors. The residential and

commercial sectors, still retain an important reduction potential, corresponding to approximately 15% of total emissions. Finally, considering the sector of non-energy uses, which covers the residual 30% of the total emission amount, it emerges, as already noted in the PNIEC (2019), the substantial difficulty in compressing emissions from agriculture/animal industry and the related industrial processes. Therefore, the continuation of current trends would not be sufficient to achieve the goal of climate neutrality by 2050: it is necessary to foresee a real change in the "Italian energy paradigm" which obviously passes through investments/choices that affect the technologies to be applied, the infrastructures but also on citizens' lifestyles.

The described European and National objectives are far from being achieved. It turns out to be increasingly necessary to find new solutions to guarantee access to clean fuel and technology. Notably, more progress is needed for integrating renewable energy resources in final applications in buildings and industry, for the conversion of existing energy systems. Public and private investments in energy also need to be increased, focusing on regulatory frameworks and innovative business models to transform global energy systems at urban and regional scales (United Nations, 2018).

The above-mentioned criticalities put into evidence the urgent need for a transition towards decarbonised energy and economic systems, which necessarily implies a more severe shift from fossil commodities to renewables (wind, solar, hydro, geothermal, biofuels). Therefore, the primary aim of energy companies has become to provide energy solutions that are increasingly sustainable and distant from those based on fossil fuels through technological development and environmental protection values. In this energetical context, geosciences can represent the key to identifying concrete solutions for the decarbonisation of energy systems. Considering the available energy resources, geothermal energy, as a weather-independent, environmentally friendly resource, represents one of the leading future energy solutions to be exploited for both power generation and direct use applications. Depending on the geological, and thermo-physical conditions such as temperature, flow rate, and geothermal waters mineralisation grade, prevailing in an area to be analysed, there are several possibilities for the industrial and economical utilisation of the thermal energy accumulated.

Geothermal energy direct-use technologies are growing in the application in metropolitan areas, including district heating, space heating using heat pumps, agricultural purposes (e.g., greenhouses), fish farming, milk pasteurization, and other purposes. Notably, through cascading exploitation of the available heat, it is possible to realize a multi-variant and extensive resource use, according to the corresponding temperature demand (Kaczmarczyk et al., 2020). Additionally, considering the resources potentially harnessable in oilfields, the clean energy production based on the exploitation of the available profound geothermal energy associated with disused hydrocarbon wells could also represent a considerable future energy solution. It could solve problems related to suspended oil and gas wells near municipalities, thereby allowing us to hypothesize long-term scenarios for exploitation — even at the end of the hydrocarbon production cycle of wells — to the benefit of end-users in the industrial, civil, and agriculture districts. Decommissioned and abandoned hydrocarbon wells in hydrocarbon fields represent suitable candidate infrastructures for allowing low-cost geothermal energy production via a retrofitted energy system. Existing boreholes, facilities and infrastructures, valuable geological and geophysical available data empower potential geothermal projects by reducing capital costs, minimizing risks and significant inconveniences (Wang et al., 2018; Liu et al., 2018; Gizzi, 2021).

Considering the temperature ranges associated with deep wells in hydrocarbon fields, energy companies and researchers have recently started to work on developing various strategies for harnessing this type of geothermal energy resource. The majority of works that have been carried out on existing abandoned petroleum wells have focused on open-loop systems designed to repurpose petroleum fields as geothermal reservoirs (Sanyal & Butler, 2010; Limpasurat et al., 2011; Kharseh et al., 2019, (Gizzi, 2021). However, open-loop technologies were found to be subject to some technical problems, including groundwater recession, corrosion, and scaling problems (Nian & Cheng, 2018b). The re-injection of fluids constitutes a further issue. Due to their physicochemical properties being unsuitable for terrestrial ecosystems, geothermal fluids must be treated before re-injection into the underground. Since these operations require the drilling and

maintenance of additional wells, the treatment and pumping of fluids often entailed higher economic costs related to potential geothermal projects. An advantageous alternative was found in the use of closed-loop deep geothermal systems (a closed-circuit of pipes).

Unlike a conventional open-loop geothermal system, heat carrier fluids in closed-loop ones circulate inside of wellbore heat exchangers (WBHEs), while no ground fluids are extracted from surrounding rocks. Besides, working fluids are not in contact with the surrounding geological formations. Moreover, corrosion and scaling problems are limited. Due to their proven advantages, a large number of researches dealing with developing closed-loop system technologies have appeared in the literature (Kujawa et al., 2006; Bu et al., 2014; Cheng et al., 2014; Wight & Bennett, 2015; Alimonti & Gnoni, 2015; Alimonti et al., 2016; Gizzi et al., 2021, Gizzi, 2021). Despite some recent successful theoretical oilfield geothermal system experiments worldwide, specific challenges remain in the large-scale harnessing of geothermal resources in oilfields (Zarrouk & Moon, 2014; Wang et al., 2016; Alimonti et al., 2018). The key factors limiting oilfield geothermal energy exploitation and utilization are mainly related to low energy conversion efficiency, insufficient involvement, inadequate assessment and planning, lack of knowledge and available economic data. Furthermore, national laws and regulations designed to accommodate available geothermal resources of oil fields are not so clear. The procedures for reconverting an existing plant in a geothermal field, especially in areas adjacent to urban aggregates, are still relatively complex to be developed.

According to the information available in the Proceedings World Geothermal Congress (2020), in Italy, there are 37 direct-use geothermal energy sites, 5 of which are for district heating, 5 for individual space heating, one industrial process site, 6 for fish farming, 4 for greenhouse heating, and 16 for swimming and bathing. At the end of 2017, the total installed capacity exceeded 1400 MW_{th}, with a corresponding heat utilization of 10915 TJ/yr. The space heating sector holds the leading share of direct geothermal use (42% of the total energy, 52% of the overall installed capacity), followed by thermal balneology (32% for both values) and fish farming (18% and 9%,

respectively). Agricultural applications, industrial processes, and other minor uses account for around 8% of the total geothermal use. Despite the potential for development in Italy, potentially available geothermal energy resources for direct uses are not fully developed, and the national current urban and regional energy paradigm relies heavily on fossil fuels. The share of geothermal heat production in Italy, excluding geothermal heat pumps, in the total thermal production from Renewable Energy Sources (RES) is limited to a percentage of 1.3% (Gestore dei Servizi Energetici S.p.A., 2018).

Over time, various hydrocarbon reservoirs have been identified and Italian sedimentary basins have been explored for both oil and gas extraction purposes. Geological and geophysical exploration campaigns into the deepest regions of such geological contexts have ascertained the coexistence of hydrocarbons and low to medium-temperature potentially exploitable geothermal energy resources (Cataldi et al., 1995; Montanari et al., 2017, Gizzi et al., 2021). Understanding the possibilities linked to the exploitation of the geothermal resources available in the described geological contexts could eventually be helping to increase the national percentage of thermal energy produced from RES (Renewable Energy Sources).

In view of the above considerations, in the presented research work, the attention was focused on analysing Italian sedimentary basins from a geological and stratigraphical point of view. Associated with these complex tectonic contexts, it was indeed defined the presence of potentially exploitable geothermal energy resources, closely related to larger hydrocarbon fields. Technical information regarding productive and dismissed hydrocarbon wells in Italy, available on the National Mining Office of the Italian Ministry for Economic Development (MISE) and VIGOR project's website, was examined. Besides, detailed litho-stratigraphic information and temperature data related to the hydrocarbon wells have been collected from the Italian National Geothermal Database (BDNG), the most extensive collection of Italian geothermal data. The research work began with a comprehensive review of Italian hydrocarbon occurrences (Chapter 3), classification of geothermal energy resources, geothermal resources potentially available in sedimentary basins that hosted oilfields (Chapter 4). Then, types

of petroleum wells capable of supplying geothermal energy resources, geothermal extraction methods from an abandoned hydrocarbon well, and heat transfer processes in wellbores located inside oilfields were described (Chapter 5).

The research work tried to answer the following main research question: can the heat of geothermal origin associated with a selected Italian hydrocarbon well represent an environmentally sustainable solution for direct thermal applications in case studies' neighboring areas (e.g., agricultural services, civil and industrial uses)?

The primary purpose was indeed to develop simplified investigation tools that can guide the comprehension of the possibility of converting existing hydrocarbon fields into geothermal ones. Due to their proven advantages, the attention was centered on two different closed-loop-type technologies. Two simplified heat exchange models (U-tube and Coaxial Wellbore Heat Exchangers) have been implemented in both Python and MATLAB software. The potential of the proposed codes has been tested on different selected national case studies (i.e., Villafortuna 1, Trecate 4, Tempa Rossa 1D, Gela 38 hydrocarbon wells) with the aim to 1) underline the differences in the extracted thermal energy amounts as a function of the specific Italian geological and depositional contexts 2) find the best closed-loop configuration that allows maximizing the heat extraction amounts.

To summarize it in a few words, the definition of new simplified approaches based on each site's geological characteristics that, together with related closed-loop configuration application codes, can allow defining the attitude of a hydrocarbon well to be converted into a geothermal one represents the primary outcome of the proposed research project.

Chapter 2

Geoscience and Decarbonisation

Rising greenhouse gas (GHG) emissions from burning fossil fuels and deforestation are leading to global heating that is destabilizing the climate, putting lives, livelihoods, and entire ecosystems at risk (IPCC, 2021). The landmark 2015 Paris Agreement aims to avoid the most devastating effects of climate change, limiting global temperature rise to no more than 2°C above pre-industrial levels. To achieve this goal, countries are aiming to reach net-zero emissions by mid-century, a point representing the balance between unavoidable GHG emissions and their removal from the atmosphere through rapid development and deployment of new clean energy technologies. According to IRENA, 2019, for reaching the global climate objectives, the deployment of renewables must be increased at least six-fold compared to current government plans. This objective would require that the impressive progress we are already witnessing in the power sector accelerate further. At the same time, efforts to decarbonise transport and heating using renewable resources would need to be stepped up significantly. Choosing renewables should be the standard for new power additions as we act resolutely to stop new fossil fuel power generation, phase out the assets, and upgrade infrastructure to ensure system flexibility that allows a higher integration of variable renewables (IRENA, 2021).

The IEA has stated that “as the major source of global emissions, the energy sector holds the key to responding to the world’s climate challenges.” In practical terms, achieving net-zero globally will require a two-pronged approach: curbing human-produced emissions and removing carbon from the atmosphere (IEA, 2021). The development and deployment of clean energy entail far more than just technological advancement. A successful transition to net-zero requires the engagement of corporates, governmental policies, and intergovernmental agreements, and buy-in from the public.

According to the information in the *Pathways to Net Zero : The Impact of Clean Energy Research Executive Summary* (2021), over the last 20 years, the share of publications in clean energy research among all outputs and the range of decarbonization solutions has increased. Besides, the commitments made by nations to reduce emissions have become more robust. The role of research and technological development as an enabler of the energy transition is crucial. Basic and applied research is fundamental in developing core technologies, such as those based on energy storage or renewable energy production. On the other hand, it is required to integrate these new technologies into the energy system, which is a very complex system with a high degree of interdependence between the parts and agents that compose it.

Energy Information Administration (EIA) forecasts that by 2050, renewables will be the most critical source of energy globally. However, despite the growing deployment of renewable energy worldwide, the share of renewables in total final energy consumption (TFEC) has seen a moderate increase. As in 2019, modern renewable energy accounted for an estimated 11.2% of TFEC, up from 8.7% a decade earlier (see Fig.1). The most considerable portion was renewable electricity (6% of TFEC), followed by renewable heat (4.2%) and transport biofuels (1.0%).

For 2020, renewable energy demand had increased by about 1% from 2019 levels, in contrast to all other energy sources. Renewable electricity generation has grown by nearly 5% despite the supply chain and construction delays caused by the Covid-19 crisis. In doing so, renewables almost reach 30% of the electricity supply globally, halving the gap with coal (from 10 percentage points in 2019) (IEA, 2020).

In Italy, the renewable energy sector has recorded a slow improvement trend. This trend is demonstrated by the latest GSE data on the production and final consumption of green energy sources. In 2019, at the electrical level, the FER (Fonti Energetiche Rinnovabili), with a total installed power of 55.5 GW, distributed among over 893,000 plants, generated 39.4% of the national electricity production. And at the same time, they covered 35% of gross domestic consumption. The source that made the most significant contribution is hydroelectric (40% of total production), followed by photovoltaics (20.4%), wind power (17.4%), bioenergy (16.9%), and geothermal energy (5.2%) (Gestore dei Servizi Energetici S.p.A., 2018).

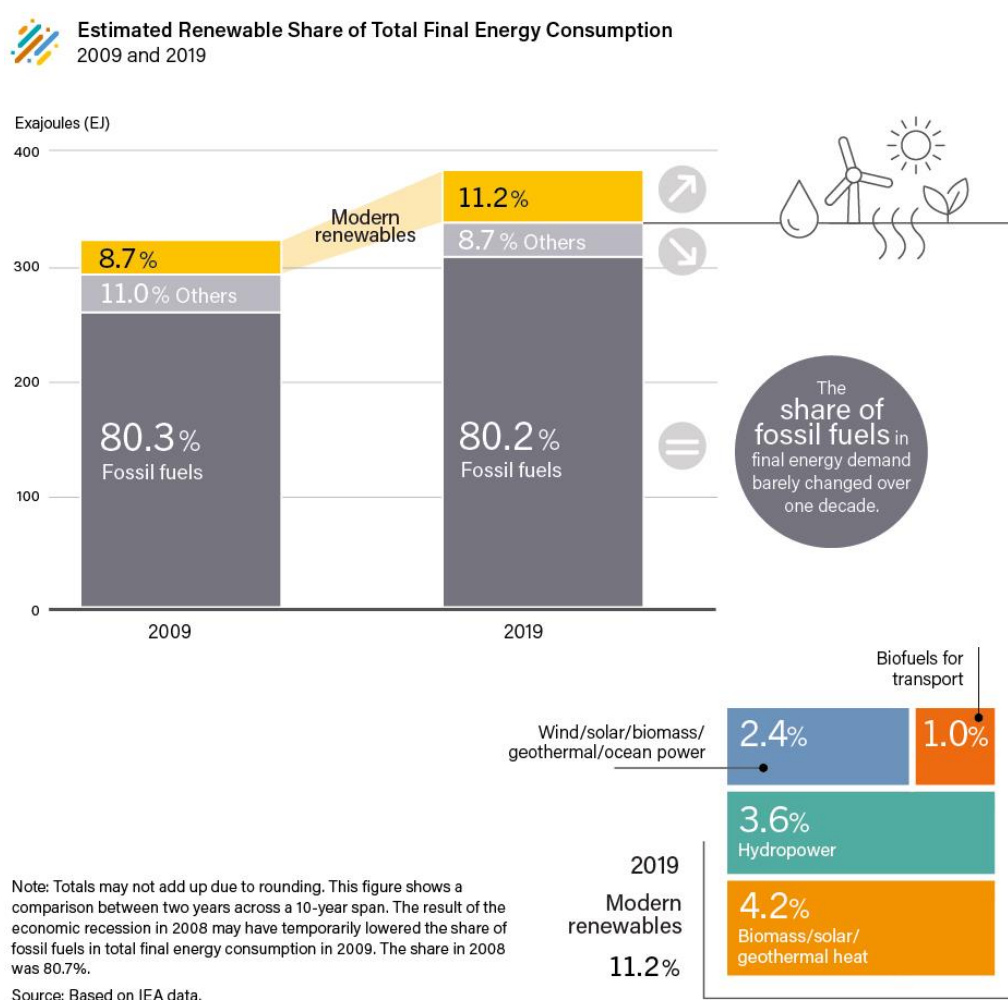


Figure 1 Estimated Renewable Share of Total Final Energy Consumption, 2009 and 2019 (IEA, 2021).

In the described international and national context, geosciences can represent a key to identifying concrete solutions for the decarbonisation of energy systems, through the development of a whole range of options that can contribute to encouraging the transition to renewable and sustainable energy sources on an urban and regional scale: the electricity production using renewable sources of power generation, the substitution of domestic heating using shallow and/or deep geothermal energy, use of carbon capture and storage (CCS) and more ambitious technologies such as bioenergy and carbon capture and storage (BECCS) that target harmful emissions (Stephenson et al., 2019). Intermittency of energy supply can be addressed by increasing the energy storage capabilities. This energy solution could include advancements in battery technologies (which rely on secure sources of minerals and metals, e.g., lithium and cobalt), as well as subsurface thermal energy storage, pumped hydro storage schemes, and compressed air energy storage. Carbon capture and storage (CCS) and bioenergy with CCS (BECCS) can have the potential to allow storing atmospheric carbon over geological timescales, removing carbon from the atmosphere permanently. Besides, across the hydrocarbon industry, moves are underway to reduce the production carbon footprint and reduce the methane intensity of operations. Oil and gas exploration strategies are shifting from quantity to quality. Companies aim to locate resources with the lowest carbon footprint and minimum impurities (e.g., no H₂S or low CO₂ cuts) and selectively develop the best.

In recent times, the topic of finding solutions for allowing the seasonal storage of large amounts of heat from solar or the exploitation and utilization of geothermal resources, using advanced geothermal technologies, has become interesting for researchers and energy companies. Bauer et al., 2015 described the possibility of seasonal storage of large amounts of heat from solar or industry. Technical options for subsurface heat storage include aquifer and borehole thermal energy storage, which enable heat storage in most subsurface geological formations. Bär et al., 2015 considered low-enthalpy geothermal systems as heat sinks, which can be used to get rid of excess heat. The extra heat from industrial processes, cogeneration power plants, or solar thermal collectors can be transferred through a borehole heat exchanger array to the subsurface during the

summer months and then be extracted in the winter for heating purposes. Such seasonal storage systems relying on in situ subsurface heat to maintain injected fluid temperature are exceptionally efficient when applied on a district heating level. Baria & Beardsmore, 2012 discussed the importance of hot dry rock and the advances that engineered geothermal systems will provide without the need for naturally convective hydrothermal resources.

Until recently, geothermal power systems have exploited resources where naturally occurring heat, water, and rock permeability are sufficient to allow energy extraction. However, through hydraulic stimulation, EGS technologies enhance geothermal resources in hot dry rocks.

As reported by different authors (Busby, 2014; Gascuel et al., 2020), hydrocarbon reservoirs and geothermal energy resources can coexist in sedimentary basin geological contexts. The hydrocarbon reservoir generation conditions in sedimentary basins are similar to geothermal ones. Hydrocarbon resources are generated under specific temperatures and pressure conditions in source rocks; groundwater is always involved in the primary migration of oil from the source rock and the secondary migration of oil and gas to the reservoir. Consequently, oil and gas reservoirs in hydrocarbon basins act as geothermal reservoirs.

According to Nasr et al., 2018, geothermal resources associated with sedimentary basins have become common targets for extending geothermal development beyond regions hosting high-enthalpy resources. Previously unexplored basins are now being considered in energy planning, but this requires accurate resource analyses and estimates based on potential reservoir temperature. However, to identify a viable geothermal system, one must consider many factors, i.e., available prospecting, drilling, and reservoir technologies, energy costs in the area, and resource durability (Caulk & Tomac, 2017). From 42–95% of the total geothermal project cost, which can be mitigated by repurposing abandoned exploratory wells in sedimentary basins, is devoted to the drilling process (Tester et al., 1994).

Hydrocarbon wells can aid in the extraction of subsurface geothermal energy. The drilled borehole provides useful geological, geophysical, and geochemical information about the sub-surface reservoirs, allowing direct access to the sub-surface heat energy (Wang et al., 2018). Globally, many candidate wells can be used for geothermal energy extraction, and they are more common in mature oilfields. Poor production of fossil fuels from a well leads to its abandonment. High bottom-hole temperature, reliable wellbore integrity, and large production capacity make a well viable candidate for geothermal energy extraction. Because geothermal energy has caught the attention of geologists and other professionals in the energy industry, there is an increasingly strong interest in modifying existing wells: abandoned hydrocarbon wells can play a vital role in geothermal resource utilization (Mehmood et al., 2019).

The work proposed within this thesis project is part of the above-described scientific and research context. Abandoned oil wells across the Italian Peninsula can represent suitable candidate infrastructures for allowing low-cost geothermal energy production via a retrofitted energy system. Exploiting geothermal sources from different Italian oilfields consists of extracting the Earth's thermal energy for use in heating needs in various applications, including heat dwellings and greenhouses, providing warm water for agricultural products in greenhouses.

Available geological, geophysical, temperature data from existing deep hydrocarbon wells can be applied to minimize the time and exploration cost for a retrofitted geothermal plant development, recovering the economic losses incurred by abandoned/dry wells by repurposing them.

Considering the medium and long-term objectives concerning the decarbonisation of the Italian Energy System that aims to reach 30% in total energy consumption from renewables by 2030¹, the described energy solution could eventually be helping to increase the national percentage of thermal energy produced from RES. As reported in Chapter 1, following the official national reporting of the Gestore dei Servizi Energetici S.p.A. (2018), the share of geothermal heat production, excluding geothermal heat

¹ <https://www.iea.org/countries/italy>

pumps, in the total thermal output by Renewable Energy Sources (RES) is, in fact, still less than 2%.

Chapter 3

Hydrocarbons

3.1 Hydrocarbon occurrences in Italy

The Alps bound Italy on the North while the Apennines cross the entire peninsula from North to South. Alps and Apennines mountain chains constitute two thrust-and-fold belts that arose during Cenozoic times due to the interaction between the European and the Adriatic–African tectonic plates (Bertello et al., 2010). The described two chains are bordered in their outer margins by well-developed sedimentary foreland basins (with foredeep and piggyback basins), especially along with the Adriatic sectors, and by relatively vast foreland areas (e.g., the Po Plain, the Adriatic Sea, and Hyblean Basin). The formation of the two orogens was preceded by a crustal stretching and extension episode, which lasted for most of the Mesozoic and was generally characterized by carbonate type sedimentation (Bertotti et al., 1993 and references therein). Most of the carbonate structures were later involved in the Cenozoic orogenesis (Bertello et al., 2010).

Due to the described Italian complex geological and sedimentary history, various petroleum systems have been developed, some of which are of economic importance, making Italy the most endowed hydrocarbon province in southern Europe.

Bertello et al. 2008, Bertello et al., 2010, Cazzola et al. 2011 and Fantoni et al. 2011 provided overviews of the Italian peninsula's geological evolution, describing how Italian hydrocarbon occurrences can be classified by their association with three main tectono-stratigraphic systems (Fig.2):

- (1) Carbonate Mesozoic substratum of the foredeep/foreland area and the external thrust belts;

- (2) Thrusted terrigenous Oligo-Miocene foredeep wedges (Southern Alps, Northern Apennines, Calabria and Sicily);
- (3) Terrigenous Pliocene-Pleistocene successions of the late foredeep basins of the Apennines in the central and northern Adriatic Sea and the Po Plain.

According to Bertello et al., 2008 and Bertello et al., 2010 at least five essential source rocks have been recognised, ranging from Mesozoic to Pleistocene. Three of the source rocks were deposited during Mesozoic crustal extension and are mainly oil-prone. Hydrocarbon occurrences associated with these types of sources are usually found in complex carbonate structures along the Apennines thrust-and-fold belt and the foreland; the Villafortuna-Trecate (Po Plain), the Val d'Agri-Tempe Rossa (Southern Apennines) and the Gela (Sicily) fields represent the most extensive oil accumulations of these systems. The two other source rocks were deposited in the foredeep terrigenous units of the foreland basins, which formed during the Cenozoic orogenesis. The older one is thermogenic gas-prone and is found in the highly tectonised Oligo-Miocene foredeep wedges; gas occurrences associated with this source are mainly concentrated along the northern Apennines margin (e.g., the Cortemaggiore field), in Calabria (e.g., the Luna field) and Sicily (e.g., the Gagliano field). The younger source is biogenic gas-prone and is located in the outer Plio-Pleistocene foredeeps.

Martinelli et al., 2012 developed a map of hydrocarbon gas seepages where the prominent gas accumulations turned out to be located along a strip parallel to the Apennines chain. In particular, the main biogenic gas accumulations occur in the foredeep due to high subsidence, synsedimentary tectonics and turbidite sedimentation (Fig.3).

Bertello et al. 2010 and Fantoni et al. 2011 clearly showed the oil-prone Villafortuna-Tredate Middle Triassic and Val d'Agri-Tempa Rossa Cretaceous systems' geographic limitation as opposed to the wide distribution of the Late Triassic–Early Jurassic system and of the biogenic gas-prone Plio-Pleistocene systems (see Fig.2).

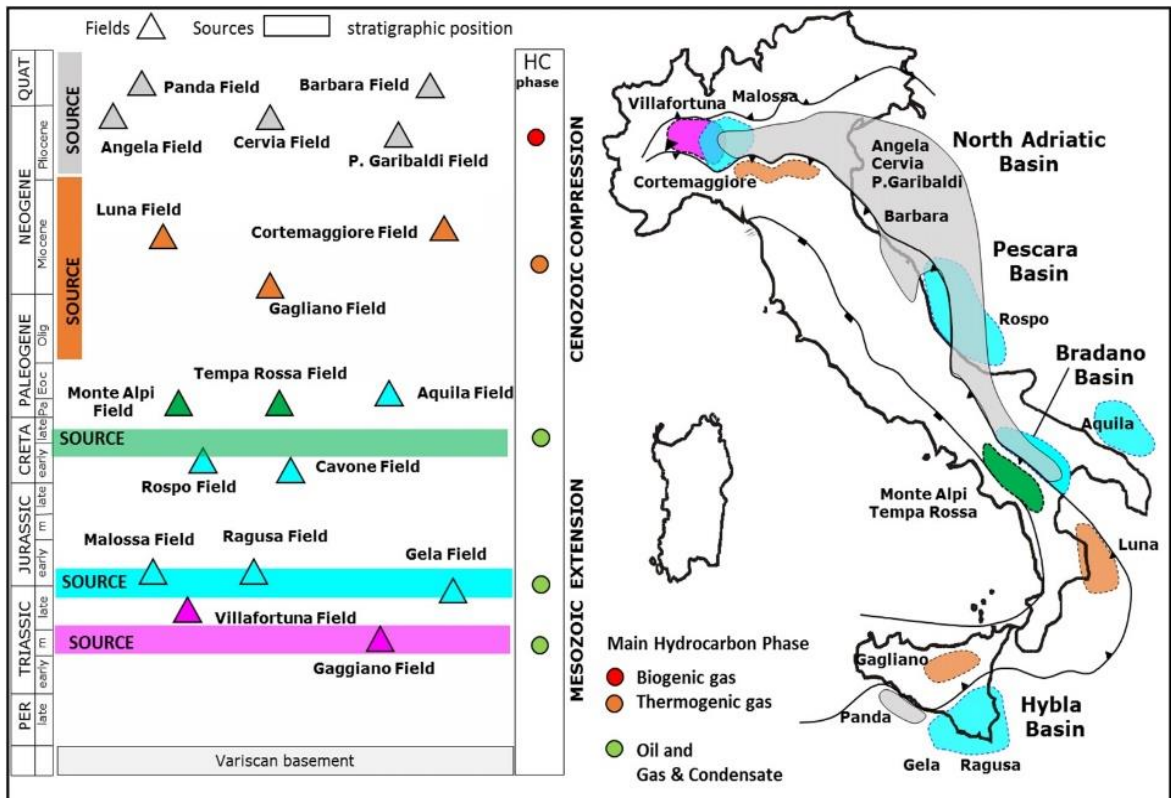


Figure 2 Stratigraphic and geographic location of the Italian petroleum systems (Modified from Cazzini, 2018. Copyright Geological Society of London, 2018).

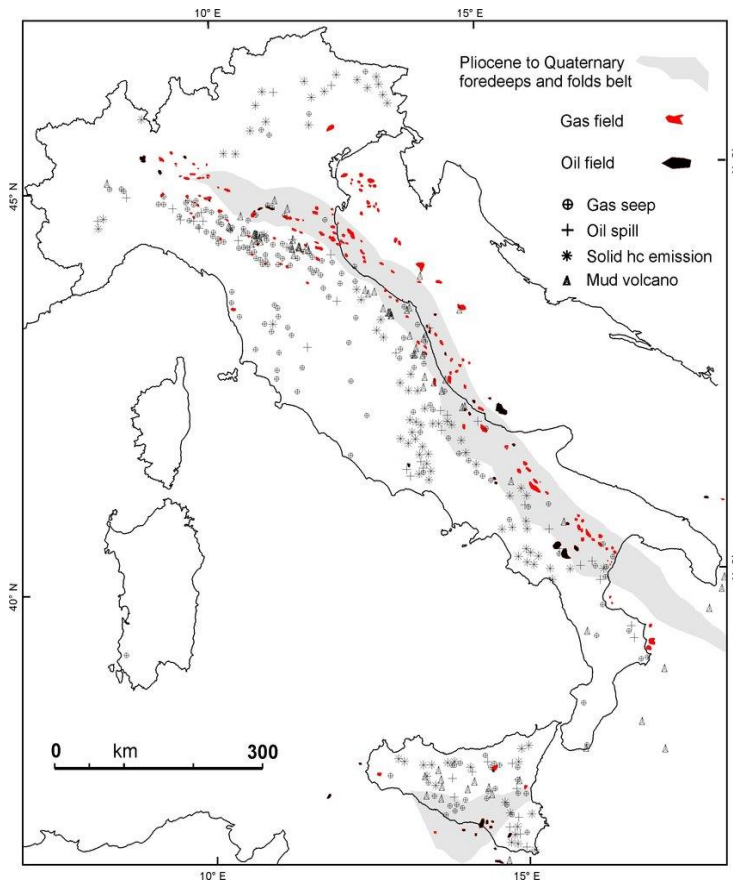


Figure 3 Spatial comparison between exploited hydrocarbon fields and natural gas seeps in Italy (Martinelli et al., 2021).

3.1.1 Oil and thermogenic gas in the Mesozoic carbonate substratum

The Middle Triassic petroleum system (**Villafortuna–Trecate Field**) is linked to the earliest stage of the Tethyan geological fragmentation. It contains dolomitised platform units of Late Triassic–Early Jurassic, which were charged by Middle Triassic carbonate source rocks deposited in the confined basins created by the rifting. The Villafortuna Field, discovered in 1984 in northern Italy, and its Trecate extension constitute the most considerable oil accumulation of this play (Bello & Fantoni, 2002; Fantoni, 2008) (Fig.4).

The petroleum system of the Villafortuna Field is developed inside the Triassic succession. It consists of two main reservoirs, made from dolomitized carbonate platform rocks and a set of source rocks deposited in the adjacent anoxic intra-platform basins (Bertello et al., 2010).

According to what was reported by Bertello et al., 2010, the lower reservoir is represented by the Anisian (Middle Triassic) Monte San Giorgio Dolomite, which was deposited in a peritidal to subtidal environment and turns out to be entirely dolomitized. The overlying Besano Shales (Anisian/Ladinian, Middle Triassic) provide the seal and are, at the same time, a source rock. The upper reservoir consists of three carbonate platform units of Norian (Late Triassic) to Hettangian (Early Jurassic) age: the Dolomia Principale, the Campo dei Fiori Limestone and the Conchodon Dolomite. Different petrophysical properties characterize the geological units due to their different original textures and subsequent diagenesis. The overlying shaly limestone of the Medolo Group (Lower Liassic) constitutes the regional seal for these three reservoirs.

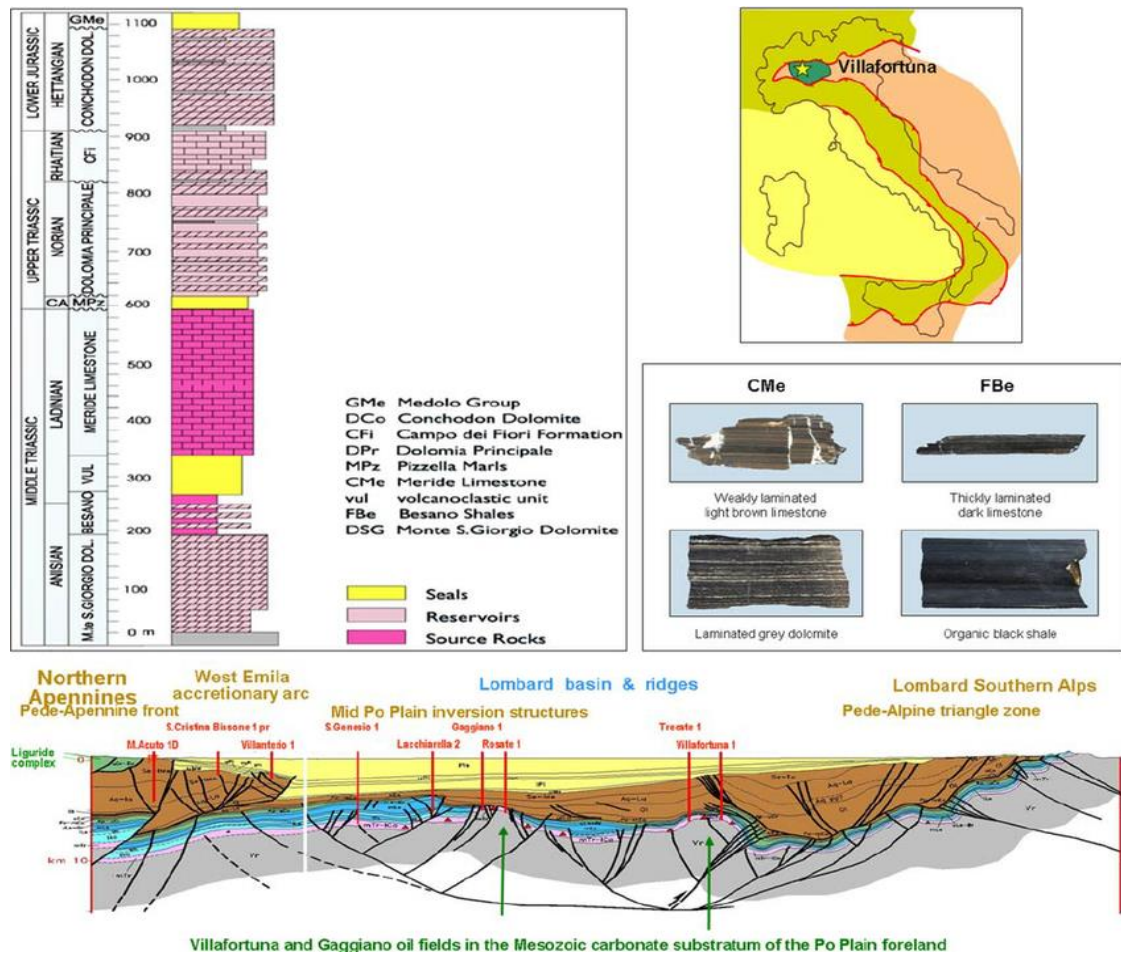


Figure 4 Villafortuna –Trestate oil field: geological sections and major hydrocarbon occurrences (vertical exaggeration 2:1) (Bertello et al., 2010).

The hydrocarbons were generated from Middle Triassic source rock formations, namely the Besano Shales (Anisian/Ladinian) and the Meride Limestone (Ladinian) (Fantoni et al. 2004).

The Late Triassic–Early Jurassic petroleum system (**Gela Field**) is linked to the main phase of the Tethyan rifting and is the most explored of the three systems, both in the foreland and in the thrust belt, and from Lombardy to Sicily. The source rocks are terrigenous or mixed carbonate/terrigenous, and they were deposited during the anoxic stage that preceded the extension of the Jurassic basins. Because of the discontinuity of the regional and local seals, the reservoirs are located in a wide chronostratigraphic range, from the coeval platform units up to the topmost carbonate units and even in the overlying terrigenous sequences (Nilde Field, Miocene, Sicily) (Bertello et al., 2010).

The Gela heavy oil field, discovered in 1956, is a remarkable example of the Late Triassic–Early Jurassic system. Its geological framework is illustrated in Figure 5.

The Gela field is located in the Ragusa Basin, in the southern part of Sicily, and extends both onshore and offshore. It represents the most significant oil accumulation of this petroleum system. The main reservoir is the Upper Triassic Sciacca Formation, consisting of dolomitized carbonate platform rocks. The Sciacca Formation is overlain by the Upper Rhaetian Noto Formation, composed of alternating laminated carbonates and euxinic shales. On top of the Noto Formation lies the shale and shaly limestone Hettangian Streppenosa Formation, which constitutes a regional seal with moderate source rock characteristics (Miuccio et al., 2000; Bertello et al., 2010 (Bertello, Fantoni, Franciosi, Gatti, Ghielmi, & Puglise, 2010)).

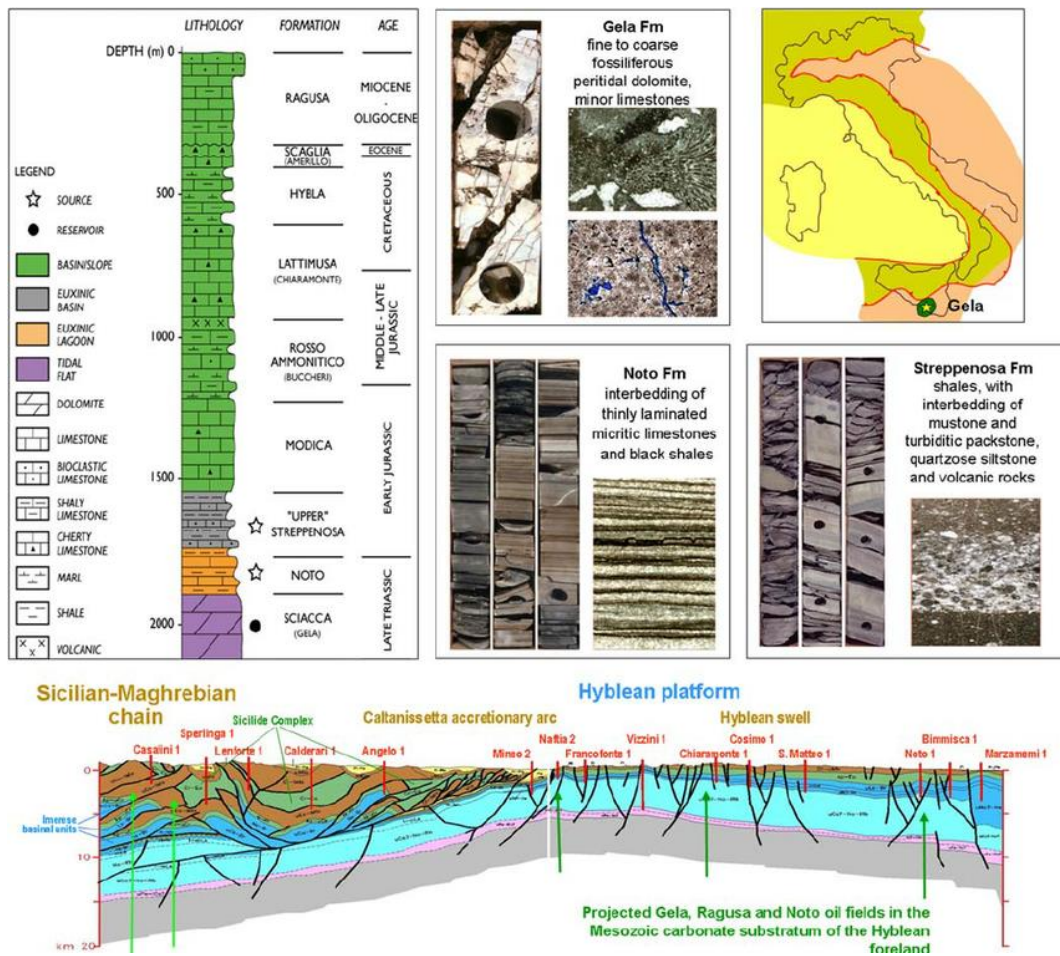


Figure 5 Gela oil field: geological sections and hydrocarbon occurrences (vertical exaggeration 2:1) (Bertello et al., 2010).

The Cretaceous petroleum system (**Val d'Agri Field**) lies in the Mesozoic carbonate substratum of the foredeep/foreland area and the external thrust belt of the southern Apennines. It bears the most significant oil and gas accumulations of Italy, namely the oil fields of Val d'Agri (composed by the Monte Alpi, Monte Enoc, and Cerro Falcone culminations) and Tempa Rossa. Because of the low permeability of its reservoirs, the Cretaceous play is most successfully explored in the highly fractured frontal structures of the thrust belt (e.g., Val d'Agri and Tempa Rossa oil fields).

The Val d'Agri giant oil field, discovered in 1988, is the most considerable oil accumulation of the Cretaceous petroleum system (Fig.6) (Bertello et al., 2010).

The reservoir is represented by the Cretaceous to Miocene limestone and dolostone of the Apulian Platform. The sedimentary evolution of this succession is complex and can be summarized, from the bottom to the top, as follows. The Early Cretaceous (Neocomian and Aptian) is characterized by a thick succession of shallow-water dolomitic limestones deposited in a restricted platform environment. The deposition of a less restricted Albian platform facies precedes the formation of intra-platform basins that developed during the Cenomanian within the Apulian Platform due to an important phase of extensional/trans-tensional tectonics (Carannante et al., 2009). These basins were probably NW–SE oriented and hosted the deposition of organic-rich laminites that constitute the source rock of this petroleum system.

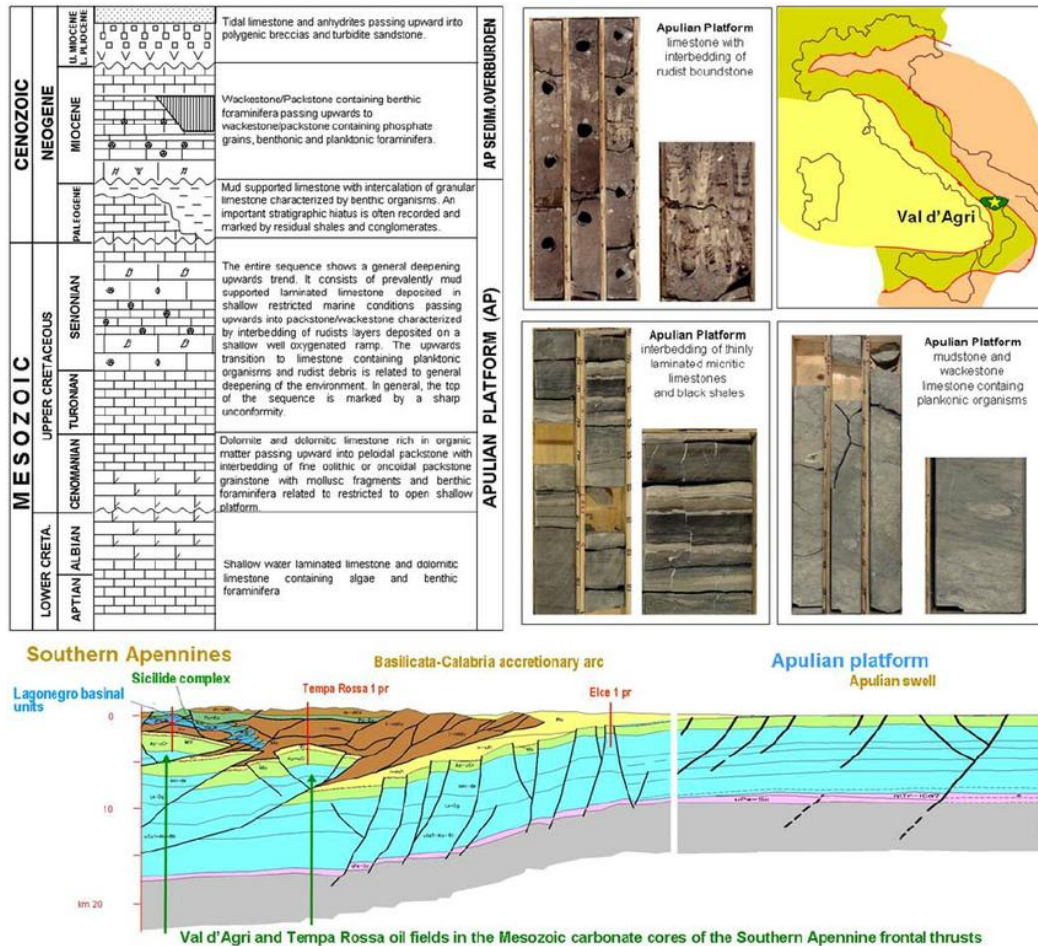


Figure 6 Val d'Agri oil field: geological sections and significant hydrocarbon occurrences (vertical exaggeration 2:1) (Bertello et al., 2010).

3.1.2 Thermogenic gas in the thrust terrigenous Oligo-Miocene foredeep sedimentary wedges

According to what was reported by Bertello et al., 2010, the Oligo-Miocene petroleum system is characterized by turbidite foredeep sedimentary wedges of the Southern Alps and the Apennines. Their successions have been tectonically involved in the thrust belts of the two chains (Fig.7).

The main hydrocarbon phase is thermogenic gas with minor amounts of condensate and light oil. The traps are usually structural. Gas occurrences related to this petroleum system have been found in the Southern Alps and the northern Apennines (e.g., Cortemaggiore and Casteggio fields), but the most important discoveries were made in the southern Apennines, in Calabria (Luna Field) and Sicily (Gagliano, Bronte and Fiumetto fields).

3.1.3 Biogenic gas in the terrigenous Plio-Pleistocene foredeep wedges

Biogenic gas fields were also found in the Plio-Pleistocene successions of the late Apennine foredeep depocentres and the outer fronts of the Apennine thrust belt, in the Po Plain, in the northern and central Adriatic Sea, in southern Italy and Sicily (Fig.7). These successions mainly consist of some thousands of meters of sand-rich turbidites (Minervini et al., 2008; Ghielmi et al., 2012; Bertello et al., 2010).

The Plio-Pleistocene clays interbedded in the turbidite successions represent the source-rock and the effective vertical seal. The derived hydrocarbon phase is biogenic gas, and the gas generation and expulsion started immediately after deposition. Exceptionally, the reservoirs may consist of Messinian conglomerates and sandstones sealed by Lower Pliocene clay (e.g., Sergnano Field, Po Plain area) or of Cretaceous Apulian Platform carbonates (e.g., Cupello and Ferrandina fields, Bradanic Foredeep).

The biogenic gas is mixed with minor amounts of thermogenic gas generated by older and deeper source rocks in these reservoirs.

The exploration of the biogenic play started during the late 1940s in the central Po Plain and progressively moved southeastward and offshore. The most important discoveries occurred in the Adriatic Sea, where hundreds of seismic bright spots were successfully tested. Among them, the Barbara gas field stands out for its giant size.

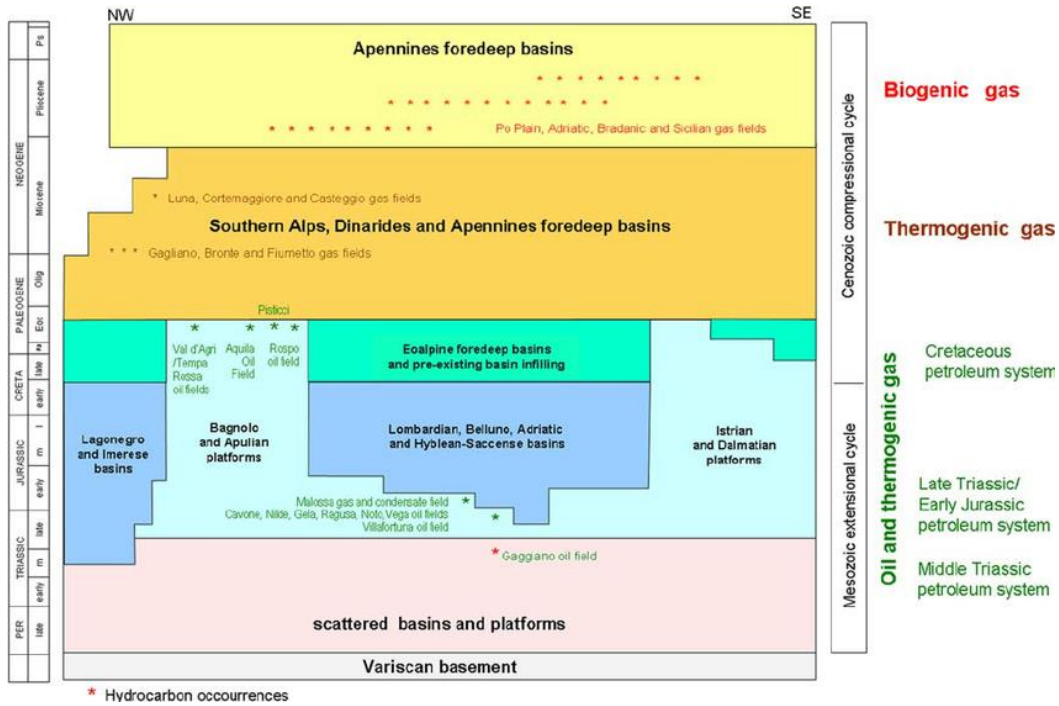


Figure 7 Tectono-stratigraphic cycles and hydrocarbon occurrences (from Bertello et al., 2010).

3.2 Hydrocarbon wells in Italian petroleum systems

As described in Chapter 3.1, Italian hydrocarbon occurrences are associated with carbonate and siliciclastic reservoir rocks, ranging in age from the Triassic to the Paleogene and from the Oligocene to the Pleistocene, respectively, distributed in thrust belt, foredeep basin, and foreland geological settings. As one of the countries with the wealthiest abundance of evidence of hydrocarbon seepages, the populations that have inhabited the Italian country during the various historical periods took advantage of these phenomena, harvesting oil and bitumen from the surface.

Cazzini (2018) provided a synthetic history of the Italian upstream oil and gas industry from its early start until today. The oil and gas production in Italy can be considered negligible before World War II. For this reason, the statistics start from 1944 until the last release of official data. According to the information available, during the late 1990s, Italy reached a remarkable total oil and gas production of close to 500 MBOE/day. The gas peak was reached in 1994 with almost 21 Bcm/year, representing 40% of the total national gas consumption (Fig.8a-b).

Compared to the peak consumption recorded in 2005 (196.1 Mtoe), Italy's energy demand in 2020 fell by more than a quarter (-26%). The overall reduction of about 15 Mtoe of energy demand in comparison with the 2019 values derives mainly from the collapse of the oil one, which has paid the most for the effects of the pandemic with a decrease of over 16% in 2019 (-9.2 Mtoe). In 2020, oil satisfied around 33% of the Italian energy demand.

Natural gas in 2020 marks a decline of 4.4% (58.3 Mtoe), substantially deriving from the lower thermoelectric production, consequent to the holding of production from renewable sources and the reduction in electricity demand. With a weight of 40% strengthening its position as the first Italian energy source, having widened the difference in weight by seven percentage oil points (UNEM, 2021).

Updated information regarding the national production rates of hydrocarbons and the relative shares distributed by Italian regions and marine areas are available on the institutional site of the Ministry of Economic Development.

Besides, the National Mining Office of the Italian Ministry for Economic Development (MISE) provides information and data regarding productive oil and gas wells and hydrocarbon and gas storage licenses in Italy.

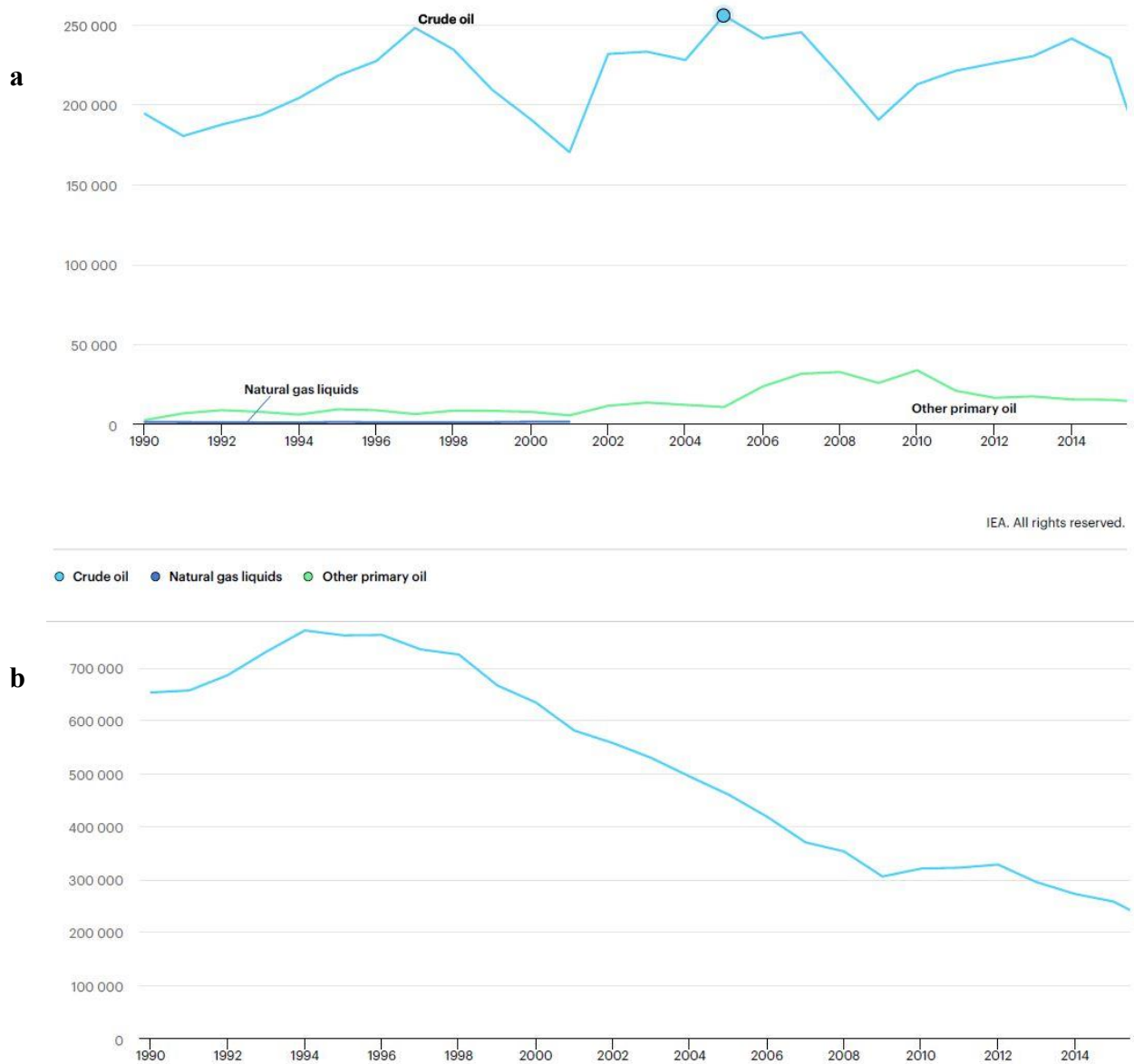


Figure 8 a. Oil production in EJ (Exajoule), Italy 1990-2020 **b.** Natural gas production in TJ-gross (Terajoule), Italy 1990-2020 (Data from IEA, 2020).

Following the data provided by MISE (2021) and progressively collected within the ViDEPI Project, at the end of September 2021, 8110 hydrocarbon wells are registered

and located on the Italian territory: 673 of these are currently productive - supplying wells. These productive wells are now used to extract hydrocarbons from the reservoir. 249 are the mining licenses for the exploration and cultivation of hydrocarbons presently registered and available for consultation (Figs.9 - 11).

3.2.1 ViDEPI Project: petroleum exploration data in Italy

The ViDEPI project², created through a collaboration between the Ministry for Economic Development UNMIG, Assomineraria and the Italian Geological Society, aims to make technical documents relating to oil exploration in Italy accessible. The available documentation concerning discontinued mining licenses and, therefore, public was deposited starting from 1957 at the UNMIG (National Mining Office for Hydrocarbons and Geothermal Energy) of the Ministry of Economic Development.

On the ViDEPI project-site, all interested researchers can access technical documents of a public nature relating to the exploration of Italian oil since 1957, deposited by the operators, in accordance with the law, with the competent mining authorities. The oil exploration activity in Italy is governed by the Law of 11 January 1957, no.6, which established UNMIG, the National Mining Office for Hydrocarbons and Georesources belonging to the Directorate General for Mineral and Energy Resources, with headquarters at the Ministry of Economic Development and peripheral offices in Bologna, Rome and Naples.

The Italian legislation establishes that the operating companies of the individual mining titles must provide the UNMIG with progressive technical reports on the activity carried out in the same tags, including copies of exemplary documents, such as geological maps, structural maps, final profiles of wells, seismic lines, etc. The same law provides that the documents delivered become publicly available after one year from the termination of the title for which they were produced.

In more than half a century, an essential database concerning the subsoil of Italian territory has been produced:

² <https://www.videpi.com/videpi/videpi.asp>

- 625 files of discontinued mining licenses;
- 230 technical reports;
- 846 attachments;
- 299 final well profiles;
- 578 seismic lines of the seismic recognition campaign of marine areas;
- 70 seismic lines of the CROP Atlas project;
- 396 seismic lines acquired in discontinued mining rights.

ViDEPI project database consists of technical information and related reports. A list of 2305 well logs (on-shore and Off-shore wells) with consultable profiles is available. Besides, data about wells listed by mining permit or concession can be found. Seismic lines acquired in expired mining permits and concessions are also downloadable and present as attachments to the technical reports listed in the technical documentation (Figs.12 - 13).

Data relating to hydrocarbon wells' geographical position, depth, construction features available, together with the stratigraphic information obtained from the analysis of the geological and seismic section, are found to be useful to properly characterise the case studies analysed (i.e., Villafortuna 1, Trecate 4, Tempa Rossa 1D, Gela 38 hydrocarbon wells).



Figure 9 Italian research permits and cultivation concessions (Data from WebGIS UNMIG. Ministero dello Sviluppo Economico).



Figure 10 Italian hydrocarbon wells location (Data from WebGIS UNMIG. Ministero dello Sviluppo Economico).

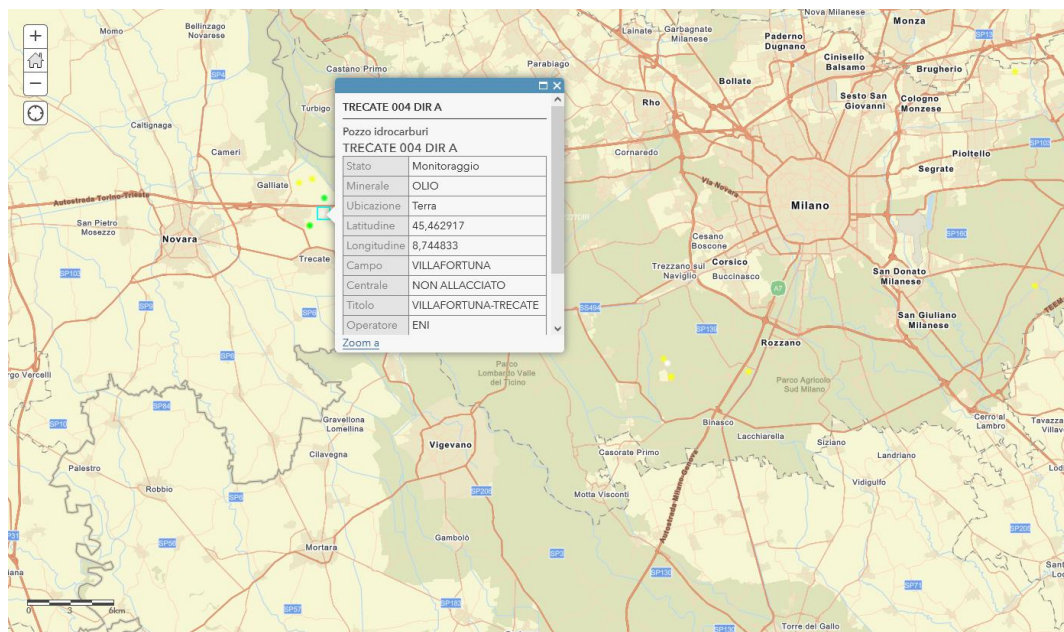


Figure 11 Trecate 004 hydrocarbon well location (Data from WebGIS UNMIG. Ministero dello Sviluppo Economico).

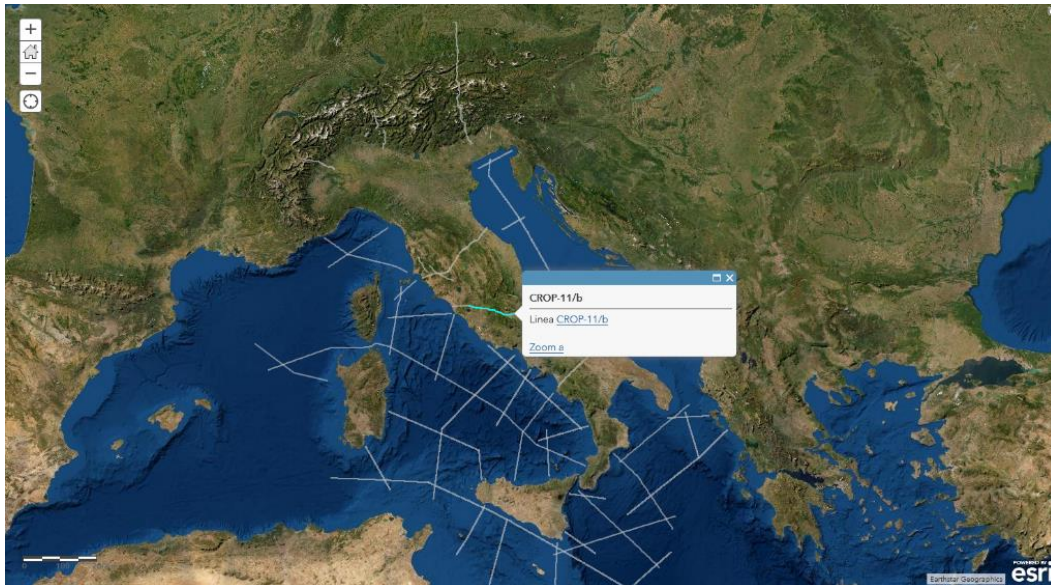


Figure 12 Seismic line of the CROP-11/b Atlas project (from VIDEPI Project UNMIG. Ministero dello Sviluppo Economico).

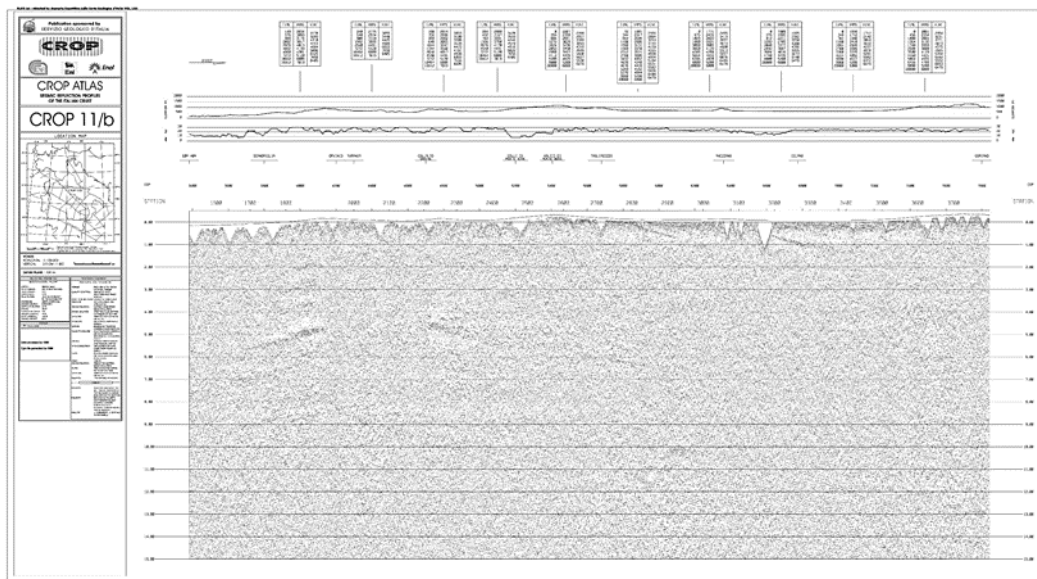


Figure 13 Seismic profile of the CROP-11/b Atlas project (from VIDEPI Project UNMIG. Ministero dello Sviluppo Economico).

Chapter 4

Geothermal Energy

4.1 Classification of geothermal energy resources

The term geothermal energy refers to the portion of the Earth's thermal energy that we can access, bring to the Earth's surface, and use for our purposes (Allansdottir et al., 2019). By 1870 modern scientific methods were being used to study the Earth's thermal regime. Still, it was not until the twentieth century and the discovery of the role of radiogenic heat that researchers could comprehend such phenomena as heat balance and the Earth's thermal history. All modern thermal models of the Earth must take into account the heat continually generated by the decay of the radioactive isotopes of uranium (U^{238} , U^{235}), thorium (Th^{232}), and potassium (K^{40}) (Lyubimova, 1968). In uncertain proportions, other potential heat sources are added to radiogenic heat, such as the primordial energy of planetary accretion. Estimates from more than thirty years ago gave the total heat content of the Earth, calculated above an assumed average surface temperature of $15^{\circ}C$, in the order of 12.6×10^{24} MJ, and that of the crust in the order of 5.4×10^{21} MJ (Armstead, 1983). Besides, geophysical data indicates the average temperature of 99% of the Earth's volume at about $1000^{\circ}C$, while the remaining 1% is characterized by an average temperature of $<100^{\circ}C$.

The emission of terrestrial heat does not occur uniformly, ranging from about 65 mW/m^2 to 101 mW/m^2 , respectively, in continental and oceanic areas (Davies, 2013).

Through the term geothermal gradient, geologists express the variation in temperature with depth that depends on the local heat flow and thermal conductivity of the rocks. The highest values, $40\text{--}80\text{ }^{\circ}\text{C km}^{-1}$, are observed in volcanic areas or where the crust is particularly thin and hot, e.g. in mid-oceanic ridges or where magma is close to the surface (Arndt et al., 2011). In subduction zones or stable continental areas, the gradient is the lowest possible, on average around $20\text{--}30\text{ }^{\circ}\text{C km}^{-1}$. Down to the depths accessible by drilling with modern technology (about 10.000 m), the average geothermal gradient is about $2.5\text{--}3^{\circ}\text{C}/100\text{ m}$. Whereas the temperature within the first few meters below ground level, which on average corresponds to the mean annual temperature of the external air, is about 15°C (Dickson & Fanelli, 2020) (Figs.14 - 15).

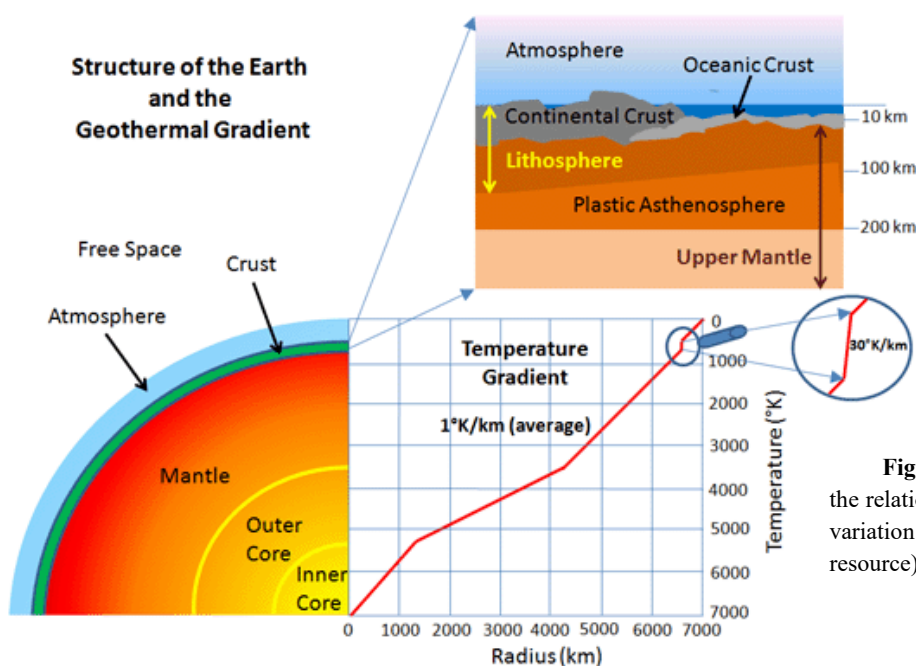


Figure 14 Simplified representation of the relationship between Earth's structure and variation of the Geothermal Gradient (Online resource).

The propagation of the heat flow from the inside of the Earth's crust occurs through conductive and convective processes. Over time, it was demonstrated that there exist areas where deep rock basement has undergone rapid sinking and the basin is filled with geologically young sediment in which the geothermal gradient is far from the average value (lower than $1^{\circ}\text{C}/100\text{ m}$). In contrast, the geothermal gradient value in specific

geological contexts (geothermal areas) is more than ten times the average value reported above.

Geothermal resources are classified on basis of heat source, heat transfer, reservoir temperature, physical state, utilization and geological settings. They can occur as the heat associated with surface emissions of steam, hot water over a wide range of temperature or as the thermal energy available at various depths below the Earth's surface. Resource classification is a key element in the characterization, assessment and development of geothermal energy.

The most common criterion for classifying geothermal resources is based on the concept of enthalpy of the characterizing geothermal fluids that act as the carrier, transporting heat from the deep hot rocks to the surface. Enthalpy, which can be considered proportional to temperature, is used to express the thermal energy content of the fluids. The geothermal resources can be divided into *low* (<90°C), *medium* (90-150°C) and *high* (> 150°C) *enthalpy resources*, according to criteria that are generally based on the energy content of the fluids and their potential forms of utilization (Muffler & Cataldi, 1978) (Tab.1).

Table 1 Geothermal energy resources classifications (Muffler & Cataldi, 1978)

	<i>Muffler and Cataldi (1978)</i>	<i>Hochstein (1990)</i>	<i>Benderitter and Cormy (1990)</i>	<i>Nicholson (1993)</i>	<i>Axelsson and Gunnlaugsson (2000)</i>
Low Enthalpy resources	< 90	< 150	< 100	≤ 150	≤ 190
Intermediate Enthalpy resources	90 ÷ 150	125 ÷ 225	100 ÷ 200	-	-
High Enthalpy resources	> 150	> 225	> 200	> 150	> 190

Besides, based on the depth and the heat (temperature) required, the Swiss Seismological Service (SED) has classified geothermal energy into two main types of resources: Shallow Geothermal Energy and Deep Geothermal Energy.

- ***Shallow Geothermal Energy***

The energy at depths lower than 400 meters below the Earth's surface, having temperature values varying between 8°C and 20°C.

- ***Deep Geothermal Energy***

The energy at a depth of at least 400 meters below the Earth's surface, having temperatures varying between 20°C and 200° C. The temperature is between 20°C and 70°C at a depth of 400 to 2000 meters, and thermal water is found at these depths that can be used for bathing and heat production. At deeper depths of 4000 meters, the temperature is found to be in the range of 150°C to 200°C, which uses some part of this energy for power (electricity) generation and the remaining for district heating.

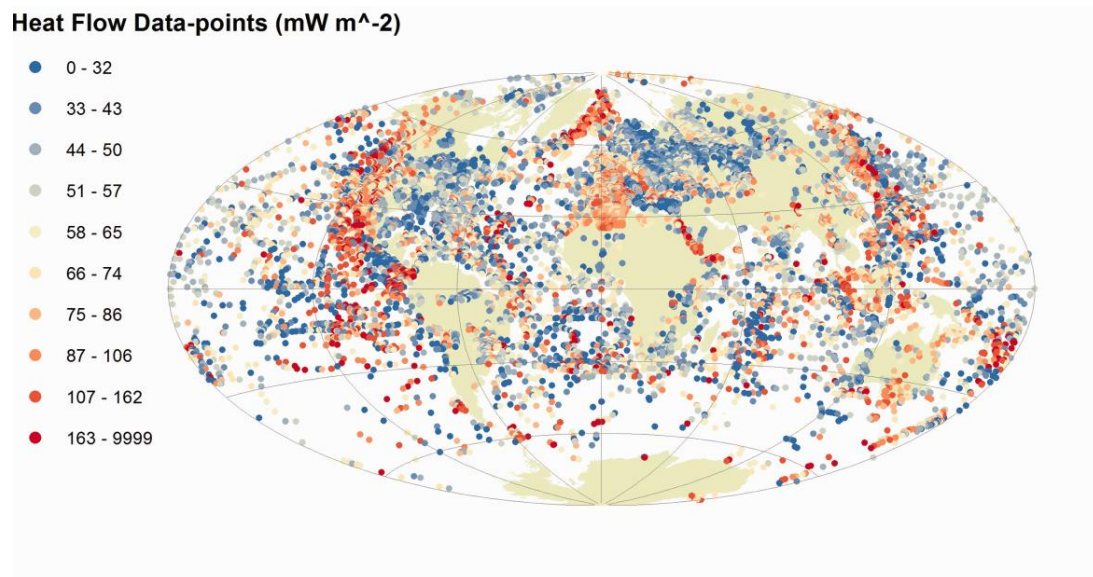


Figure 15 Map of heat flow measurement points (Davies, 2013).

Considering the Italian regulation, the Legislative Decree No. 22/2010 states that geothermal energy qualifies as mineral resources that fall under the non-disposable patrimony of the Italian State or of the relevant region depending on the national or local interest of such resources. It regulates the research and management of geothermal resources and defines the different geothermal resources based on temperature ranges of characterizing fluids: high enthalpy resources (fluid temperature $>150\text{ }^{\circ}\text{C}$) are considered of national interest, heritage of state, whereas medium (fluid temperature of $90\text{--}150\text{ }^{\circ}\text{C}$) and low enthalpy (fluid temperature $<90\text{ }^{\circ}\text{C}$) resources are declared of local interest (Pellizzone et al., 2019).

Geothermal energy has usually been classified as clean, renewable and sustainable. Renewable describes a property of the considered energy source, whereas sustainable describes how the resource is used. The most critical aspect of considering geothermal energy as a renewable energy source is the rate of energy recharge. In exploiting natural geothermal systems, energy recharge takes place by advection of thermal water at the same time scale as production from the resource. This recharge modality justifies our classification of geothermal energy as a renewable energy resource.

In contrast, in the case of hot, dry rocks, and hot water aquifers in sedimentary basins, energy recharge is only by thermal conduction. Due to the slowness of the latter process, however, these types of reservoirs should be considered as finite energy resources (Axelsson & Stefansson, 2003). Considering what has been described, it is essential to accurately know its nature, geological characteristics, and energy recharge modalities to exploit a type of geothermal system correctly. Besides, identifying the geological features of a potentially available geothermal field is increasingly necessary for elaborating energy production scenarios in areas where it is currently not possible to exploit other types of renewable resources. The investigation and assessment of geothermal resources rely not only on direct underground geological data, mainly from wells, but also require their integration with indirect sources, from geochemical and geophysical surveys and remote sensing data.

The characteristics of the source or geothermal field influence the choice of geothermal exploitation technology for the production of electricity, for the direct use of heat for

civil services (residential heating/cooling, district heating), for agricultural and industrial processes.

4.1.1 Direct and indirect uses of geothermal energy resources

Depending on their temperature ranges, geothermal energy resources can have several types of direct (i.e., district heating, domestic heating and/or cooling of small and medium buildings, agricultural and zootechnical uses, industrial uses, thermal uses) and indirect uses (i.e., electricity generation).

The main areas of application of geothermal technologies, based on the type of geothermal resource exploited, can be summarized as follows:

- Production of electricity and direct use of heat through the exploitation of hydrothermal systems, or hot fluids from underground aquifer systems (*Deep Geothermal Energy Resources*)

- Direct use of heat through the use of geothermal heat pumps (GSHP, Ground-Source Heat Pump) that take advantage of the thermal stability of the subsoil within 200m depth (*Shallow Geothermal Energy Resources*).

Technologies for traditional geothermal energy direct uses like district heating, geothermal heat pump systems are already used in urban areas, especially in temperate climate zones (Violante & Guidi, 2020).

High-temperature geothermal resources are generally used for electricity production, such as hydrothermal steam and dominant water reservoirs (Fig.16).

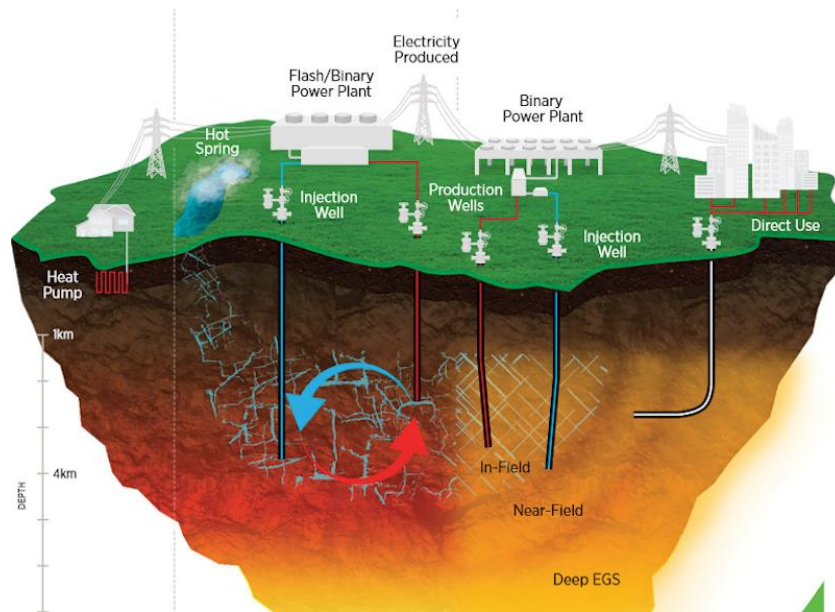


Figure 16 Geothermal energy overview (from GeoVision report by the U.S. DOE).

The various possible applications of geothermal resources, together with the corresponding temperature demand, are illustrated by the Lindal diagram reported in Fig.17 (Kaczmarczyk et al., 2020). By a cascading exploitation mode of the available heat, researchers intend a multi-variant and extensive use of the resource. As shown in Fig.17, depending on specific geological, hydrogeological, and thermo-physical conditions such as temperature, flow rate, and geothermal waters mineralisation, prevailing in an area to be analysed, there are several possibilities for the industrial and economic utilisation of the heat energy accumulated (Gizzi, 2021).

The possible uses range from the electricity generation to the use of heat for the air conditioning of environments, for thermal purposes, for agricultural services (heating greenhouses, pasteurization of dairy products, drying and fermentation of food products), aquaculture, and for uses industrial, up to the use of the so-called low-temperature geothermal energy.

- ***Electricity generation***

Electricity generation mainly occurs in **conventional steam turbines** and **binary plants**, depending on the geothermal resource's features.

Conventional steam turbines require fluids at a temperature of at least 150°C and are available with either atmospheric (backpressure) or condensing exhausts. The steam, direct from dry steam wells or, after separation, from wet wells, is passed through a turbine and exhausted into the atmosphere. Generating electricity from low-to-medium temperature geothermal fluids and the waste hot waters from the separators in water-dominated geothermal fields have made considerable progress since binary fluid technology improvements have been made. The binary plants utilize a secondary working fluid, usually an organic fluid, with a low boiling point and high vapour pressure at low temperatures compared to steam. The secondary fluid is used through a Conventional Organic Rankine Cycle (ORC): the geothermal fluid yields heat to the secondary fluid through heat exchangers, in which this fluid is heated and vaporizes; the vapour produced drives a typical axial flow turbine, which is then cooled and condensed, and the cycle begins again. By selecting suitable secondary fluids, binary systems can be designed to utilize geothermal fluids in the temperature range 85-175°C.

- ***Direct heat uses***

Direct heat use is one of the oldest, most versatile, and most common ways of using geothermal energy. Space and district heating, agricultural applications, aquaculture, and industrial uses are the best known and most widespread forms of utilization. Still, other forms are already in use or in the late planning stages. Geothermal district heating systems are capital intensive. The main costs are initial investment costs for production and injection wells, downhole and transmission pumps, pipelines and distribution networks, monitoring and control equipment, peaking stations, and storage tanks. Operating expenses, however, are comparatively lower than in conventional systems and consist of pumping power, system maintenance, control, and management. A crucial factor in estimating the system's initial cost is the thermal load density or the heat demand divided by the ground area of the district. A higher heat density determines the economic feasibility of a district heating project since the distribution network is expensive. Some economic benefits can be achieved by combining heating and cooling

in areas where the climate permits. The load factor in a system with integrated heating and cooling would be higher than the factor for heating alone, and the unit energy price would consequently improve (Allahvirdizadeh, 2020).

Geothermal space conditioning (heating and cooling) has expanded considerably since the 1980s, following the introduction and widespread use of heat pump systems. Ground-Source Heat Pump systems (GSHPs) represent one of the most promising high-efficiency technologies in the heating and cooling of the building sector. GSHPs use the ground, ground or surface water resources as a heat source/sink to provide space heating and cooling and domestic hot water. This technology can offer higher energy efficiency for air-conditioning than conventional air-conditioning (ASHP) systems because the underground environment provides higher temperature for heating and lower temperature for cooling, experiencing less temperature fluctuation than ambient air temperature change (Sarbu & Sebarchievici, 2014).

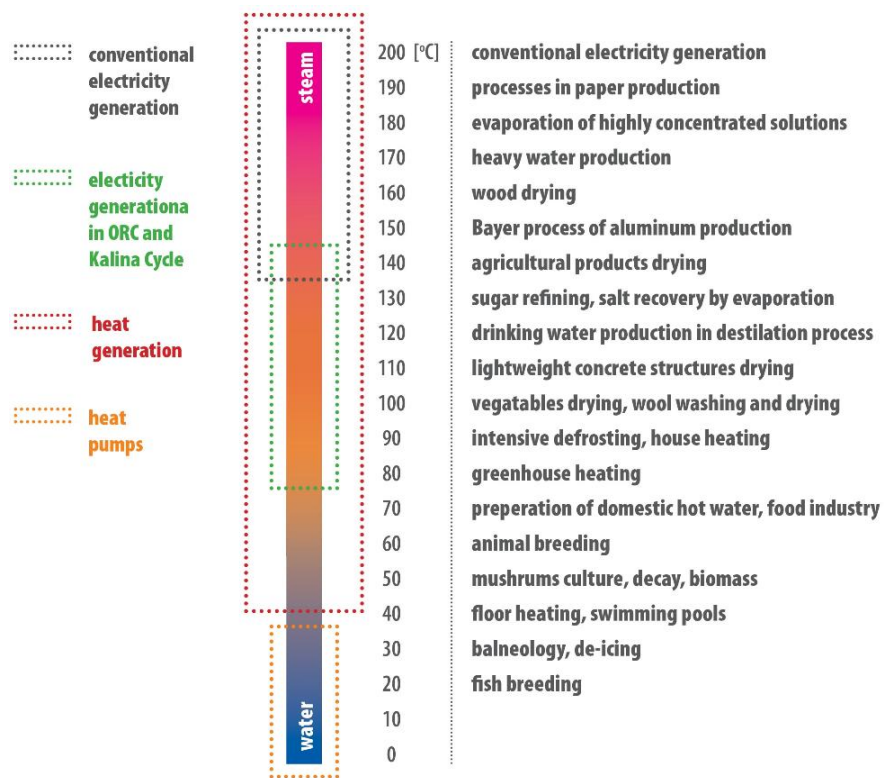


Figure 17 Modified Lindal diagram (Gudmundsson et al., 1985; Operacz and Chowaniec, 2018).

From a technological point of view, a GSHP system, in addition to the different types of external heat exchangers through which heat is absorbed or transferred to the ground or a mass of water (earth connection subsystem), includes two other main components: a heat pump subsystem, a heat distribution subsystem (Fig.18).

The agricultural applications of geothermal fluids consist of open-field agriculture and greenhouse heating. Thermal water can be used in open-field agriculture to water and/or heat the soil.

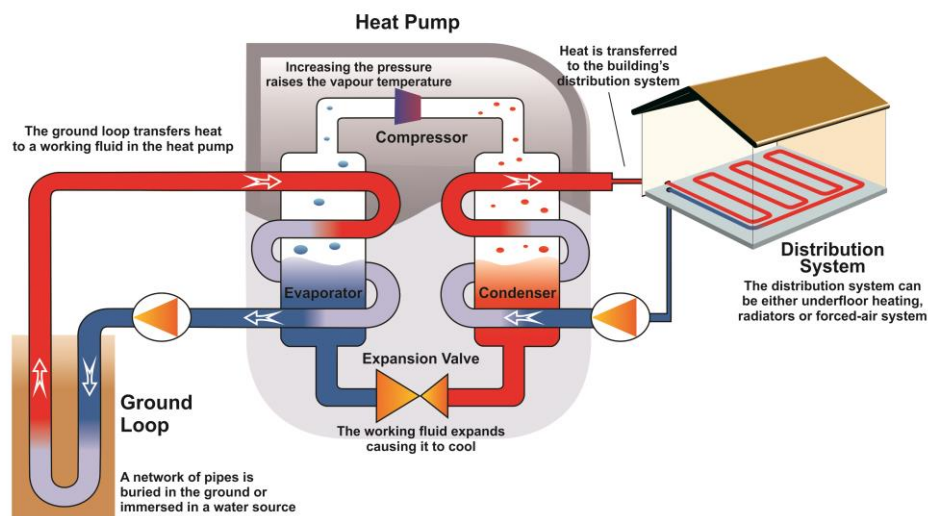


Figure 18 Ground source heat pump (GSHP) system schematic diagram (from Moon et al., 2019).

The main advantages of temperature control in open-field agriculture are: (a) to prevent any damage ensuing from low environmental temperatures, (b) to extend the growing season, increase plant growth, and boost production, and (c) to sterilise the soil (Barbier & Fanelli, 1977). However, the most common application of geothermal energy in agriculture is greenhouse heating, which has been developed on a large scale in many countries. Planting vegetables and flowers out-of-season or in an unnatural climate can now draw on a widely experimented technology. Various solutions are available for achieving optimum growth conditions, based on the optimum growth temperature of each plant (Fig.19), and the quantity of light, the CO₂ concentration in the greenhouse environment, the humidity of the soil and air, and on-air movement. The exploitation of

geothermal heat in greenhouse heating can considerably reduce their operating costs, which in some cases account for 35% of the product costs (vegetables, flowers, house plants, and tree seedlings) (Beall & Samuels, 1971).

Farm animals and aquatic species, and vegetables and plants can benefit in quality and quantity from optimum conditioning of their environmental temperature. In many cases, geothermal waters could be used profitably in a combination of animal husbandry and geothermal greenhouses. The energy required to heat a breeding installation is about 50% of that needed for a greenhouse of the same surface area so a cascade utilization could be adopted. Breeding in a temperature-controlled environment improves animal health, and the hot fluids can also be utilised to clean, sanitize and dry the animal shelters and waste (Barbier & Fanelli, 1977).

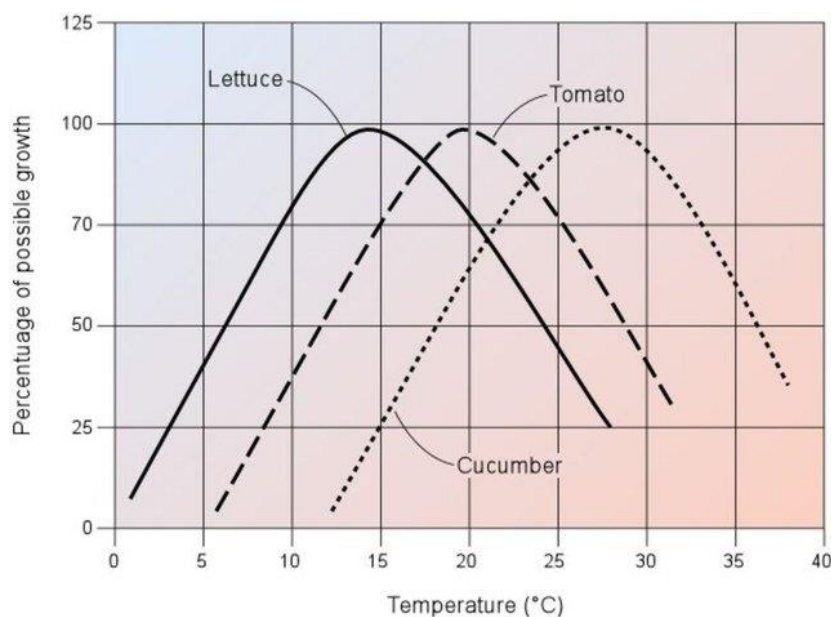


Figure 19 Growth curves for some crops (from Beall and Samuels, 1971)

As described by Barbier & Fanelli, 1977, aquaculture, the controlled breeding of aquatic forms of life, is gaining worldwide importance due to increasing market demand. Control of the breeding temperatures for aquatic species is of a greater extent than for land species. By maintaining an optimum temperature artificially, we can breed more exotic species, improve production, and even, in some cases, double the reproductive cycle. The typically raised species are carp, catfish, bass, tilapia, mullet, eels, salmon,

sturgeon, shrimp, lobster, crayfish, crabs, oysters, and clams scallops, mussels and abalone.

Eventually, as shown in the Lindal diagram in Fig.17, the entire temperature ranges of geothermal fluids, whether steam or water, can be exploited for industrial applications: heating, evaporation, drying, distillation, sterilization, washing, de-icing, salt, and chemical extraction, as well as oil recovery processes.

Industrial process heat has applications in 19 countries, where the installations tend to be large and energy consumption high. Examples include concrete curing, bottling of water and carbonated drinks, paper and vehicle parts production, oil recovery, milk pasteurization, leather industry, chemical extraction, CO₂ extraction, mushroom growing, and laundry use, salt extraction, and diatomaceous earth drying, pulp and paper processing, and borate and boric acid production (Lund, 2010; Lund & Toth, 2021).

The information reported below on the topic of direct applications of geothermal heat was extracted from the proceedings of World Geothermal Congress, 2020 (Lund & Toth, 2021), based on country update papers submitted and covering the period 2015-2019. In Table 2, it was summarized, by region and continent, the installed thermal capacity (MWt), the annual energy use (TJ/yr and GWh/yr), and the capacity factors through 2019. The total installed capacity, reported at the end of 2019 for direct geothermal utilization worldwide, is equal to 107,727 MWt, with a percentage increase of 52% over WGC, 2015. The total annual energy use is 1,020,887 TJ (283,580 GWh), indicating a 72.3% increase over WGC, 2015 and a compound annual growth rate of about 11.5%. The growth rates of installed capacity and annual energy use over the past 30 years are summarized in Figure 20.

Table 2 Summary of direct-use data worldwide by region and continent, 2019 (Modified from Lund & Toth, 2021)

Region/Continent	MW _t	TJ/year	GWh/year	Capacity Factor
Africa (11)	198	3,730	1,036	0.597
Americas (17)	23,330	180,414	50,115	0.245
Central America and Caribbean (5)	9	195	54	0.687
North America (4)	22,700	171,510	47,642	0.24
South America (8)	621	8,709	2,419	0.445
Asia (18)	49,079	545,019	151,394	0.352
Commonwealth of Independent States (5)	2,121	15,907	4,419	0.238
Europe (34)	32,386	264,843	73,568	0.259
Central and Easter Europe (17)	3,439	28,098	7,805	0.259
Western and Northern Europe (17)	28,947	236,745	65,762	0.259
Oceania (3)	613	10,974	3,048	0.568
Total (88)	107,727	1,020,887	283,580	0.300

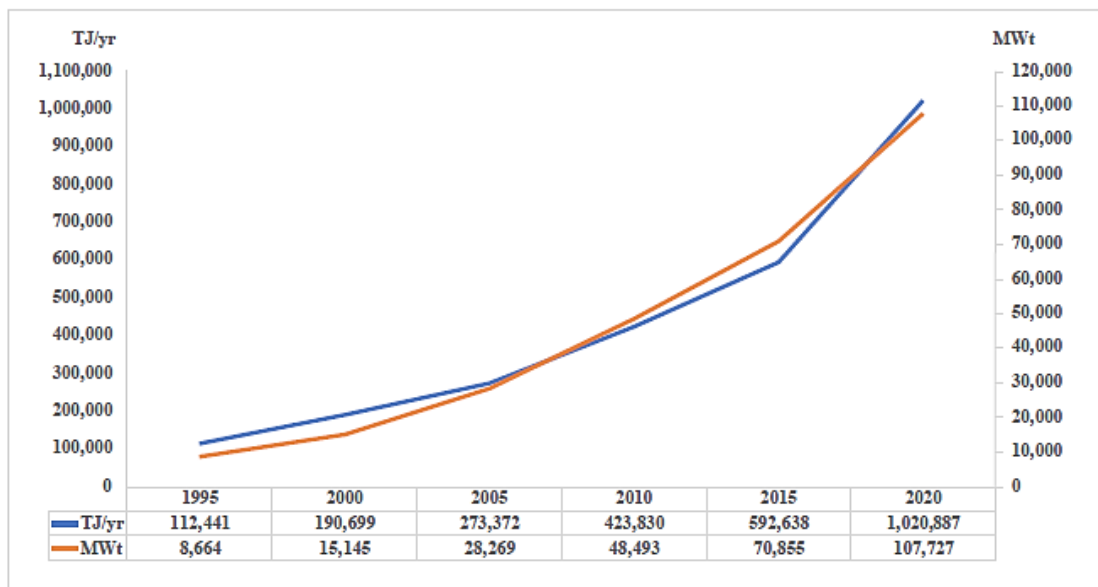


Figure 20 Worldwide installed direct-use geothermal capacity and annual utilization from 1995-2020 (from Lund & Toth, 2021).

Geothermal heat pump systems

Geothermal GSHPs have the most considerable geothermal use worldwide, accounting for 71.6 % of the installed capacity and 59.2 % of the annual energy use. The installed capacity of 77,547 MWt, and the energy use is 599,981 TJ/yr. Although most of the installations occur in North America, Europe, and China, the number of countries with installations increased from 26 in 2000 to 33 in 2005, 43 in 2010, 48 in 2015, and 54 in 2020. The equivalent number of installed 12 KW units (typical of USA and Western European homes) is approximately 6.46 million. This value represents a 54% increase over the number of installed units reported in 2015 and over twice the number of units registered in 2010. The size of individual units, however, ranges from 5.5 kW for residential use to large units over 150 KW for commercial and institutional installations. The leaders in installed units (MWt) are China, United States, Sweden, Germany, and Finland, accounting for 77.4 % of these units, and the leaders in energy produced (TJ/yr) are also: China, United States, Sweden, Germany and Finland accounting for 83.5 % of the output.

Space heating

Space heating, including individual space heating and district heating, has increased 68.0% in installed capacity and 83.8% in annual energy use over 2015 (Lund & Boyd, 2016). The installed capacity now totals 12,768 MWt, and the annual energy use is 162,979 TJ/yr. In 2019, the leaders in district heating in terms of both capacity and yearly energy use were China, Iceland, Turkey, France, and Germany. In contrast, in the individual space heating sector in installed capacity (MWt), Turkey, Russia, Japan, United States, and Hungary are leaders.

In the annual energy use (TJ/yr), the leaders were Turkey, Japan, Russia, the United States, and Switzerland. These five leaders account for about 90% of the world's total use in district heating and about 75% of the world's space heating.

Greenhouses and covered ground heating

Worldwide use of geothermal energy for greenhouse and covered ground heating increased by 24 % in installed capacity and 23 % in annual energy use. The installed capacity is 2459 MWt and 35,826 TJ/ yr in energy use. A total of 32 countries report geothermal greenhouse heating (compared to 31 from WGC, 2015). The leading countries in annual energy use (TJ/yr) are Turkey, China, Netherlands, Russia, and Hungary, accounting for about 83 % of the world's total.

The main crops grown in greenhouses are vegetables and flowers; however, tree seedlings, cacti, and fish in ponds (USA), and fruit such as bananas (Iceland) are also grown. Covered ground heating has been reported using geothermal heat pumps in Iceland (vegetables) and Greece (asparagus). Since labor is one of the high costs in this sector, developing countries have a competitive advantage compared with more developed countries. Using the average energy requirement determined from WGC, 2000 of 20 TJ/yr/ha for greenhouse heating, the 35,826 TJ/ yr corresponds to about 1791 ha of greenhouses heated worldwide – a 23.4 % increase over 2015.

Aquaculture pond and raceway heating

Aquaculture use of geothermal has increased over WGC, 2015, amounting to a 36.5 % increase in installed capacity and 13.5 % increase in annual energy use. The installed capacity is 950 MWt, and the energy use is 13,573 TJ/yr. Twenty-one countries report this type of use. The main ones in terms of annual energy use are China, United States, Iceland, Italy, and Israel – the same countries reported in WGC, 2015, accounting for 92 % of the annual use. Tilapia, salmon, bass, and trout seem the most common species cultivated, but tropical fish, lobsters, shrimp, and prawns, as well as alligators, are also being farmed.

Industrial process heat

This industrial process heat has applications in 14 countries. Examples of industrial processes that use geothermal heat include concrete curing (Guatemala and Slovenia), bottling of water and carbonated drinks (Bulgaria, Serbia and the United States), milk

pasteurization (Romania and New Zealand), leather industry (Serbia and Slovenia), chemical extraction (Bulgaria, Poland and Russia), CO₂ extraction (Iceland and Turkey), pulp and paper processing (New Zealand), iodine and salt extraction (Vietnam), and borate and boric acid production (Italy).

The installed capacity in 2019 was 852 MWt, and the energy use was 16,390 TJ/yr, an increase of 38.8% and 56.8%, respectively, compared to WGC, 2015.

Bathing and swimming

Despite almost every country having spas and resorts with swimming pools heated by geothermal water, including balneology, the treatment of diseases with water, related data are the most complicated information to collect and quantify. Actual usage and installed capacity data are challenging to find. There are known installations in Denmark, France, Mozambique, Nicaragua, Singapore, and Zambia for which no information was available. The most considerable reported annual energy uses for bathing and swimming are from China, Japan, Turkey, Brazil, and Mexico, accounting for 79.5 % of the annual use.

Other direct uses

This category includes animal husbandry, spirulina cultivation, de-salination, and sterilization of bottles. The most important use is in New Zealand, where it is applied in irrigation, frost protection, and a geothermal tourist park, followed by Japan (cooking) and Kenya (boiling water). Besides, Snow melting applications for streets and sidewalks operate in Iceland, Japan, Argentina, the United States, and Slovenia, and to a limited extent in Poland and Norway. An estimated 2.5 million square meters of pavement are heated worldwide, the majority in Iceland (74%). The installed capacity for snow melting is 415 MWt, and the energy use is 2,389 TJ/yr.

4.1.2 Direct uses of geothermal energy resources in Italy

Geothermal resources are abundant in Italy, ranging from those for shallow applications through the medium ($>90^{\circ}\text{C}$) to high ($>150^{\circ}\text{C}$) temperature systems. Italian geothermal resources potentially harnessable within 5 km depth are in the range of 21 Exajoule (about 500 million tonnes of oil-equivalent – MTOE). Two-thirds have temperatures below 150°C (Buonasorte et al., 2011) (Fig.22 a-c).

Resources at temperatures suitable for electricity generation ($T>80\text{-}90^{\circ}\text{C}$), at costs currently competitive with those of other energy sources, exist only in areas with intense heat flow anomalies: the Tuscany-Latium-Campania pre-Apennine belt, the two main Italian islands, and some volcanic islands of the Tyrrhenian Sea, all located in western and south-western Italy. Conversely, medium- and low-temperature resources ($T<80\text{-}90^{\circ}\text{C}$) suitable for direct uses are found not only in the above areas of high heat flow, but in many other zones. Additionally, using heat pumps, even resources at lower temperature ($T<30^{\circ}\text{C}$) and small depths could be exploited almost everywhere in Italy. Within accessible depths, Italy is endowed with geothermal resources of any kind and temperature in many significant areas, especially for direct uses (Buonasorte et al., 2011).

The exploitation of high-temperature geothermal energy resources for electricity production started at the beginning of the last century in the Larderello and Travale areas (Tuscany region). In the second half of the 20th, energy production activities were extended to several areas of new potential interest, located in the Tyrrhenian pre-Apennine belt of central-southern Italy and the Aeolian Islands. Enel and Agip performed these exploration activities in the Latium region in many areas North of Rome (Latera caldera, Vico Lake, Cesano, Bracciano Lake) and South of Rome (Alban Hills). In southern Italy, geothermal exploration was performed in Campania, the Phlegraean Fields and Ischia Island, and Sicily, Vulcano and Pantelleria. Unfavorable characteristics of the potential reservoirs (poor permeability, aggressive fluid, etc.), together with other logistical or environmental problems (urbanization, tourist nature of

zones, etc.), limited geothermal development in many of the reported areas (Bertini et al., 2005).

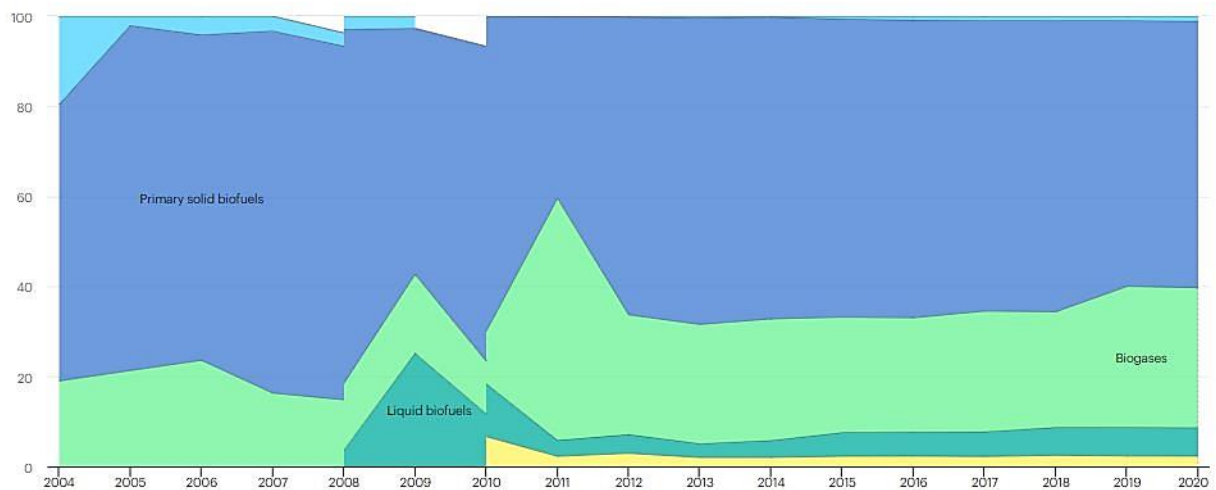
Non-electric uses of geothermal energy in Italy are mainly associated with the spa business, agricultural utilisations (greenhouses and fish farming) followed by space heating, including district heating (DH). Considering the direct-use geothermal areas, 37 sites are present in Italy, 5 of which are for district heating, 5 for individual space heating, one an industrial process site, 6 for fish farming, 4 for greenhouse heating, and 16 for swimming and bathing.

At the end of 2017, the **total installed capacity**³ exceeded 1400 MWth, with a corresponding heat utilization of 10915 TJ/yr. The main share of direct geothermal use turns out to be held by the **space heating sector** (42% of the total energy, 52% of the overall installed capacity), followed by **thermal balneology** (32% for both values) and **fish farming** (18% and 9% respectively). Agricultural applications, industrial processes, and other minor uses account for around 8% of the total geothermal use. Ground-source heat pumps (GSHPs) account for 38% of the installed capacity and some 30% in terms of energy. District heating (DH) systems represent about 8% of the total geothermal heat utilization. If we refer to the heating power available for the end-user systems (i.e., the condenser output), the nominal thermal energy of GSHPs is almost 780 MWth (Lund & Toth, 2021).

The major DH systems are located in Tuscany, within the geothermal electrical power production area. The fluid used to feed the DH networks is produced by the same deep wells feeding the power plants and is delivered as waste or valuable steam. The other main Italian geothermal DH application is in Ferrara, where a 14 MWth capacity system with two production wells of about 2 km depth produces pressurized hot water at almost 100°C, all of which is then reinjected into a third well. The other two systems are located in Milano, where ground-source heat pumps are used to deliver heat to the network, and Bagno di Romagna (Manzella et al., 2019; Lund & Toth, 2021). The most important

³ The maximum instantaneous geothermal energy deliverable by the system under well-defined and declared operational conditions

agribusiness facilities include greenhouses at Amiata and Pantani (in central Italy) as well as the fish farms of Orbetello (Tuscany), Brindisi and Sannicandro (Apulia). Following the official national reporting (Gestore dei Servizi Energetici S.p.A., 2018), the share of geothermal heat production, excluding geothermal heat pumps, in the total thermal output by Renewable Energy Sources (RES) is limited at 1.3% (Fig.21). Most of RES heat production is from solid waste (68%), followed by heat pumps (25.9%). Of the latter, only a minor part is represented by GSHPs, about 0.07% in the number of appliances and 0.62% in heat production. In Italy, most of the heat consumption from RES is for residential heat (38.2%) and services (36.4%), with only 3% dedicated to industrial uses. About 22% of RES heat production is lost in the transmission.



IEA. All rights reserved.

● Industrial waste ● Primary solid biofuels ● Biogases ● Liquid biofuels ● Geothermal ● Solar thermal

Figure 21 Heat generation from renewables and geothermal sources, Italy 2004-2020 (Data from IEA, 2020).

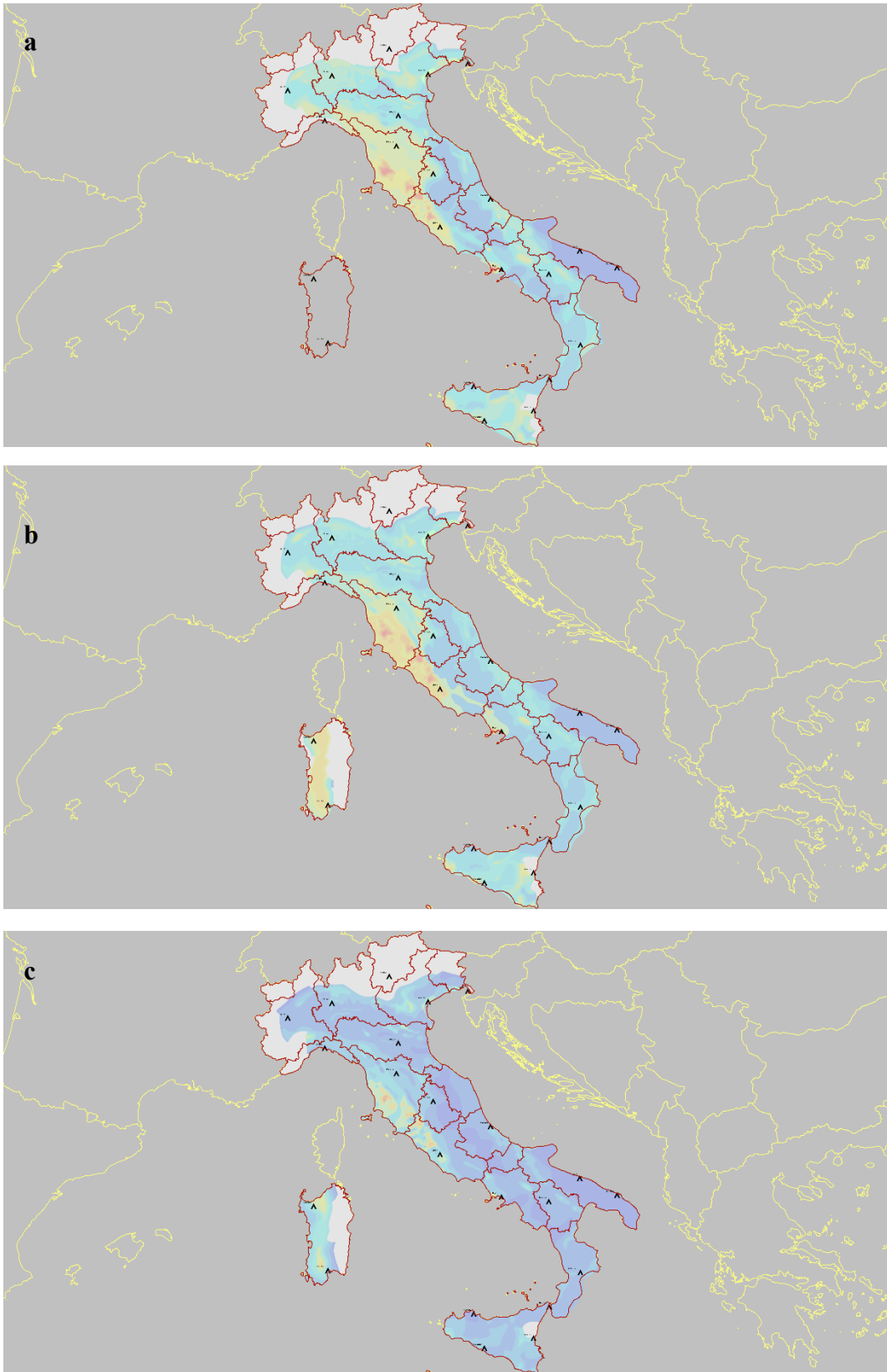


Figure 22 Temperature values recorded in the Italian territory at **a.** 3000 depth ($^{\circ}$ C), **b.** 2000 depth ($^{\circ}$ C), **c.** 1000 depth ($^{\circ}$ C). Representations not to scale. (Modified from Inv. Ris. Geotermiche Italiane, 1986).

4.2 Geothermal energy in sedimentary basins

In their works, Bethke et al. (1988), Raffensperger & Vlassopoulos (1999), Cacace et al. (2010) described that a significant portion of potentially exploitable deep geothermal energy resources is hosted in sedimentary basins. The study of the Italian sedimentary basins from a geological and stratigraphical point of view turns out to be therefore necessary as, together with geothermal resources, the major oil and gas fields of the world can be closely associated with these complex tectonic contexts.

As briefly mentioned in Chapter 3.1, sedimentary basins are areas of the earth's crust that is underlain by a thick sequence of sedimentary rocks. They usually differ in origin and lithology, and they are individually unique. Hydrocarbon resources commonly occur in those geological contexts and are absent in areas characterised by igneous and metamorphic rocks (North, 1971).

Sedimentary basins are formed over hundreds of millions of years by a combined action of deposition of eroded material and precipitation of chemicals and organic debris within a water environment. When first deposited, the sediments are soft and have high water content while, as they are buried by succeeding sediments, water is squeezed out by compaction. While compaction's effects are fully reversible at shallow depths, at greater depths, the deposits gradually become consolidated by compaction and diagenesis, mineralogical and chemical changes that take place under the influence of subsurface temperatures and pressures, and electrochemical environment. Eventually, the grains are cemented together by the deposition of minerals from siliceous or calcareous formation waters, forming sandstones, indurated shales, and claystone. Formations composed of sands and silts are named arenaceous. Those composed of clays and mixtures of clays and silts are argillaceous (Fig.23).

Because of tectonic forces in the earth's crust, the surface may go through cycles of elevation and depression. Thus, old sedimentary basins may be raised above sea level and overlain by or intermingled with other sediments, such as carbonates, sulfates, and rock salt, which are laid down by evaporation of saturated water solutions in lagoons and inland lakes. Therefore, it is sometimes essential to pay attention to all the broader

aspects of the sedimentary basin, analysing the geodynamic, tectonic and sedimentary contexts.

The formation of geothermal resources in sedimentary basins is the result of the interactions between different coupled processes comprising groundwater flow, mechanical deformation, mass transport, heat transfer, and different water-rock interaction mechanisms. Understanding the relative impact of fluid and other heat driving processes on the resulting geothermal field as well as the subsurface flow dynamics is of crucial importance in the planning phase of the geothermal energy fields exploitation. Besides, quantifying the processes mentioned above, interpreting the physical and chemical conditions that contribute to the temperature field is essential for adequately conducting a geothermal exploration campaign. Geological, geophysical studies can also play an indispensable role in all phases of geothermal research, right up to the siting of exploring and producing boreholes.

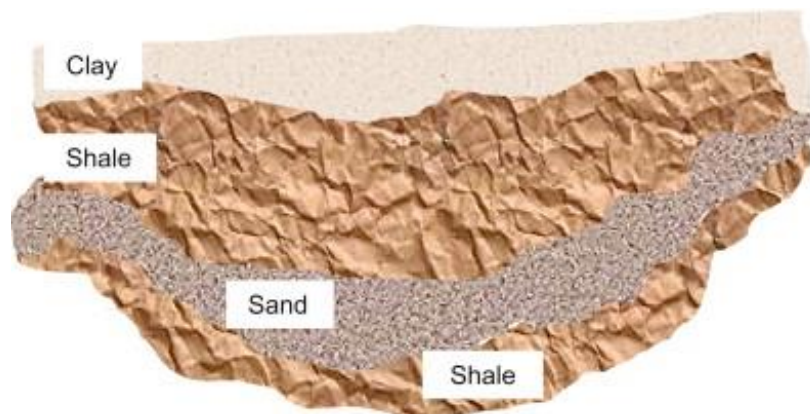


Figure 23 Conceptualized basin sedimentary formations (modified from Onajite, 2014 - Seismic Data Analysis Techniques in Hydrocarbon Exploration).

Considering the heat transfer mode in sedimentary basins from a physical point of view, they occur through conduction and convection processes. As a temperature gradient exists, experience has shown an energy transfer from the high-temperature regions to the low-temperature areas. The energy is transferred by conduction and the heat-transfer rate per unit area is proportional to the normal temperature gradient. Therefore,

conduction describes the energy transfer from matter to adjacent matter by direct contact, without intermixing or flow of any material.

Convection is the heat exchange between two surfaces by fluid in motion through molecular interaction. As for conduction, the heat transfer occurs if a temperature gradient exists. Convection heat transfer mode depends on the fluid's viscosity and its dependence on the thermal properties of the fluid medium (thermal conductivity, specific heat, density) (Levenspiel, 1984).

Under favorable geological and hydrogeological conditions, advection energy transfer mode, the transport of a substance or quantity by bulk motion of a fluid, may be as effective as conduction in sedimentary basin contexts. According to what was reported by Moeck (2014), geothermal energy fields in such tectonic settings where no asthenospheric anomalies occur are mainly conduction-dominated, as exemplified by the conductive settings of sedimentary basins.

Understanding the relative impact of the described heat transfer mode in sedimentary basins that hosted oilfields, estimating the rate at which the exchange will take place under certain conditions is crucial in the planning phase of a new geothermal energy field exploitation project. A proper interpretation of the physical behavior of the different modes of heat transfer in sedimentary basins contexts is a prerequisite for understanding the possibility of exploiting oilfields as sources of potentially exploitable geothermal resources.

4.2.1 Geothermal energy in Italian hydrocarbon fields

Over the past decades, the potential of the hydrocarbon reserves has made Italy one of the most important hydrocarbon provinces of southern Europe. Italian sedimentary basins have been explored for both oil and gas exploration and extraction activities. Consequently, deep hydrocarbon wells are found and continue to be drilled in these geological contexts. Well logs, temperature distribution profiles, and reservoir vertical cross-section and properties, such as depth to basement and geological formation thickness, are generally well known and available for consultation.

As reported in Chapter 3.2, since 1985, more than 8000 wells have been drilled for hydrocarbon extraction in Italy. Associated with the described variety of oil and gas reservoirs, geological and geophysical exploration campaigns into the deepest regions of such geological contexts have ascertained the coexistence of hydrocarbons and the low- to medium-temperature geothermal energy resources (Cataldi et al., 1995; Montanari et al., 2017b).

Several recent investigations have attempted to assess the geothermal potentials, modeling heat transfer modes and different water-rock interaction mechanisms in sedimentary basins, exploring deep geothermal resources in various Italian regions, and reconstructing heat flow maps at different depths (Trumpy et al., 2016; Trumpy & Manzella, 2017). These reported research works were carried out within the VIGOR project⁴, a three-year program dedicated to a comprehensive assessment of geothermal energy potentials and applications in four regions of Italy (Puglia, Calabria, Campania, Sicily). The VIGOR project had a broad interdisciplinary approach and included classic geological, geophysical, and engineering analyses and studies on economic, juridical, and social issues concerning implementing geothermal energy in Italy. Consistent with this framework, the VIGOR project originated from an agreement between the Italian Ministry of Economic Development and the Italian National Council (CNR) to locate and develop interventions to expand the exploitable geothermal energy potential of four Italian Regions (Apulia, Calabria, Campania and Sicily). VIGOR aimed to study a wide array of geothermal applications, from low to high enthalpy, depending on the natural resources and the economic and social aspects of the reference territories. Consistent with the RRI approach and the studies presented above, the VIGOR Project was investigating the geothermal potential of southern Italy by adopting a comprehensive approach that includes social studies (see Albanese et al., 2014). The results reported in Trumpy et al., 2016 highlighted how regional mapping of deep regional reservoirs, temperature, petrophysical parameters and flow properties based mainly on

⁴ <http://www.vigor-geotermia.it/>

hydrocarbon industry data, can provide a significant resource base of geothermal energy for direct heat and power production (Figs.24 – 25). Estimations proposed highlighted a total amount of thermal energy available up to 5 km depth in the order of $4 \cdot 10^7$ PJ for the studied areas. This energy guarantees a technical potential of 2082 GWth, 2168 GWth or 77 GWe for district heating, district heating, cooling and electrical power production, respectively assuming a lifetime of 30 years and a recovery factor of 10%. The maps obtained in their work represent important tools for all geothermal stakeholders: i) decision-makers can use them to establish new policies aimed at fostering geothermal energy, ii) investors can establish where the most promising locations for geothermal exploitation are and calculate the amount of energy available for a specific application.

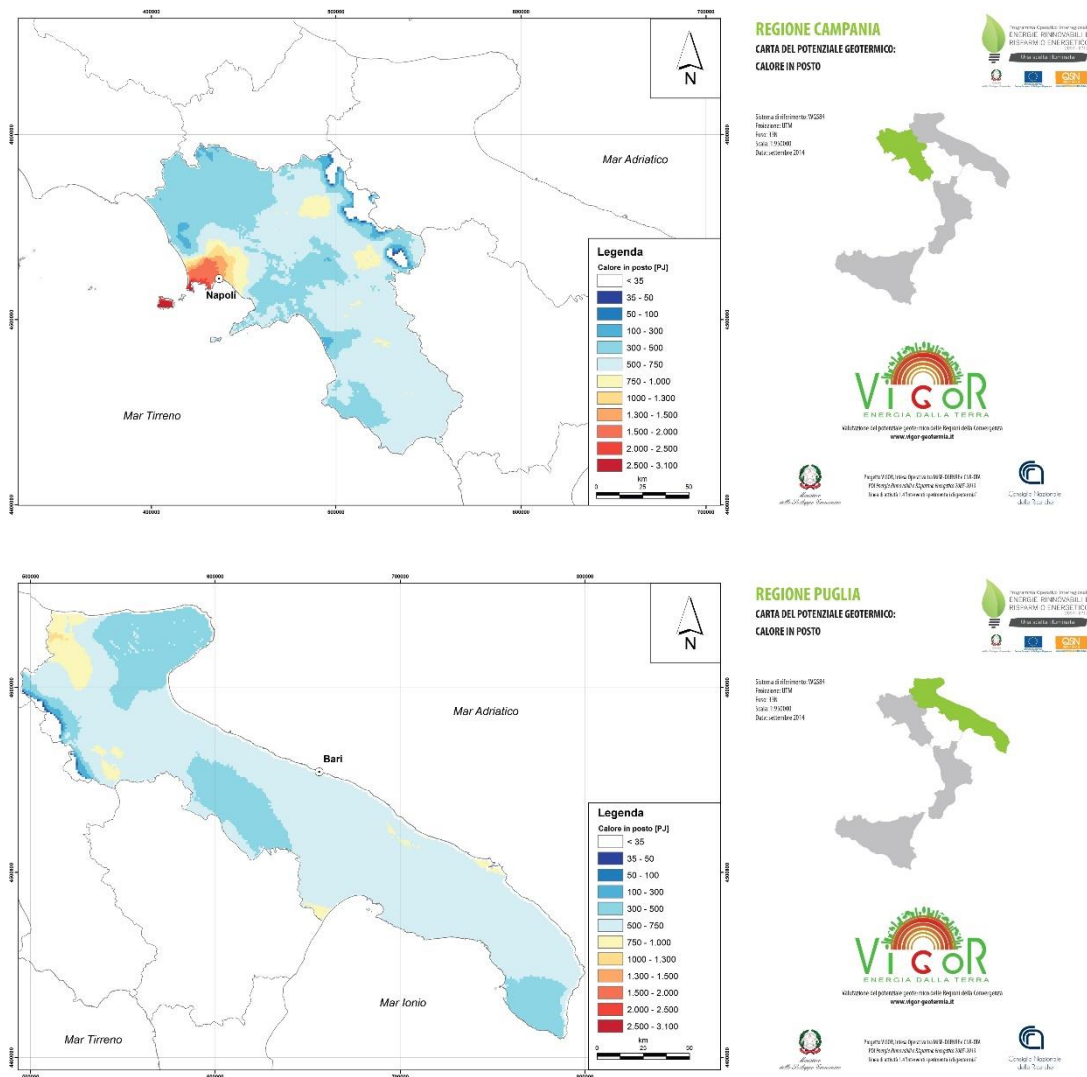
Research works that are part of the described scientific context turn out to be fundamental to broaden the knowledge of the geothermal potential available in the different sedimentary contexts of the Italian peninsula.

Additionally, in order to determine heat conductivity values at the regional and local scales of Italian sedimentary basins geological formations, Di Sipio, 2016 investigated the thermal conductivity of 200 rock samples collected from four different regions of southern Italy (Calabria, Campania, Apulia and Sicily), measuring in both dry and wet conditions. Moreover, Pasquale et al., 2011 utilised the framework of the MIUR–2008 project ‘Geothermal resources of the Mesozoic basement of the Po Basin: groundwater flow and heat transport’ to accurately estimate the thermophysical properties of a wide variety of sedimentary and intrasedimentary volcanic rocks from the Po Basin through laboratory measurements of density and porosity.

Alimonti et al., 2021 produced a vision of the geothermal potential stored in the depleted fields in Italy, using the available information provided by the Ministry of Economic Development, the published data on hydrocarbon fields, and the estimated temperature at depth from the Italian National Geothermal Database.

The volume method has been applied to assess the geothermal potential of five different most promising fields, producing a vision of the geothermal potential and describing how the available heat in Italian hydrocarbons fields is encouraging.

The information contained and made available following the publication of the results of the above-described projects was fundamental for the aim of the proposed work. Applying a strategy for understanding the possibility of crossover from hydrocarbons to geothermal energy production represents a chance for Italy to increase the share of renewable energy production, reduce the waste heat, and reconcile the social architecture with an industrial sector.



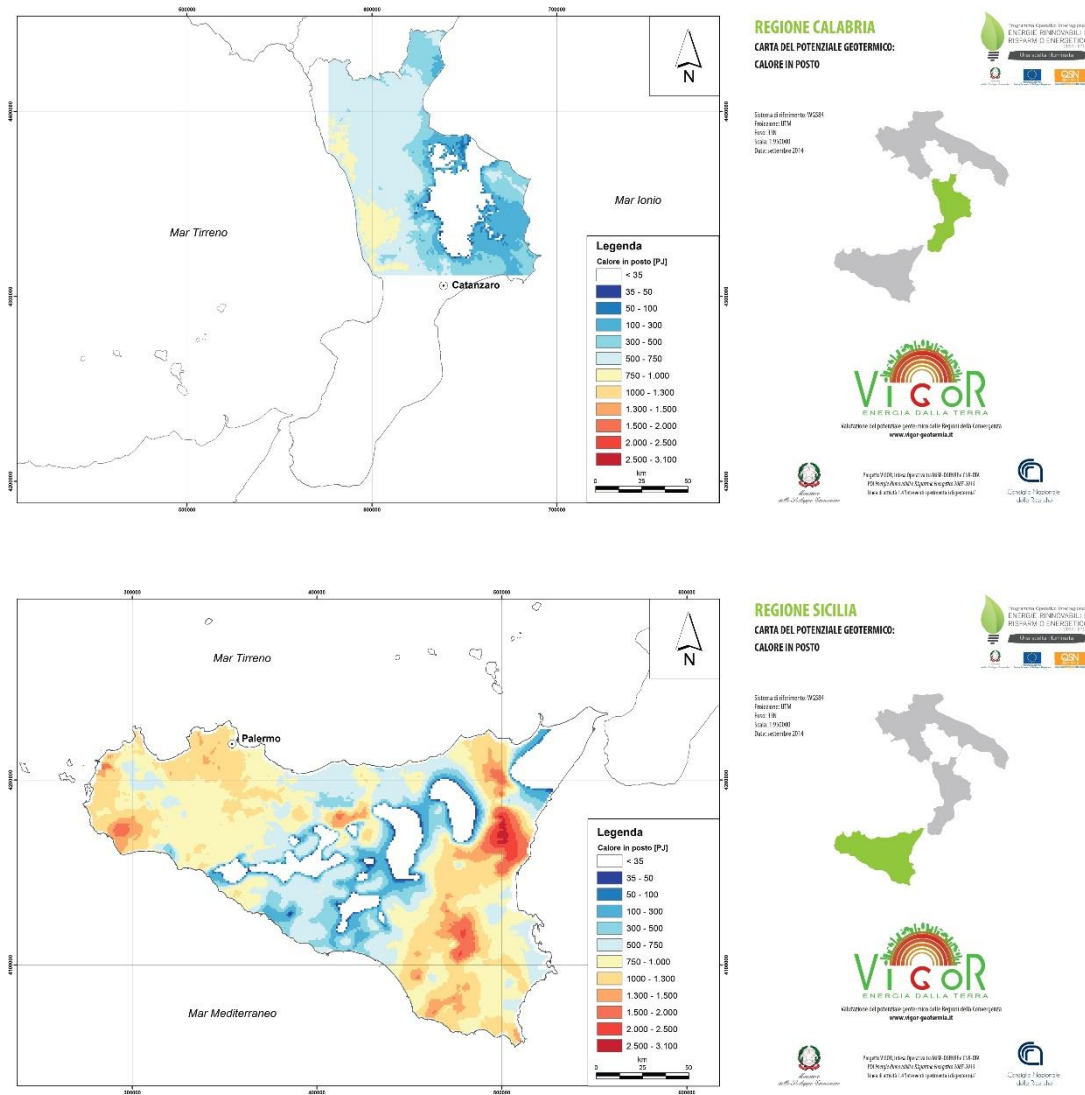


Figure 25 Deep Geothermal Potential **a.** Regione Calabria **b.** Regione Sicilia (VIGOR Project from VIGOR Project - online resources).

4.2.2 Thermal properties of rocks in Italian hydrocarbon fields

Thermal properties of the subsoil rock formations turn out to be necessary for assessing the ground's ability to allow heat exchange phenomena (Yasar et al., 2008, Pouloupatis et al., 2011, Liebel et al., 2010).

As reported above, conduction is one of the principal heat transmission modes in the Earth's subsurface. Thermal conductivity is an essential thermophysical rock property needed for deep thermal regime determination and reconstruction of the thermal history of a sedimentary basin. Therefore, it turns out to be necessary to properly know the thermal conductivity values ($\text{Wm}^{-1}\text{K}^{-1}$) of geological formations involved by ground heat exchangers, providing a distribution map to be associated with other fundamental parameter representations, potentially useful for geothermal system planning.

The thermal conductivity is strongly temperature dependent. It is generally accepted that the thermal conductivity of rocks decreases with increasing temperature and increases with increasing pressure, and the effects of temperature and pressure counteract each other (Labus & Labus, 2018).

The thermal conductivity of rocks usually falls in the range of $0.40\text{--}7.00 \text{ Wm}^{-1}\text{K}^{-1}$ (Kukkonen et al., 1999). Lower values are characteristic for dry, not consolidated sedimentary rocks, as gravels and sands. Higher thermal conductivity values are for most sedimentary and metamorphic rocks, while very high values are typical for felsic igneous rocks. The best heat conductors are rocks with high quartz content (e.g., quartzite, sandstone) and water-saturated stones. Blackwell & Steele, 1989 provided thermal conductivity values for sandstones in the range of $2.50\text{--}4.20 \text{ Wm}^{-1}\text{K}^{-1}$, shale: $1.05\text{--}1.45 \text{ Wm}^{-1}\text{K}^{-1}$, and claystone siltstone: $0.80\text{--}1.25 \text{ W m}^{-1}\text{K}^{-1}$. Although many thermal conductivity measurements of the igneous and metamorphic rocks have been made, little attention has been paid to sedimentary rocks (terrigenous and carbonatic) and heat flow in sedimentary basins as geological contexts.

In 2016, Di Sipio et al. and the VIGOR project team (See Chapter 4.2.1) highlighted the need for a reasoned choice of heat conductivity values to be assigned at a regional and local scale when planning a geothermal plant in Italy. In the first phase of their study, a general review of the thermal conductivity values described in the literature for rocks and loose materials has been performed (Lee & Deming, 1998; Vosteen et al., 2003; Waples & Waples, 2004; Davis et al., 2007; Gruescu et al., 2007; Alishaev et al., 2012). Data regarding about 90 lithologies were organized in a reference database. Besides, as

a local scale the different climate and environmental conditions, together with the structural and geological features of the territory, can modify porosity (i.e., water content), texture and homogeneity of the material, leading to thermal conductivity values, an overview of the geological and hydrogeological features of the four regions involved in the VIGOR Project (Calabria, Campania, Apulia and Sicily) was performed (see Tab.3). In order to validate the proposed thermal conductivity values ($Wm^{-1}K^{-1}$) of rocks and loose materials, obtained from the screening of international literature, the authors carried out an extensive sampling campaign in the summer of 2012. Selected samples, representative of the main geological units (i.e., having the most considerable areal extent and present in the most urbanized areas) were collected all over the territory and tested for thermal conductivity values using a specific thermal conductivity analyser (Tab.4). Through their work, Di Sipio et al., 2016 created an Italian regional database of thermal conductivity for geological materials, comparable with the one made from literature data (Tab.5). As the presence or absence of water can significantly improve the ability to conduct heat, particular attention was paid to measuring wet and dry material.

Table 3 The geological unit selected considering the four different Italian region (VIGOR Project)

	Selected geological unit	Area (km²)
Calabria	<i>Granites and granodiorites – Paleozoic cycle</i>	2004
Campania	<i>Clays, limestones and clay unit (turbiditic) - Paleogene</i>	1864
Apulia	<i>Skeletal limestones of neritic and carbonate platform facies - Upper Cretaceous</i>	4955
Sicily	<i>Clays and marls – middle-lower Miocene</i>	2924

Table 4 Thermal conductivity values ($\text{Wm}^{-1}\text{K}^{-1}$) of the main geological units derived by direct measurements on samples (dry condition).

Selected geological unit	n° of samples	λ dry min	λ dry max	λ dry
<i>Granites and granodiorites</i>	8 granite	1.3	3.5	2.4
	3 granodiorites			
<i>Clays, limestones and clay unit (turbiditic)</i>	3 marls	0.4	3.2	2.0
	1 clay			
	1 calcarenite			
	1 sandstone			
<i>Skeletal limestones of neritic and carbonate platform facies</i>	7 limestone of Altamura	1.7	3.7	2.5
	20 limestone of Bari			
	3 dolomite of Galatina			
	1 limestone of Melissano			
<i>Clays and marls</i>	2 clay	0.9	2.0	1.6
	3 marl			

Table 5 Comparison between thermal conductivity values ($\text{Wm}^{-1}\text{K}^{-1}$) measured in dry and wet conditions and derived by literature

Selected geological unit	λ dry	λ wet	λ bibliography values
<i>Granites and granodiorites</i>	2.4	2.8	2.8
<i>Clays, limestones and clay unit (turbiditic)</i>	2.0	-	2.3
<i>Skeletal limestones of neritic and carbonate platform facies</i>	2.5	-	2.9
<i>Clays and marls</i>	1.6	2.8	2.2

In 2011, within the framework of the MIUR–2008 project ‘Geothermal resources of the Mesozoic basement of the Po Basin: groundwater flow and heat transport’, Pasquale et al. proposed a valuable analysis of thermal properties, density and porosity of clastic, chemical/ biochemical and intrasedimentary volcanic rocks collected from petroleum exploration wells of the Po Basin (Northern Italy). The Po Basin is a several hundred-kilometer-wide sedimentary basins, mainly filled with clastic and chemical/biochemical deposits, enclosed between the Alps and Apennines orogenic belts. Their work aimed to understand better the geothermal potential of the Po Basin deep sedimentary

sequences. In detail, they presented the results of laboratory measurements of thermal properties, density, and porosity of rock samples recovered from several petroleum wells drilled in the basin.

More than 100 core samples from 25 petroleum exploration wells, scattered in the Po Basin, made available by the Italian national oil company (Eni E&P Division San Donato Milanese, Milan), were tested. The cores provide a broad collection of the basins primary lithologies up to 6500 m depth. Most of them were sedimentary and include elastic and chemical/biochemical rocks (i.e., marls and silty marls of marine origin). A few samples were effusive rocks belonging to intrasedimentary volcanic bodies. The sampled lithotypes were macroscopically isotropic, except some siltstones, shales and silty shales exhibiting horizontal bedding of sheet silicates.

The results obtained and reported in Table 6 were then tested with mixing models to predict thermal conductivity and volumetric heat capacity, based on the volume fractions of the rock-forming minerals.

As reported in Chapter 4.2, during the preliminary phases of a new geothermal energy field exploitation project it is required to properly define the relative impact of the different heat transfer mode, estimating the rate at which the exchange will take place under certain conditions. In the specific case for research work proposed within this thesis work, having relative values of the thermal conductivities for several geological formations available was found to be fundamental for modeling the heat transfer from matter (rocks formations) to adjacent matter (infrastructure represented by the analysed hydrocarbon well) by direct contact, without intermixing or flow of any material. As emerges from the reading of the results Chapter, the values defined by Pasquale et al., 2011 and Di Sipio, 2016 were used to determine the thermophysical parameters of the associated geological formations and the geological model associated with each of the selected case studies.

Table 6 Laboratory results of physical properties from Pasquale et al., 2011. k_r is the thermal conductivity of water-saturated isotropic samples, ϕ is the porosity, $\rho_r c_r$ and ρ_r are the volumetric heat capacity and the density, respectively, of both isotropic and anisotropic dry samples. The standard deviation (in brackets) and the number n of samples are listed.

Rock	Code/Lithotype	n	k_r ($W m^{-1} K^{-1}$)		$\rho_r c_r$ ($kJ m^{-3} K^{-1}$)		ϕ (per cent)		ρ_r ($kg m^{-3}$)	
			Range	Mean	Range	Mean	Range	Mean	Range	Mean
Clastic	1-Marl	19	2.15–3.08	2.77 (0.23)	1310–2038	1808 (176)	6.0–37.0	15.1 (8.4)	1787–2530	2278 (240)
	2-Silty marl	18	2.85–3.66	3.16 (0.26)	1790–2150	1937 (125)	2.0–20.0	12.8 (5.5)	2150–2670	2359 (156)
	3-Calcareous marl	6	1.99–2.37	2.17 (0.13)	1406–1617	1495 (72)	22.0–35.0	30.8 (5.0)	1693–2008	1801 (123)
Chemical–biochemical	4-Argillaceous limestone	3	3.58–3.63	3.60 (0.03)	1977–2094	2036 (59)	7.5–12.0	9.3 (2.4)	2477–2588	2520 (80)
	5-Argillaceous sandstone	6	2.60–3.40	3.00 (0.29)	1630–2059	1884 (155)	8.0–25.0	15.1 (6.2)	1990–2560	2330 (222)
	6-Siltstone	4	–	–	1853–2145	2003 (119)	6.0–18.0	11.1 (5.4)	2368–2560	2492 (107)
Carbonate	7-Shale	6	–	–	1780–1970	1854 (63)	4.8–22.0	15.9 (6.3)	2120–2400	2220 (106)
	8-Silty shale	6	–	–	1680–1830	1739 (55)	5.0–21.0	13.2 (6.3)	2200–2570	2340 (145)
	9-Calcarenite	3	2.18–2.50	2.34 (0.16)	1370–1810	1590 (220)	25.0–32.0	29.0 (3.6)	1834–1997	1917 (82)
	10-Mudstone	5	3.04–3.48	3.30 (0.16)	2090–2188	2148 (36)	0.5–6.0	2.7 (2.1)	2550–2695	2630 (59)
	11-Wackestone	5	3.10–3.20	3.16 (0.04)	1980–2190	2108 (80)	3.0–10.0	6.0 (3.0)	2500–2670	2590 (75)
Siliceous Evaporitic	12-Packstone	4	3.00–3.45	3.23 (0.18)	2014–2109	2058 (39)	3.0–6.0	4.3 (1.3)	2550–2655	2620 (59)
	13-Grainstone	5	2.95–3.36	3.12 (0.16)	1950–2070	2010 (55)	6.5–12.0	8.8 (2.5)	2400–2540	2480 (73)
	14-Dolostone	5	4.25–5.45	4.60 (0.49)	2240–2400	2331 (58)	1.5–7.5	3.8 (2.4)	2800–2630	2735 (73)
	15-Radiolarite	4	3.16–3.46	3.37 (0.14)	1953–2107	2021 (69)	0.5–5.5	2.4 (2.2)	2550–2650	2600 (48)
	16-Anhydrite	5	3.15–3.65	3.39 (0.22)	1930–1970	1945 (17)	0.5–5.0	2.7 (1.8)	2680–2780	2730 (52)
Igneous	17-Gypsum	5	1.40–1.64	1.54 (0.09)	2325–2500	2445 (71)	0.5–7.0	2.4 (2.6)	2260–2400	2350 (61)
	18-Dacite	4	3.56–3.91	3.73 (0.18)	2140–2160	2151 (8)	1.5–7.5	3.3 (2.8)	2690–2500	2610 (102)

4.2.3 Geothopica: The Italian National Geothermal Database

The harnessing of non-conventional geothermal energy resources for the energy production, together with updated atlantes illustrating the geothermal resources, have a strategic value in the sustainable development of the territories, potentially functioning as an investment attraction and launch-pad for an energetic economy that may bring back Italian's geothermal role as an essential renewable energy resource.

Because it is stored in subsurface geological formations and associated with hydrocarbons, available geothermal energy resources must be extracted before it can be used. Decommissioned or disused wells, especially those in mature oilfields, are good candidates for geothermal heat exploitation and may provide access to subsurface energy resources.

Georesources assessment strongly relies on reliable underground data. Direct information on the underground is produced mainly by geothermal, mining and oil and gas companies, which carry out surveys and drilling to improve the knowledge of the resources and increase production. Italian regulation requires that underground information related to explored resources, which are the state's property, is provided to public administrations and guarantees that such information remains confidential until the end of the leasing period. Thus, only a tiny portion of the data from wells is publicly available, and a minor part is readily accessible (Law of 11 January 1957, no.6) (Trumpy & Manzella, 2017).

The Italian National Geothermal Database (BDNG) represents the most extensive collection of Italian Geothermal data. It was set up in 1988 and implemented by the International Institute for Geothermal Research (Institute of Geosciences and Earth Resources - IGG) of the National Research Council (CNR) of Italy, as the completion of the inventory of deep geothermal resources by CNR, ENEA (Agenzia Nazionale per le nuove tecnologie, l'energia e lo sviluppo economico sostenibile – Italian National Agency for new Technologies, Energy and Sustainable Economic Development), ENEL (Ente Nazionale per l'Energia Elettrica – National Agency for Electricity) and ENI (Ente Nazionale Idrocarburi – National Body for Hydrocarbons), under law 896 of

1986 (Trumpy & Manzella, 2017). Besides geothermal production data, the geoinformation required by the geothermal sector is also intended to assess geological, hydrogeological, geochemical, geophysical, and thermal underground conditions. Therefore, geothermal databases of underground information such as the BDNG, storing lithological and temperature data from deep wells and fluid chemistry data from wells and thermal springs appear to be of fundamental importance for analysing the geothermal resources available at different depths.

According to the description reported in Trumpy & Manzella (2017) “the original BDNG database was used as a back-end of a desktop application. It was possible to browse geothermal wells or springs through a user interface to obtain the location and relevant data. A toolbar also enabled users to further explore specific thematic data reports (e.g., temperature data, litho-stratigraphic data, technical data, reservoir characters). The application could use a geographical data viewer to search through geothermal data. In 2008, a software improvement and data update were performed with the Institute of Geosciences and Earth Resources, the coordination of Saipem, the financial support of ENI Refining & Marketing, R&S management, and in collaboration with UNMIG (Ufficio Nazionale Minerario per gli Idrocarburi e le Georisorse – National Office for Mining Hydrocarbons and Earth Resources), a department of the National Ministry of Economic Development, who guaranteed the access to a new dataset. This improvement led to an upgrade with the resulting BDNG (the acronym was slightly changed) to become the most complete and organized underground (wells and thermal springs) data repository at a national level. The BDNG was also made accessible by a dedicated website named Geothopica.

The BDNG is the core of the Geothopica website, whose webGIS tool allows different types of users to access geothermal data, visualize multiple types of datasets, and perform integrated analyses. The webGIS tool has been recently improved by two specially designed, programmed, and implemented visualization tools to display well lithology and underground temperatures” (Figs.26 - 28).

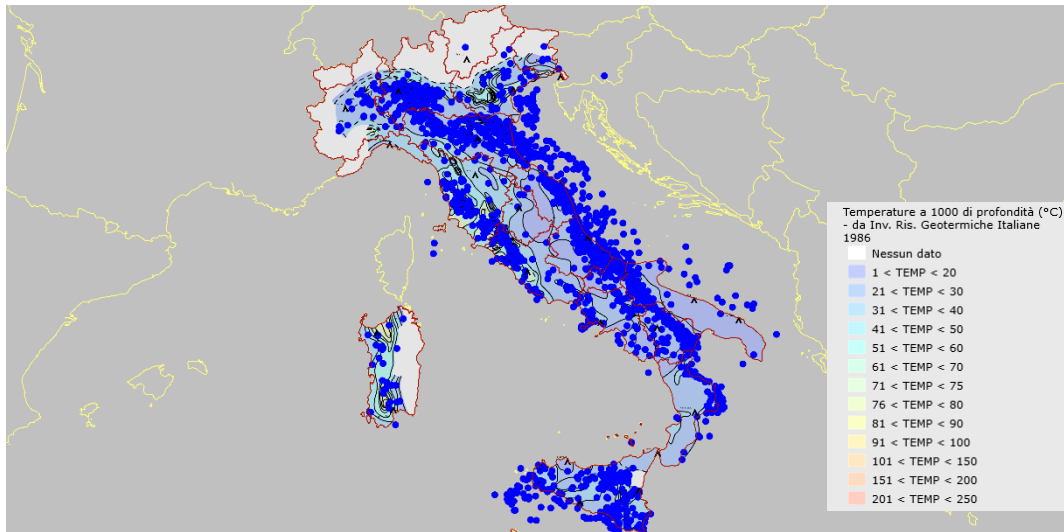


Figure 26 Geothopica webGIS – Italian hydrocarbon wells location (image above is not to scale).

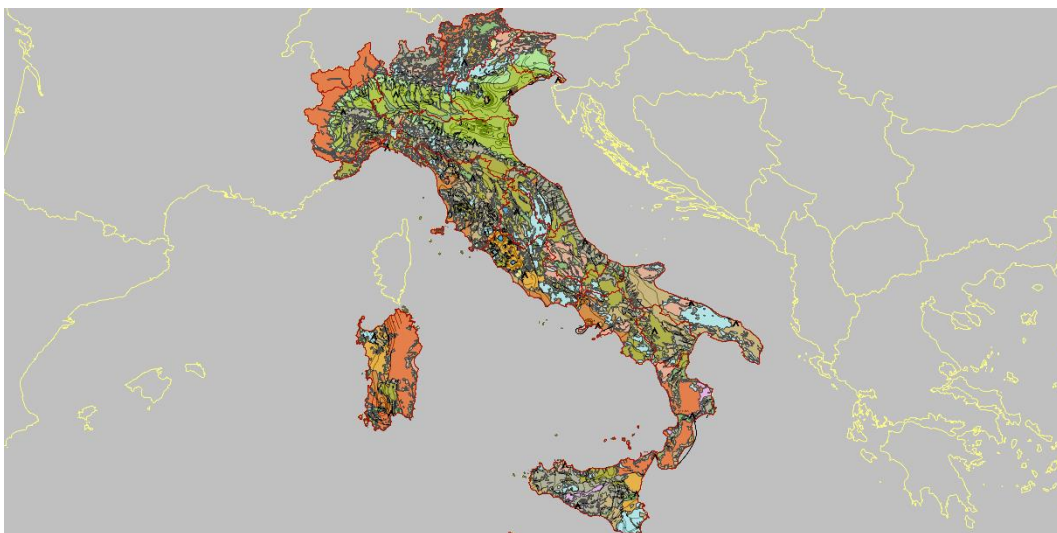


Figure 27 Geothopica webGIS – Hydrogeological Complexes of Italy - from the Atlas of Water Resources of the European Community (image above is not to scale).

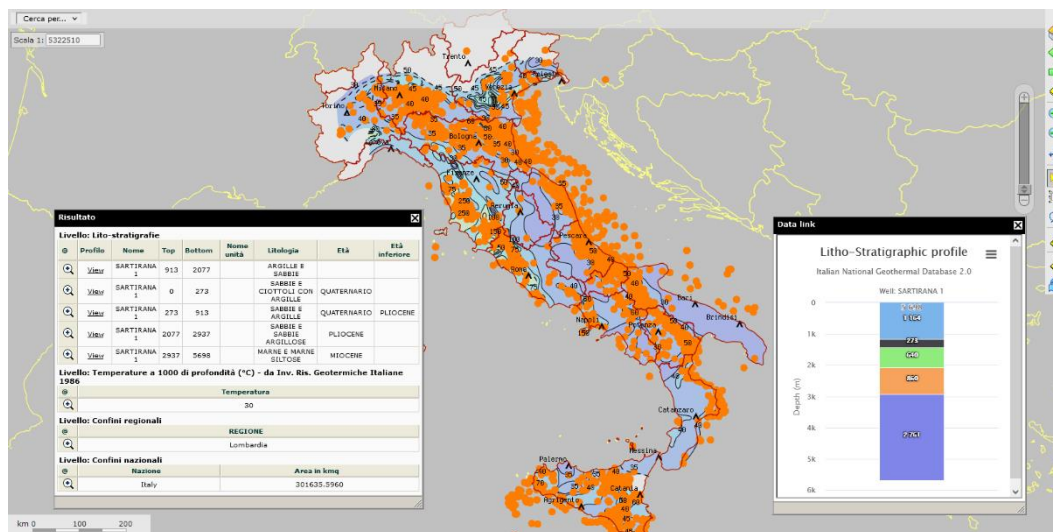


Figure 28 Geothopica webGIS – Lito-stratigraphic profile and selected hydrocarbon well information.

“The described database also contains data from deep and shallow geothermal exploration and production wells and thermal springs and surface manifestation (with temperatures $>30^{\circ}\text{C}$). Useful underground information is also retrieved from hydrocarbon wells, both onshore and offshore, which provide information on the underground nature: considering a total number of 3434 wells, 1041 are geothermal, 2349 are hydrocarbon, and 43 are very shallow wells drilled for civil use. Besides the underground data, the BDNG has five thematic maps: three temperature maps at different depths from ground-level (i.e., 1, 2, 3 km) and two different versions of the surface heat flux density. These maps were computed and published by Cataldi et al., 1995 and Della Vedova et al., 2001 based on the underground data stored in the BDNG. Since 2008, stored data have been reviewed and controlled, and new data have been added. All original hard copy documents (ENEL et al., 1988; AGIP, 1977, 1986, 1994; ENI, 1972) were also checked. New hydrocarbon well data were then added, drawing from the VIDEPI project, which collects a comprehensive dataset of hydrocarbon well-logs in pdf format. Data retrieved from well-logs were digitized and archived in the database (see Fig.22). Spring data were retrieved from scientific literature and reports. After this data update, the archived data increased from 2649 to 3434 wells, and from 460 to 586 thermal springs” (Trumpy & Manzella, 2017).

4.2.4 Rete Geotermica Italiana e Unione Geotermica Italiana

According to the information available on the Rete Geotermica Italiana website⁵, the Geothermal Network is an association of companies born from the desire of some operators holding research permits to create a supply chain capable of enhancing the geothermal resource widely present in the national territory, especially in the Tuscany Region. The guiding principle is to improve the use of this resource as a driving force for the socio-economic development of the environments concerned. The environmental sustainability of this development is the reason why some of the partners representing the Network are industrial entities of national importance capable of providing the supply chain with the skills necessary to develop innovative technologies, such as to minimize the environmental impacts deriving from geo-thermoelectric installations.

The union of sector operators and industrial groups has made it possible to create a network with complete know-how for the correct management of all activities related to the geothermal sector, from the resource analysis phase to the plant's design and management. The Geothermal Network, in addition to having the objective of increasing, individually and collectively, the innovative capacity and market competitiveness, is driven by the firm belief that the geothermal resource must be the driving force of other production initiatives relating to other sectors, among which the agricultural and civil one, through projects compatible with the will of the communities of the territories concerned.

The formalization of the Geothermal Network as a legal entity took place on 21 October 2013 and is made up of the following holders of research permits: Graziella Green Power Spa, ToscoGeo Srl, Magma Energy Italia Srl, Sorgenia Geothermal Srl, Geoenergy Srl, Exergia Toscana Srl, Gesto Geothermal Italy, Geotermics Italy and industrial entities such as Termomeccanica Ecologia Spa, Exergy International Srl, Sintecnica Srl, Samminiatese Pozzi Srl, Idrogeo Engineering & Consulting, Hydro Drilling Srl, Turboden, Isolver Spa, also benefits from the collaboration of the

⁵ <http://www.retegeotermica.it/it-it/home>

consortium Floramiata. However, the Network's wish is to be able to bring together all the operators holding permits to be the sole representative of the voice of all those realities that are now operating in the geothermal sector.

In accordance with the estimations proposed by Di Sipio et al., 2016, the potential of geothermal energy in Italy is significant. The conditions for exploiting geothermal resources in Italy are indeed highly advantageous. An additional 3000 MW could be installed compared to what is currently operational and could cover 12% of the national needs. Besides, based on estimates made by UGI (Unione Geotermica Italiana) and EGEC (European Geothermal Energy Council), the potential geothermal development from extractable resources from depths up to 5 km is equivalent to approximately 500 MTEP (million tonnes of oil equivalent).

Identifying new engineering solutions, economically and environmentally sustainable, that would favor exploiting deep geothermal energy resources available within the Italian territory is increasingly necessary to reach energy production levels close to those estimated. The work proposed fits into this scientific research context.

As reported below in Chapters 5 and 6, the application of the methods and models described required the identification and definition of preliminary data and information of a different nature: information shared by authorities, companies, professional associations, organizations and institutions that operates in the geothermal sector in Italy and worldwide, available on UGI⁶ and Geothermal Network websites, have been consulted while the detailed litho-stratigraphic and temperature data visualisation related to the Italian hydrocarbon wells, contained in the Italian National Geothermal Database (BDNG), turned out to be indispensable. Moreover, technical information regarding productive and dismissed hydrocarbon wells in Italy, available on the National Mining Office of the Italian Ministry for Economic Development (MISE) and the website of the VIGOR project, promoted by MISE-DGRME (Direzione Generale Risorse Minerarie ed Energetiche) and the Italian Geological Society and the Assomineraria Association were also used.

⁶ <https://www.unionegeotermica.it/>

Chapter 5

Materials and Methods

5.1 Background of geothermal resources utilization in oilfields

In the current energy industry framework, oil companies are searching for more innovative ways to reduce operating costs, and extending hydrocarbon fields' life. Petroleum wells are dismissed and abandoned when the oil/gas reservoir becomes unfeasible for hydrocarbon extraction activities or a dry hole is drilled. At the end of their productive time-span, wells are plugged with cement and decommissioned, becoming an enduring financial and environmental liability.

When a hydrocarbon field turns to be depleted, the geological system could potentially be converted into a geothermal reservoir. However, in order to guarantee the cost-effectiveness and environmental sustainability of a reconversion project, it's crucial to correctly identify the exploitation technology best suited to the specified site (Soldo & Alimonti, 2015).

Even though the concept of extracting heat from a hydrocarbon well is relatively novel, a lot of preliminary studies have started to appear in recent years (Davis & Michaelides, 2009; Cheng et al., 2013; Templeton et al., 2014; Wight & Bennett, 2015; Caulk & Tomac, 2017; Kharseh et al., 2019). As reported in Soldo & Alimonti (2015), the precursor of these studies is the demonstration power plant of the Pleasant Bayou field, carried out by Riney (1991), where existing wells were used to extract both gas and hot water and produce electricity.

The first aspect that must be considered with the purpose of guaranteeing the possibility of harnessing heat from hydrocarbon fields correctly is to identify their heat-recovery potential.

A lot of data needs to be collected to determine an acceptable range of parameters that makes geothermal power production from mature oil and gas fields possible as well as to define screening from suitable candidate sites. As reported in Chapter 4.2.3, sometimes, a large amount of data is made available for consultation and use in national databases and archives.

Assessment of geothermal resources is not simply an estimation of the resource base in a given area. Still, it requires evaluation of that part of the resource base that can be recovered under specified economic and environmental conditions. Accordingly, geothermal resource assessment depends on a variety of factors that can be grouped as follows (Muffler & Cataldi, 1978) (Fig.29):

Geological and physical factors

- Distribution of temperature and specific heat values of geological formations
- Total and the effective porosity
- Permeability
- Pattern of fluid circulation
- Fluid phase (steam or water)
- Reservoir depth

Technological factors

- Drilling technology
- Extraction technology
- Plant and application systems

Economic factors

- Value of the geothermal energy (direct use or electricity production)
- Costs of the different elements of the utilization plant
- Economic convenience of multipurpose projects
- Costs of the substitute source of energy

As a type of energy stored in subsurface geological formations, geothermal resources in oilfields require to be extracted before utilization. In current practice, geothermal resources are mainly harvested by a liquid medium from existing wells and applied in the form of hot fluid. The liquid medium could be the produced water from an active production well or a working fluid rejected to and circulated out from an abandoned hydrocarbon well.

Sanyal & Butler (2010) described the main features of three identified types of petroleum wells, potentially capable of supplying geothermal energy resources:

- (a) a producing oil or gas well with a water cut amount
- (b) an oil or gas well abandoned because of a high water cut amount
- (c) a geo-pressured brine well with dissolved gas

The power capacity of wells of the first category (a) is determined primarily by the production rate (Q) and the produced water temperature (T), ambient temperature and the conversion efficiency of the geothermal power system. If the produced water has adequate temperature, it is possible to extract the geothermal energy and generate power before injecting it. No drilling cost would presumably be involved in such a power generation project from co-produced water from active oil or gas wells compared to a conventional geothermal project, where the drilling cost typically amounts to 30% to 40% of the total capital cost of a project.

Depending on the type of geothermal configuration applied (open or closed-loop kind of system), the power capacity of wells in the second category - abandoned gas well (b) - can depend on production rate (Q) and produced water temperature (T), ambient temperature, the conversion efficiency of the geothermal power system, water salinity, gas content in the produced fluid, heating value of the gas and the characteristics of the equipment used to generate power from the produced gas. Besides, the production rates of water from such a well depend on the hydraulic properties of the formation, gas content in the formation water, formation temperature and pressure, well technical design.

All of the factors considered above for an abandoned oil or gas well plus the amount of overpressure in the formation determine the power capacity of a geopressed well (c). Different from geothermal extraction from producing wells, in which produced water is dominated by oil production, heat extraction in abandoned wells is more manageable with flexibility for adjustments, such as the type of geothermal configuration system (open or closed-loop kind of system), the injection fluid selection, the injection rate and injection fluid temperature. This flexibility enables the operators to manage and control the whole process of geothermal energy extraction. In general, the main factors that influence the wellhead temperature of the produced fluid are geological formations temperature, hydrocarbon well depth, well diameters and production rate.

In 2018, Liu et al. investigated the heat recovery potential of several giant hydrocarbon fields worldwide. The main goal of their data collection work was determining an acceptable range of the various geological parameters that make geothermal power production from mature fields possible employing **open-loop systems**, as well as defining screening criteria for a suitable candidate:

1. Flow rate

High production flow rates are generally required for geothermal power generation from low-to medium-temperature water resources.

2. Wellhead temperature

As a general criterion, the wellhead temperature value should be higher than the minimum temperature required for thermal energy use.

3. Water cut

High water cut is a universal feature of mature, active oil and gas fields in their later life. Most mature fields require a long-term, stable water supply, such as water injection or natural fluids recharge at the reservoir boundaries to sustain hydrocarbon production. Due to its high heat conductivity, water is a natural heat carrier usable to exploit the geothermal resource associated with the hydrocarbon reservoirs.

4. Average reservoir temperature and geothermal gradient

The stored heat in subsurface systems can be estimated from the average reservoir temperature. A general conclusion is that reservoir temperature increases with depth. According to Liu et al. 2018, average reservoir temperatures vary from 100 to 200 °C, suggesting that reservoir temperatures lower than may not be suitable for heat recovery.

5. Permeability and porosity

The permeability describes the ability of the fluid flow to go through porous media: it partly controls how much heat can be transferred from the formation to the produced fluids through convection.

Flow in porous media is also affected by natural fracture networks. The Porosity is the pore volume fraction of the total volume of the rock: it can be used to represent the amount of fluids in place in the reservoir.

6. Water flooding and steam flooding

Water injection is one of the most popular methods for the secondary recovery phase of oil and gas fields: it can complement reservoir pressure effectively and create a sizable volume of water underground at the same time. This large volume of water can become a favorable transmission medium for geothermal energy.

7. Type of geothermal plant

All the geothermal projects analysed in Liu et al, 2018 recommended using an ORCs plant for geothermal energy conversion oil and gas fields. However, as widely reported in Chapter 4.4.1, depending on their temperature ranges, geothermal energy resources can have several types of direct uses (i.e., district heating, domestic heating and/or cooling of small and medium buildings, agricultural and zootechnical uses, industrial uses, thermal uses). Furthermore, as mentioned above, Liu et al., 2018 focused their attention on analysing the different parameters that make geothermal power production from mature fields possible exclusively using **open-loop systems**.

An open-loop system consists of an injection and an extraction well. A fluid is pumped through the injection well into a reservoir, where it gains heat from surrounding rocks before it is circulated through an extraction well.

It is possible to state that the majority of works that have been carried out on existing abandoned petroleum wells have focused on open-loop systems designed to repurpose petroleum fields as geothermal reservoirs. Over time, many types of scientific research have supported works about retrofitting abandoned petroleum resources with open-loop geothermal technologies (Barbacki, 2000; Reyes, 2007; Limpasurat et al., 2011; Falcone et al., 2018; Kharseh et al., 2019; Raos et al., 2019).

Although open-loop systems in sedimentary formations may provide a sustainable solution where the geothermal potential and heat demand coincide, these technologies are subject to not negligible technical problems, including groundwater recession, corrosion and scaling (Nian & Cheng, 2018a; Kamila et al., 2021; Gizzi, 2021) Further issues are represented by the reinjection of geothermal fluids and the complex additional exploration activities (Perez Donoso et al., 2020). Due to the physicochemical properties being unsuitable for terrestrial ecosystems, extracted geothermal fluids must be treated before the re-injection into the underground. Since these operations require the drilling and maintenance of additional wells, the treatment and pumping of fluids often entailed higher economic costs related to potential geothermal projects.

An effective alternative for relatively low energy demand is represented by the use of closed-loop geothermal systems that allow thermal energy extraction from abandoned hydrocarbon wells by using a selected working fluid that circulates within a piping system with defined geometry. The central concept associated with this extraction method is to repurpose a depleted petroleum reservoir into a geothermal one, harnessing the heat using a selected fluid that plays the role of both heat extractor and heat carrier. The common practice is injecting fluid at the surface. The surrounding geological formation will gradually heat up the selected working fluid as it flows down. When the injected fluid reaches the bottom of the heat exchanger, where it gains the maximum temperature, it changes the direction, flows upward, and ascends to the wellhead.

Unlike conventional open-loop geothermal systems, heat carrier fluids in closed-loop systems circulate inside a wellbore heat exchanger (WBHE), while no ground fluids are extracted from the surrounding rocks. Therefore, a closed-loop system does not require a water management system, whereas a water management system is compulsory for open-loop configurations. Moreover, corrosion and scaling problems are limited. The capital costs for a geothermal project can be further diminished by employing a closed-loop design (i.e., a closed circuit of pipes), which can be retrofitted to a single well (Kharseh et al., 2019) (Fig.30).

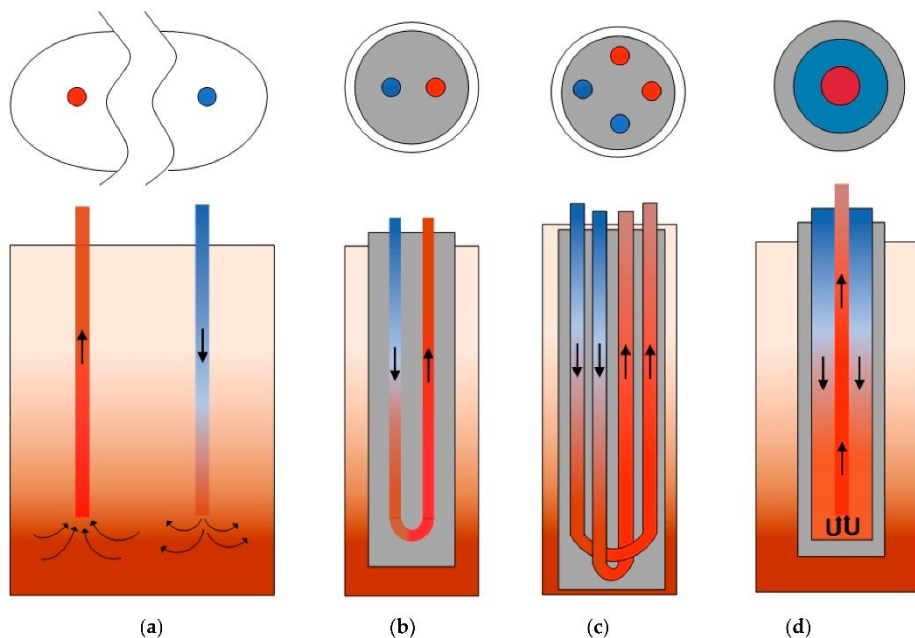


Figure 30 Extraction geothermal technologies: (a) producer-injector doublet (open-loop system), (b) wellbore heat exchanger single U-tube, (c) wellbore heat exchanger double U-tube, (d) coaxial wellbore heat exchanger (Raos et al., 2019).

Closed-loop configurations usually require a lower pumping power than an open-loop one, due to the passive heat exchange connected with natural convection phenomena (thermosiphon effect) in a closed system (Gehlin et al., 2003). Lastly, closed-loop configurations have the advantageous option of using a non-aqueous fluid with a lower boiling point than water to increase the heat exchange with the subsoil.

All the described advantages associated with the closed-loop type of geothermal systems led the researchers and industry experts to start focusing their attention on the analysis

of the potential connected to the implementation of such configurations (WBHEs) for abandoned hydrocarbon well energy conversion in contexts of natural sedimentary basins. The methodological study reported below is inserted in this specific scientific context.

5.1.1 Closed-loop geothermal systems: Wellbore Heat Exchangers (WBHEs)

In current practice, two main kinds of closed-loop systems are used to extract geothermal energy resources by taking advantage of disused boreholes in oilfields: U-tube and Coaxial double-pipe wellbore heat exchanger (WBHE) technologies (Wang et al., 2018; Lo Russo et al., 2020; Gizzi et al., 2021). Both kinds of systems allow for heat extraction from the ground without extracting or re-injecting any geothermal fluids. (Figs.31 - 32).

In U-tube heat exchangers (U-tube WBHE) fluid is pumped through one tube string and comes out of the other (Fig.31). By this action of flowing through the well, the fluid can gain heat energy from the surrounding geological formations.

On the other hand, the coaxial heat exchanger (Coaxial WBHE) is composed of two concentric pipes, as shown in Figure 32. Circulating working fluid is injected into an outer pipe (injection pipe), flows down to the lower part of the exchanger, and is gradually warmed up by acquiring heat from the rocks. After the fluid reaches the bottom hole of the well, it flows upwards through an installed pipe with an inferior diameter that acts as the inner pipe (extraction pipe). Both the outer wall of the inner and the outer pipes are thermally insulated, while the bottom hole is sealed. The gap between internal pipes is filled with an insulating material. Heat exchange occurs both on the outside wall of the exchanger (between the geological formation and the fluid flowing through the injection pipe) and between the fluid in the injection pipe and the fluid flowing through the extraction pipe (Gizzi et al., 2021; Gizzi, 2021).

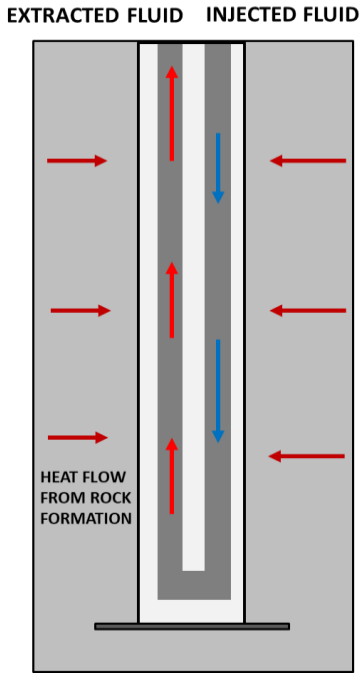


Figure 32 Schematic representation of a U-tube heat exchanger (U-tube WBHE) geometry (Lo Russo et al., 2020).

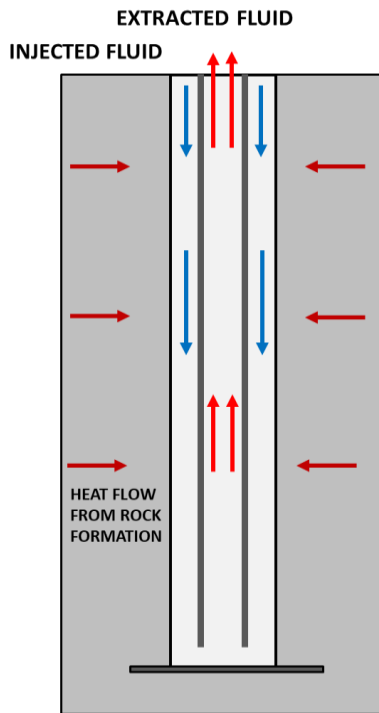
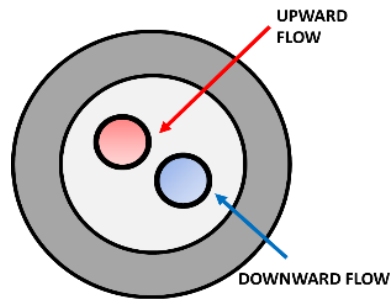
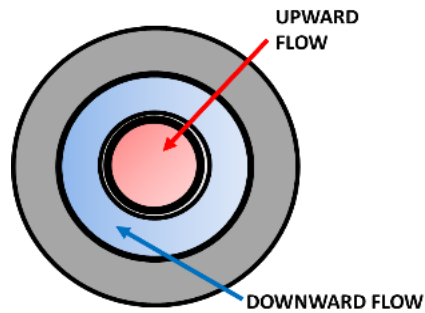


Figure 32 Schematic representation of a single Coaxial heat exchanger (Coaxial WBHE) geometry (Lo Russo et al., 2020)



Corrosion must be considered when selecting a closed-loop type of configuration: it may be ideal for heat exchange but, at the same time, it may also reduce the system's operational life. Due to its low cost and its heat transfer and storage capacity, water is still one of the most commonly used fluids. Besides, the operating parameters of subsurface closed-loop systems, such as fluid flow rate and pipes diameters, should be selected to guarantee transient turbulent flow conditions, since these conditions facilitate heat transfer, and low hydraulic head losses, since this indicates lower energy expenditure on circulation pumping.

Compared to U-tube heat exchangers, Coaxial heat exchangers have the advantages of a higher surface area and volume of the working fluid, through which heat exchange occurs. As a result, under the same injection rate conditions (q), the fluid flow velocity in the coaxial pipe system and the hydraulic pressure required for fluid circulation can be lower, resulting in decreased energy consumption from pumping (Wang et al., 2018; Gizzi et al., 2021; Gizzi, 2021). Additionally, since the outer pipe (casing) is already present, retrofitting a coaxial heat exchanger inside an abandoned well also requires significantly reduced construction times than adapting a U-tube heat exchanger. Finally, the coaxial geometry of a double-pipe heat exchanger has the advantage of reducing the thermal resistance between the circulating fluid and the wellbore piping.

For all these different listed advantages of coaxial pipe geometry, researchers have recently started to shift their attention to Coaxial WBHEs as an alternative to U-shaped configurations to provide and develop increasingly accurate thermal simulation methods and heat transfer models.

5.2 Heat transfer process in wellbores in oilfields

Heat transfer is defined as the thermal energy in transit due to a spatial temperature difference between material bodies (Bergman et al. 2011).

As long as the temperature of wellbores in oilfields and surrounding geological formations is different, energy exchange will occur. Conduction and convection phenomena are responsible for the energy transfer in wellbores during the heat extraction process. As reported in Chapter 4.2, conduction can be defined as the heat transfer through direct contact between substances (solids or stationary fluids) in which a temperature gradient exists. The heat flux by conduction in the x -dimension (one-dimensional form), or rate of heat transferred per unit area, q_x , through a plane wall, is given by the following Eq.1:

$$q_x = -kA \frac{dT}{dx} \quad (1)$$

Where dT/dx is the temperature gradient in the x -direction (heat flow direction), the positive constant k is the thermal conductivity of the substance. Equation 1 is called Fourier's law of heat conduction after the French mathematical physicist Joseph Fourier, who made very significant contributions to the analytical treatment of conduction heat transfer. The negative sign is inserted so that the second principle of thermodynamics will be satisfied: it implies that the direction of heat flow goes from hot to cold along the temperature gradient.

Convection describes the heat transfer between two surfaces by fluid in motion through molecular interaction. The heat transfer mechanisms involved are diffusion and advection, which is the energy transfer through fluid bulk movement if a temperature gradient is present. To express the overall effect of convection, the Newton's law of cooling (Eq.2) is used:

$$q = hA(T_w - T_\infty) \quad (2)$$

where T_{∞} is the temperature of the free stream outside the velocity boundary layer, T_w is the temperature of the surface on which convection is considered.

The term h introduces the convective heat transfer coefficient, which depends upon the system's geometry, the thermodynamic properties of the fluid, the thermal properties of the solid medium, and the systems boundary conditions. Values of h have been measured and tabulated for commonly encountered fluids and flow situations. Besides, for circular tubes, they can be determined using the Nusselt number Nu and the correlation functions available in the literature and listed in Tab.7 (Eq.3):

$$h_f = \frac{Nu\lambda_f}{2r} \quad (3)$$

where $2r$ is the equivalent diameter of the circular tube.

The relationship between conduction and convection for fluid flow through circular tubes, where there exists a temperature difference between the flowing fluid temperature and the tube walls, may be estimated through correlations obtained experimentally, identified for various flow conditions and geometry. The most common correlations for forced convection in circular tubes are available for turbulent and laminar flow regimes. In Table 7, the Prandtl number Pr is the ratio of momentum diffusion rate to thermal diffusion rate. Re is the Reynold's number that predicts the flow behavior of the fluid, or rather the onset of laminar, transitional, or turbulent flow. The laminar region is for $Re \leq 2300$, the transitional region is for $2300 < Re \leq 4000$, and the turbulent region is for $Re > 4000$.

Table 7 Various forced convection correlations for circular tubes (Bergman et al. 2011)

Nusselt correlation	Author	Flow conditions
$N_u = 0.023Re^{4/5}Pr^n$	Dittus and Boelter (1930)	$0.7 \leq Pr \leq 160$ $Re \geq 10000$
$N_u = 0.027Re^{4/5}Pr^{1/3}\left(\frac{\mu}{\mu_s}\right)^{0.14}$	Seider and Tate (1936)	$0.7 \leq Pr \leq 16700$ $Re \geq 10000$
$N_u = \frac{(f/8)(Re-1000)Pr}{1+12.7(f/8)^{1/2}(Pr^{2/3}-1)}$	Gnielinski (1976)	$0.5 < Pr < 2000$ $2300 < Re < 500,000$
$N_u = 4.36$		$Re < 2300$

Understanding the relative impact of the described heat transfer modes associated with wellbores in oilfields, estimating the rate at which the exchange will take place under certain geological conditions is crucial in the planning phase of a new geothermal energy field exploitation project. Besides, a correct interpretation of the physical behavior of heat transfer in different closed-loop systems (U-tube and Coaxial WBHEs) is a prerequisite for understanding the possibility of using abandoned wells as facilities for potentially exploiting geothermal resources in sedimentary basins.

5.3 Heat transfer in Coaxial WBHEs

In coaxial WBHEs, the steel downward is in contact with the hole in the well. The general energy balance of the fluid in the injection pipe can be expressed with the following Eq.4 (Nian & Cheng, 2018a; Blank et al., 2021; Gizzi, 2021)

$$\frac{\partial((\rho c)_f A_o T_{fo})}{\partial \tau} + \frac{\partial((\rho c)_f A_o v_f T_{fo})}{\partial z} = -\frac{dQ}{dz} + \frac{dQ_{io}}{dz} \quad (4)$$

where T_{fo} is the fluid temperature in the outer pipe, A_o and v_f are the outer pipe area and fluid velocity, respectively, dQ/dz is the heat extraction from the formation at unit well depth (W/m). The term dQ_{io}/dz represents the heat flux from the inner pipe to the outer pipe: although insulation is used to prevent heat loss from the inner pipe fluid, heat is partly transferred between the two pipes. Therefore, the energy equation for the inner tube can be described by the following Eq.5:

$$\frac{\partial((\rho c)_f A_i T_{fi})}{\partial \tau} + \frac{\partial((\rho c)_f A_i v_f T_{fi})}{\partial z} = -\frac{dQ_{io}}{dz} \quad (5)$$

By assuming steady heat transfer and constant heat flux in wellbore components (insulation, casing, cement), the heat extraction from formation dQ/dz can be assumed to be equal to the heat flux through the outside surface of the wellbore (interface of wellbore/rock formation) to the injected fluid (Nian and Cheng, 2018) (Eq.6):

$$\frac{dQ}{dz} = 2\pi r_w k_w (T_{fo} - T_w) = (T_{fo} - T_w)/R_w \quad (6)$$

where T_w is the temperature at the interface of the wellbore/formation, r_w is the radius of wellbore outside, k_w is the heat transfer coefficient between outer pipe fluid and wellbore exterior, R_w is the thermal resistance between the outer pipe and surrounding rocks (Tab.8 and Tab.20).

At the well bottom, the heated fluid is forced to enter and flow through the internal pipe of the coaxial WBHE. Proceeding upwards to the wellhead, heat transfer occurs only through the inner pipe wall. Thus, dQ_{io}/dz is determined by considering the

temperature difference between the outer pipe and inner pipe fluids, together with the estimated thermal resistance of the insulation (Eq.7):

$$\frac{dQ_{i0}}{dz} = 2\pi r_0 k_{i0} (T_{fi} - T_{f0}) = (T_{fi} - T_{f0}) / R_{i0} \quad (7)$$

where T_{fi} is the fluid temperature in the inner pipe, k_{i0} is the heat transfer coefficient between the outer pipe and inner pipe, and R_{i0} is the thermal resistance between the outer pipe and inner pipe (Tab.8 and Tab.20).

Table 8 Coaxial WBHE–geometric parameters.

Coaxial Wellbore Heat Exchanger - Geometric Parameters	Symbol	Unit of Measure
Outer pipe area	A_0	[m ²]
Inner pipe area	A_i	[m ²]
Radius of outside wellbore	r_w	[mm]
External radius of the external casing	r_c	[mm]
Internal radius of the external casing	r_i	[mm]
Radius of the internal casing	r_0	[mm]
Thicknesses of the pipe exchanger	d	[mm]
Depth	z	[m]

5.3.1 Coaxial WBHE: coefficient of heat exchange between outer-pipe fluid and the wellbore exterior

A proper estimate of the parameter k_w is fundamental for a correct evaluation of the heat exchange between the outer-pipe fluid and the drilled geological formations in coaxial WBHE.

For a coaxial WBHE, the heat exchange coefficient for the injection pipe can be expressed as the sum of heat transfer components in terms of thermal resistance values (R_w) (Eq.8) (Nian and Cheng, 2018; Gizzi et al., 2021; Gizzi, 2021)

$$R_w = R_s + R_a + R_c \quad (8)$$

where R_s is a function of time representing the thermal resistance due to conductive heat transfer in the rock, R_a represents the thermal resistance due to convection into the pipe. R_c is the thermal resistance due to conductive heat transfer through the casings of the well.

In evaluating the total thermal resistance, the conductive term prevails; consequently, the thermal exchange is directly proportional to the convective transfer coefficient.

Conductive thermal resistance (R_s) can be expressed as follows (Eq.9):

$$R_s = \frac{1}{2\lambda_s} \ln \frac{2\sqrt{\alpha_s t}}{r_w} \quad (9)$$

where λ_s (W/mK) is the thermal conductivity of the rock and α_s (m²/s) is the thermal diffusivity of the rock. In Eq.9, the numerator of the argument of the natural logarithm represents the time-dependent radius of the thermal influence of the well (r_s). This parameter considers the change, over time, of the heat flux into WBHE surroundings geological formations (Alimonti & Soldo, 2016) (Tab.20).

Convective thermal resistance (R_a) can be determined by the following equation (Eq.10):

$$R_a = \frac{1}{2r_c h_f} \quad (10)$$

where r_c is the external radius of the outer casing, h_f is the convective heat transfer coefficient, calculated by using the Nusselt number (Nu) and the form of Dittus-Boelter equation assuming turbulent flow inside the tubes (Reynolds number ≥ 104) (Davis and Michaelides, 2009) (See Tab.7):

$$h_f = \frac{Nu\lambda_f}{2r_c} \quad (11)$$

$$Nu = 0.023Re^{0.8}Pr^{0.4} \quad (12)$$

where $Pr = \frac{\rho c_f \mu}{\lambda_f}$ and $Re = \frac{\rho v_f 2r_c}{\mu}$.

Finally, thermal resistance to heat conduction through the casings of the well (R_c) can be determined as follows:

$$R_c = \sum_{i=1}^n R_{\lambda i} = \frac{1}{2} \sum_{i=1}^n \frac{1}{\lambda_i} \ln \frac{r_{c,i+1}}{r_{c,i}} \quad (13)$$

where λ_i is the thermal conductivity of the rock in correspondence with the different casings of the well. Generally, due to the high thermal conductivity of the steel piping, the total thermal resistance of the casing is negligible compared with the rock's thermal resistance.

As a result, the heat exchange coefficient k_w can be determined as follows (Charnyi 1948, 1953):

$$\frac{1}{k_w} = \frac{2r_c}{2\lambda_s} \ln \frac{4\sqrt{a_s t}}{2r_w} + \frac{1}{h_f} \quad (14)$$

where $r_c = r_w$ as the thickness of the external tube is negligible (Tab.20).

5.3.2 Coaxial WBHE: coefficient of the heat exchange between the outer-pipe fluid and the inner pipe

Unlike in the injection pipe, the total heat flux in the upward pipe (extraction pipe) is determined by a **conductive component** of the composite pipe and by **two convective components**: one on the internal wall and one on the external wall of the WBHE. Consequently, the total heat exchange coefficient k_{i0} for the extraction pipe can be calculated as follows (Eq.15):

$$\frac{1}{k_{i0}} = \frac{r_0}{r_{0+d}} \frac{1}{h_i} + r_0 \sum_{i=1}^n \frac{1}{\lambda_i} \ln \left(\frac{r_{i+1}}{r_i} \right) + \frac{1}{h_0} \quad (15)$$

where r_0 is the radius of the inner pipe, d is the thicknesses of the pipe exchanger, h_0 and h_i are the coefficients of convective heat transfer to the inner and outer wall, respectively, and λ_i is the thermal conductivity of the pipe material (air and steel).

5.3.3 Coaxial WBHE: current methodological developments

A significant number of published scientific articles model the heat transfer in abandoned petroleum wells, estimate the potential of heat production and perform sensitivity studies to determine the optimal conditions for operating the geothermal wells (Sui et al., 2019).

The works carried out by Kujawa et al. (2005) and (2006) represent the pioneering researches for the evaluation of the possibility to retrofit abandoned oil and gas wells for geothermal energy exploitation, utilising a coaxial WBHE. In their studies, they proposed a 2870-m-long coaxial WBHE for a Jacho'wka K-2 well with an external casing constituted by a column of steel pipes with diameters of 244.5/222.0 mm and a new column of pipes with diameters of 60.3/50.7 mm, located concentrically inside the exchanger. Due to their starting assumptions of a steady-state and a constant temperature at the interface of wellbore/formation, they considered a simplified heat exchange model in which the heat flux penetrating from the external fluid is equal to the heat flux conducted through the multilayer cylindrical barrier and to the heat flux penetrating the internal fluid. In detail, they started from the formula of linear density of the heat flux transferring from one medium reported in Eq.6 and estimated the overall heat transfer coefficient between the outer pipe fluid and wellbore outside (k_w) by using equations provided by Charnyi 1948, 1953 (Eq.14) and Dyad'kinMoon & Gendler, 1985 (Eqs.16, 17):

$$k_w = \frac{k'_w}{1 + Bi \ln(1 + \sqrt{\gamma F0})} \quad (16)$$

$$\frac{1}{k'_w} = \frac{1}{h_f} + \frac{D_1}{2} \sum_{i=1}^n \frac{1}{\lambda_i} \ln \frac{D_{i+1}}{D_i} \quad (17)$$

where $Bi = \frac{h_f r_c}{\lambda_s}$ is the Biot number, $Fo = \frac{a_s t}{r_c^2}$ is the Fourier number and $\bar{\gamma}$ is the parameter depending on the Biot number (if $Bi > 30$, $\bar{\gamma} = \pi$. In other cases, $\bar{\gamma} = 2$). By performing calculations for selected volume flow rates of injection fluid (water) flowing through the heat exchanger (2, 10, 20 and 30 m³h⁻¹) and temperatures respectively equal to 10, 15, 20, and 25°C, the authors demonstrated the practical significance of reusing the existing well for only two injection flow rate values: 2 and 10 m³h⁻¹, with associated temperatures at the extracted fluid of 65°C and 47°C, respectively.

Furthermore, Bu et al., 2012 began to consider heat transfer from geological formations as associated with two-dimensional heat conduction phenomena by replacing the assumption of constant temperature at the interface of wellbore/formation in Kujawa et al. (2005, 2006) and Davis & Michaelides, 2009. Through analysing abandoned wells that were 4000 m deep with an associated geothermal gradient of 25°C/km and 45°C/km, Bu et al., 2012 and 2014 discretised energy balance equations for coaxial WBHE using the finite volume method and solved it using the tri-diagonal matrix algorithm (TDMA) (Tao, 2001). Although they considered the heat transfers from geological formations as transient in their study, a finite boundary was set for surrounding rocks assuming that rock temperature became constant at a radius of surrounding rocks over 200 m.

For their elaborations, the diameter of the injection well on the top part was fixed to 340/300 mm with a length of 2500 m, while the bottom diameter was 330/300 mm with a length of 1500 m. The inner diameter of the extraction well was 100 mm.

The results of Bu et al. (2012, 2014) works were fundamental to understanding how the amount of geothermal energy that can be extracted from abandoned oil and gas wells significantly depends on the injection fluid flow rates and on the recorded regional geothermal gradient. For a selected geothermal gradient of 45°C/km, they estimated net power output for the analysed single well of 53.70 kWe with an outlet temperature is 129.88°C. The optimal flow velocity of the fluid at which they attained the maximum

net power was 0.03 ms^{-1} , while the maximum value of heat from rocks was acquired at a flow rate of 0.05 ms^{-1} .

Different from Bu et al. (2012, 2014), Cheng et al., 2013 and Cheng et al., 2014a examined the effects of formation heat transfer with an infinite boundary and conducted a theoretical analysis of geothermal power generation from abandoned wells using isobutane as the working fluid. In their study, they started from Ramey's (1962) definition of radial heat flow from the formation at the heat exchanger/formation interface. They introduced a novel transient heat conduction function $f(t)$, as follows (Eq. 18):

$$\frac{dQ}{dz} = \frac{2\pi\lambda_s(T - T_w)}{f(t)} \quad (18)$$

where T is the formation temperature at an infinite distance from the well axis, T_w is the heat exchanger/formation interface temperature and λ_s is the thermal conductivity of the rock formation.

Different from the traditional $f(t)$ introduced by Ramey (1962) that only considered the effect of time, the novel transient heat conduction function obtained by Cheng et al., 2011 and allowed the consideration of the impact of time and heat capacity of the wellbore on heat extraction from the formation (Eq. 19):

$$f(t) = \frac{16\omega^2}{\pi^2} \int_0^\infty \frac{1 - \exp(-t_D u^2)}{u^3 \Delta(u, \omega)} du \quad (19)$$

where $t_D = \frac{\alpha_s t}{r_i^2}$ is defined as dimensionless time, r_i is the inner radius of the injection well, α_s is the thermal diffusivity of the formation, ω is the ratio of the formation heat capacity and the wellbore heat capacity, u is the variable for integration and the function $\Delta(u, \omega)$ is associated to the following relation (Eq. 20):

$$\Delta(u, \omega) = [uY_0(u) - \omega Y_1(u)]^2 + [uJ_0(u) - \omega J_1(u)]^2 \quad (20)$$

where J_0 and J_1 are the zero-order Bessel function of the first kind and the first-order Bessel function of the first kind, respectively. Y_0 and Y_1 are the zero-order Bessel

function of the second kind and the first-order Bessel function of the second kind, respectively.

The results of their studies, which were performed on an abandoned well with a depth of 6000 m, clearly showed for the first time how the formation of heat transfer mechanisms strongly influences geothermal power generation. Furthermore, they determined that the outlet temperature of working fluid tends to gradually decrease with increasing operating time, eventually approaching a steady state. The inlet velocity of isobutene in the injection well was also a binding parameter, as the heat obtained from the abandoned well and fluid outlet temperature strongly decreased with increasing fluid inlet velocity.

Meanwhile, Templeton et al., 2014 also developed a two-dimensional cylindrical model by incorporating Fourier's three-dimensional diffusion law, two different terms describing the unsteady state heat transfer in the heat exchanger, the advective and conductive effects of the working fluid into the energy conservation equation, to generate a partial differential equation that adequately describes the heat transfer mechanisms.

Comparing the results obtained from the proposed model with the ones reported in Kujawa et al., 2006 and Bu et al. (2012), they clearly showed that using a one-dimensional model tends to overestimate the performance of a coaxial WBHE.

More recently, Alimonti & Soldo, 2016 also focused on optimising a coaxial WBHE structure to maximise the heat extraction from an abandoned oil and gas well located in one of the largest European oil fields, the Villafortuna Trecate Oilfield. The main reservoir associated with this site was identified at between 5800 m and 6100 m depth with an available temperature of approximately 160–170°C.

The same approach described by Kujawa et al., 2005 was proposed and implemented in a C-computation code for simulating formation heat conduction mechanisms. By fixing the sizing of the inner and outer tubes, as well as the final casing size as reported in Table 9 with an inlet temperature of the heat carrier fluid equal to 40°C, they analysed

variations in the temperature of the extracted fluid as a function of different fluid flow rate values.

Despite the availability of geological and geophysical data relating to drilled rock formations acquired during the prospecting phases in Italian oilfields, the authors considered the properties of rocks to be uniform with depth (λ_s 2.5 Wm⁻¹ K, ρ 2600 kgm⁻³ and pc_s 800 Jm⁻³K). Their results demonstrate how the fluid temperature reaches a maximum value of approximately 120 °C for an injection fluid flowrate of 10 m³h⁻¹. Also, the increase in injection flowrate values tended always to cause a decrease in the recorded temperatures at the wellhead.

In addition to the work proposed by Alimonti & Soldo, 2016, very few works available in the bibliography comprehensively considered the influence of vertical and horizontal variations in geological. Over time, authors have in fact primarily focused their attention on analysing the impacts on energy performance caused by changes in working fluid-related parameters such as initial temperature and injection flow rate values. Many other studies have also been conducted to identify the optimal design configurations for the selected WBHE. However, due to the geological complexity of sedimentary basins, correct estimates of geothermal energy that can be extracted from an abandoned hydrocarbon well cannot be performed without a proper analysis of the geological model surrounding the analysed boreholes. As described in the section dedicated to introducing the results (Chapter 6), in the proposed work, the assumption that the thermophysical parameters (thermal conductivity, volumetric heat capacity and rock density) are constant values has been overcome. The detailed stratigraphic data of each selected case study (hydrocarbon wells) was adequately considered in each elaborated code.

Table 9 Coaxial WBHE tube sizing in Alimonti and Soldo, 2016 – ID: internal diameter, OD: external diameter

Tube sizing	ID (mm)	OD (mm)
3½ inches	77.9	88.9
5½ inches	121.4	139.7
Casing 7 inches	150.4	177.8

5.4 U-tube WBHE: thermal resistances model

As described in Gizzi (2021), the hole between the tubes and the well in U-tube WBHE is filled with grout (bentonite) to prevent direct leakage between the ground and pipes, avoiding a connection between the ground and Earth’s subsurface. The grout material needs to be characterized by good thermal conductivity to maximize the heat exchange. Different approaches have been proposed to reproduce the thermal behaviour of different U-tube WBHE configurations (Yang, Cui and Fang, 2010). The general approach is based on the line and cylindrical heat source theories to model the heat transfer between the borehole wall and the surrounding soil, neglecting the heat transfer inside the borehole.

In this proposed work, in order to obtain the temperature profile in the U-tube configuration using a one-dimensional heat exchange, the model with a set of equivalent thermal resistances described and proposed by Ruiz-Calvo et al. (2015) was applied.

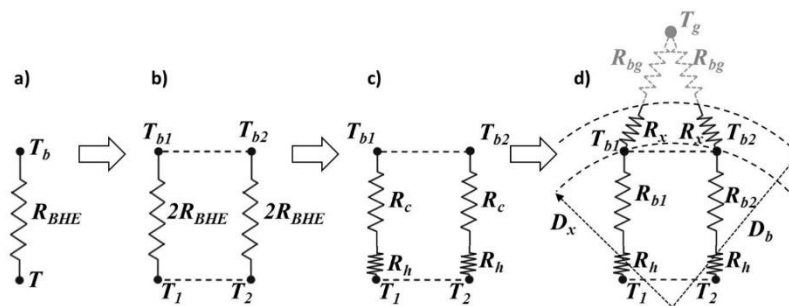


Figure 33 Thermal resistances definition steps: (a) borehole resistance, (b) parallel borehole resistances, (c) convective and conductive resistances and (d) final resistances configuration (reproduced from Ruiz-Calvo et al. 2015. Copyright Elsevier, 2014).

Six thermal resistances were considered at each depth, including the thermal properties of the ground, the grout, and the pipes (Fig.33).

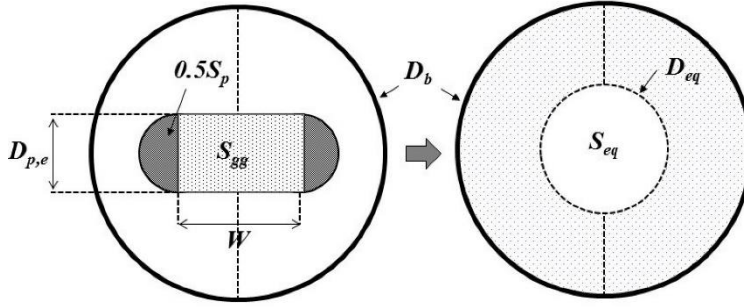


Figure 34 Geometrical model characteristics for calculating the equivalent diameter (reproduced from Ruiz-Calvo et al. 2015. Copyright Elsevier, 2014).

The thermal resistances between the grout (bentonite) and pipe depend on the overall borehole thermal resistance R_{bhe} . This parameter represents the average thermal resistance between the fluid in the pipe and the borehole wall, and it is usually determined after experimental tests. The grout area is divided into two zones according to the pipe numbers; thus, R_{bhe} was also considered as divided into two parallel resistances that connected each pipe with the corresponding grout zone. This parameter can be further divided into a convective (R_h) and a conductive (R_c) term (Eq.21).

$$2R_{bhe} = R_h + R_c \quad (21)$$

where R_c represents the conductive thermal resistance, considering the total conductive resistance between the pipes and the borehole wall. As the grout node can be located at a certain distance D_x , R_c is divided into two different resistances (Eqs. 22, 23).

$$R_c = R_b + R_x \quad (22)$$

$$R_b = R_{b1} = R_{b2} \quad (23)$$

where R_b represents the conductive resistance between the pipe and the considered node. R_h is calculated using the following Eq.24, where r_i is the internal pipe radius, h_f is the convective heat coefficient, and Nu is the dimensionless Nusselt number, calculated through Eq.12:

$$R_h = \frac{1}{2\pi r_i h_f dz} = \frac{1}{\pi \lambda_f Nu dz} \quad (24)$$

The R_c value is estimated using a calculation method that requires the estimation of the pipe equivalent surface S_{eq} and its diameter D_{eq} (Eq. 25) (Tab.10).

$$D_{eq} = 2 \sqrt{\frac{S_{eq}}{\pi}} \quad (25)$$

The pipe equivalent surface (S_{eq}) can be calculated by following the approach proposed by Pasquier and Marcotte (2012), considering the sum of S_{gg} and S_p as reported in Fig.34. Consequently, D_{eq} is obtained through the following Eq. 26:

$$D_{eq} = D_{pe} \sqrt{\frac{4W}{\pi D_{pe}} + 1} \quad (26)$$

Using the equivalent diameter, the conductive thermal resistance R_b and R_x are calculated considering a semi-cylindrical conductive heat transfer:

$$R_b = R_{b1} = R_{b2} = \frac{\ln(D_x/D_{eq})}{k_b \pi dz} \quad (27)$$

$$R_x = \frac{\ln(D_b/D_x)}{k_b \pi dz} \quad (28)$$

where k_b is the borehole grout thermal conductivity.

Usually, when the pipes are near the borehole wall, D_x can be located at the same distance from the borehole wall; thus, $D_x = D_b$ and, consequently, the R_x part of the conductive resistance can be neglected.

Finally, the correlation as reported in Eq.9 is used for the estimation of the ground thermal resistance. The total resistance value related to the analysed single tube includes convective (R_a), grout conduction ($R_b + R_x$), and ground resistance (R_s) terms.

Table 10 U-tube WBHE - Geometric parameters

U-tube wellbore heat exchanger - Geometric parameters	Symbol	Unit of measure
Borehole diameter	D_b	[mm]
Grout node position	D_x	[mm]
External U-pipe diameter	D_{pe}	[mm]
External U-pipe diameter	D_{pi}	[mm]
External U-pipes radius	r_i	[mm]
Equivalent pipes surface	S_{eq}	[m ²]
Equivalent pipes diameter	D_{eq}	[mm]
Shank spacing (center-to-center)	W	[mm]
Depth	z	[m]

5.5 Pressure losses

The heat-exchange modalities are not the only aspect that must be considered to correctly analyse the heat transfer mechanisms associated with Coaxial and U-tube WBHE. In order to carry out an analysis as complete as possible, pressure loss phenomena also need to be analysed as they affect pumping cost and are not negligible in the management of closed-loop geothermal systems. Closed-loop configurations usually require a lower pumping power than an open-loop one, due to the passive heat exchange connected with natural convection phenomena (thermosiphon effect) in a closed system (Gehlin et al., 2003).

Pressure losses can be estimated through the use of the following equations Eqs 29,30:

$$dP = \rho g dz - dP_{f\text{Downward}} \quad (29)$$

$$dP = -\rho g dz - dP_{f\text{Upward}} \quad (30)$$

where the first term strictly depends on the elevation; the second is due to friction, and it depends on velocity (Eq.31):

$$dP_f = \frac{f dz}{D} \rho \frac{v_f^2}{2} \quad (31)$$

where f is the friction factor, D is the diameter of the specific circuit considered, and v_f is the fluid velocity. The pressure loss due to elevation is zero, as upward and downward components are added together.

The components' friction-related values are not zero and, consequently, the pumping rates must be settled to provide the power needed to balance this component. Upward and downward pressure loss values are not equal because the tubes' thermal fluid velocity and diameter vary across the different configurations considered.

For the evaluation of the friction factor, both in the inner tube and the annulus, and subsequently the calculation of the pressure drops, the Haaland equation (Haaland, 1983), an approximate explicit equation which combines experimental results of studies of laminar and turbulent flow in pipes pipes, can applied.

5.6 The Codes

5.6.1 WBHEs models assumptions

PYTHON and MATLAB are software for numerical and statistical calculations that allow algorithms to be solved easily. They were both adopted to be used to perform the analysis of the selected WBHEs by implementing the above-described simplified models (Coaxial and U-tube-WBHE) using their programming languages.

According to the Coaxial and U-tube WBHEs models reported in chapters 5.3.1, 5.3.2 and 5.4, energy transfer in the geological reservoir occurs through conduction; heat propagation inside the wellbore tubes takes place through conduction and convection phenomena. In both models, the geological reservoir was built by considering a single well located at the center of a circular area.

Considering the existing temperature profile, it was assumed to be constant in the radial direction. There is no temperature gradient in the annulus or the inner tube: due to the turbulent flow inside the pipes, enhanced mixing phenomena occur, which decrease the radial temperature gradient.

The temperature changes only in the annulus and the inner tube vertical direction. Consequently, the temperature profile is considered unidirectional (vertical temperature profile).

The analytical models were built under steady-state conditions and considering constant heat flux in wellbore components. There were no temperature variations over time: each point of the tubes (annulus and inner tubes) maintains the same temperature for the system's lifecycle. These assumptions can be considered to be suitable, especially on a long-term basis, because the heat transfer in a wellbore is more rapid than that in larger-scale formation and takes less time to reach a stable state.

In addition, the described models consider the resistance associated with tube thickness to be negligible. The tube material had very high conductivity (15 W/mK), so its resistance could be regarded as minor compared to the other resistances that define the

system. Moreover, the thermal conductivity value of the insulating material for both Coaxial and U-tube-WBHE is set 0.025 W/mK

The properties of the selected heat carrier fluid were assumed to be constant. As the fluid used in the proposed study was water (100°C, 2 bar), no variations occurred due to pressure or/and temperature gradients.

For the estimation of resistance associated with the rock (see Equation (9)), the time value used was 3 years. From a preliminary analysis carried out through the study of the R_s variation value over the time it emerged as, in the period preceding the three years (1–3 years), the system turns out to ensure more significant heat exchange phenomena with the possibility of causing overestimation in energy performances

Considering the U-tube WBHE configuration, heat exchange was assumed to occur in a semicircular area that was half the area of the casing pipe. At the same time, the interaction between the downward and upward tubes was neglected.

Both proposed analytical models follow the path of the working fluid with an approach that could be called step-by-step. In detail, they considered intervals of length dz (heat flow direction direction) in which the inlet and outlet temperatures were calculated by solving the specific energy balance equation for each considered volume dv .

For the estimation of the energy exchange in the radial direction, the mean value of the temperature in the volume dv was used and calculated using the arithmetic mean (Eq.32).

$$T_m = \frac{T_{inlet} + T_{outlet}}{2} \quad (32)$$

All the energy exchanged in the radial direction in the volume dv was absorbed by the water (the working fluid) (Eq.33):

$$P = mcp_w(T_{outlet} - T_{inlet}) \quad (33)$$

where m is the fluid mass, T_{in} is the working fluid inlet temperature, T_{out} is the outlet temperature of working fluid.

The factors influencing the wellhead temperature of the selected working fluid are geothermal gradient, hydrocarbon well depth, well and heat exchanger pipe radius, inlet

flow rate, temperature of the fluid entering the well. The different parameters listed above must be adequately defined before applying the models relating to the different wellbore heat exchanger configurations. For this purpose, appropriate sections have been prepared within the developed models. The codes' structure, described in detail in the following Chapters 5.6.2 and 5.6.3, is characterized by different parts. A section is strictly dedicated to defining the technical input parameters; a second section describes the heat exchanger to be considered and analysed for the hydrocarbon well's energy conversion project. Besides, section two contains the reconstruction of the geological model with the assignment of the geological formations' thermal parameters (See figs.36 - 39).

5.6.2 The Python Code

Python is a high-level programming language with an object-oriented approach described by van Rossum, 1995. Python extension libraries are available for several tasks, including science and engineering applications, for which Python has become increasingly popular. Python is a pseudocompiled language: an interpreter analyses the source code (text files with .py extension) and, if syntactically correct, executes it. It is free software: the interpreter software downloads as well as using Python in own applications are completely free.

Python software was chosen to analyse the WBHEs by implementing the described models (Coaxial and U-tube-WBHE models) in different codes with the general structure illustrated in Figure 35. The proposed Code uses the Numerical Python library (<http://numpy.scipy.org/>) to enable efficient numerical computations.

The code named “setting.py” was developed to allow the definition of the input parameters needed to carry out the analysis. It is able to communicate with the proposed WBHE codes (Sensibility analysis models; WBHE models). Consequently, following the selection phases of the case studies and the definition of site-specific input parameters, it is possible to carry out an analysis of the energy performance according to the closed-loop system selected.

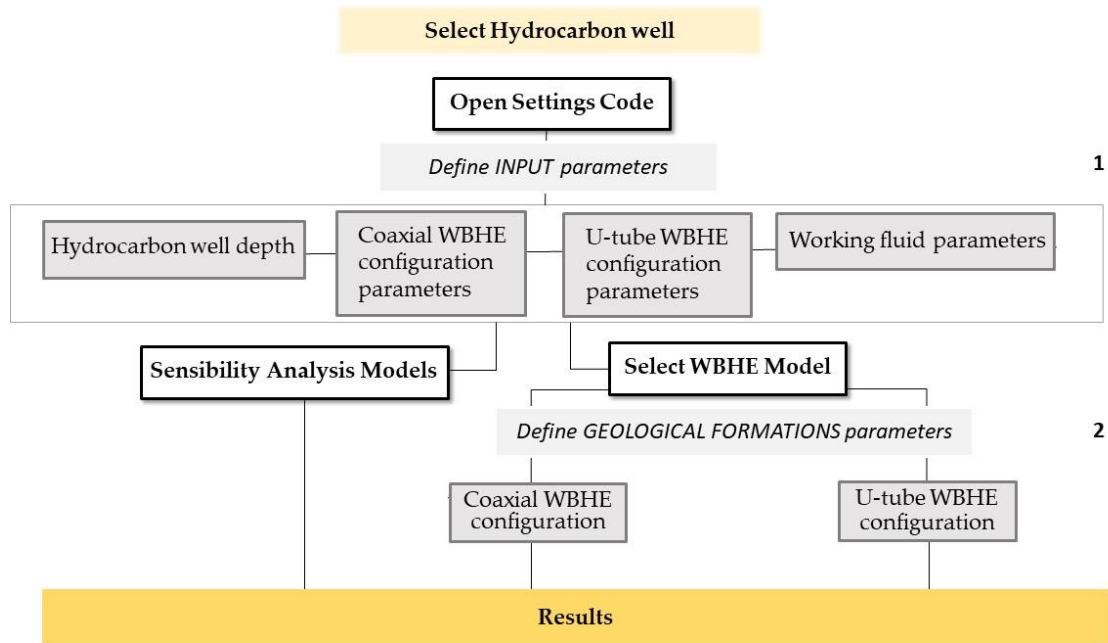


Figure 35 Python codes simplified research flowchart.

The Anaconda distribution of Python was used to manage the developed codes. Besides, the IDE Spyder (included in anaconda) was applied as a graphical interface.

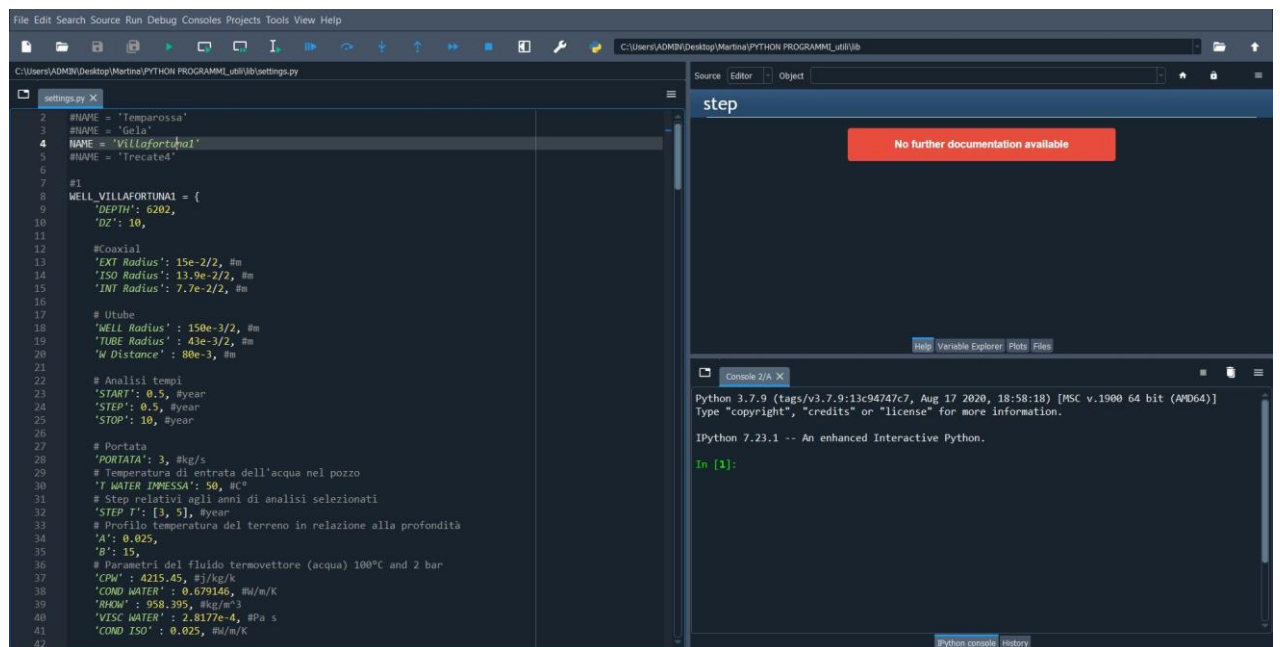
The proposed codes named “Coaxial WBHE configuration” and “U-Tube WBHE configuration” allow the reconstruction of the working fluid temperature profile associated with the selected hydrocarbon well, assessing both the outlet temperature and recoverable thermal energy. Also, “sensibility analysis codes” can be applied for performing specific analyses of the geological parameters' influence on the heat exchange mechanisms between rock-wellbore. Eventually, a specific section in the "sensibility analysis code" is finally dedicated to analysing pressure loss phenomena.

The IDE Spyder user interface, containing the text editor window, allows consultation of the Python codes made available and helps its use and compilation.

The results can be presented in different graphic elaborations. The output values and figures can be easily exported in various electronic formats (e.g., PDF, jpeg, png, Tiff files).

In the repository folder provided are made available for their application:

- Lib folder, which contains the standalone setting.py code (Settings.py code) (Fig.36)
- Source code files: Sensibility.py, Alpha parameter.py (geological formations' thermal properties analysis), Coaxial.py model codes, U-tube.py model codes (Fig.37, 38)



```
2  #NAME = 'Temparossa'
3  #NAME = 'Gela'
4  #NAME = 'Villafortuna1'
5  #NAME = 'Trecate4'
6
7  #1
8  WELL_VILLAFORTUNA1 = {
9      'DEPTH': 6202,
10     'DZ': 10,
11
12     #Coaxial
13     'EXT Radius': 15e-2/2, #m
14     'ISO Radius': 13.9e-2/2, #m
15     'INT Radius': 7.7e-2/2, #m
16
17     # Utube
18     'WELL Radius': 150e-3/2, #m
19     'TUBE Radius': 43e-3/2, #m
20     'W Distance': 00e-3, #m
21
22     # Analisi tempi
23     'START': 0.5, #year
24     'STEP': 0.5, #year
25     'STOP': 10, #year
26
27     # Portata
28     'PORTATA': 3, #kg/s
29     # Temperatura di entrata dell'acqua nel pozzo
30     'T WATER IMPRESSA': 90, #C°
31     # Step relativi agli anni di analisi selezionati
32     'STEP T': [3, 5], #year
33     # Profilo temperatura del terreno in relazione alla profondità
34     'A': 0.025,
35     'B': 15,
36     # Parametri del fluido termovettore (acqua) 100°C and 2 bar
37     'CPM': 4215.45, #J/kg/K
38     'COND WATER': 0.679146, #W/m/K
39     'RHOW': 958.395, #kg/m^3
40     'VISC WATER': 2.8177e-4, #Pa s
41     'COND ISO': 0.025, #W/m/K
42
```

The screenshot shows a Python IDE with a code editor on the left displaying the 'settings.py' file. The code defines a dictionary 'WELL_VILLAFORTUNA1' with various parameters for well depth, radii, time steps, and material properties. On the right, there is a 'step' window with a red error message: 'No further documentation available'. Below that is a console window showing the Python version (3.7.9) and IPython version (7.23.1).

Figure 36 Developed Python Settings.py code structure.

```

116
117
118 #Parametri relativi alle Formazioni geologiche
119 if NAME == 'Temparossa':
120     condrockfunz = lambda bb: 3.0*(bb<2912)+2.34*(bb>=2912)*(bb<depth) #W/m/K
121     rhothrockfunz = lambda bb: 2330*(bb<2912)+1917*(bb>=2912)*(bb<depth) #kg/m^3
122     cprockfunz = lambda bb: 808.6*(bb<2912)+829.4*(bb>=2912)*(bb<depth) #j/kg/K
123     WELL = WELL_TEMPAROSSA
124 elif NAME == 'Villafortuna1':
125     condrockfunz = lambda bb: 0.3*(bb<1258)+1.61*(bb>=1258)*(bb<1405)+3.16*(bb>=1405)*(bb<5493)+3.5*(bb>=5493)*(bb<depth) #W/m/K
126     rhothrockfunz = lambda bb: 1700*(bb<1258)+1890*(bb>=1258)*(bb<1405)+2359*(bb>=1405)*(bb<5493)+2480*(bb>=5493)*(bb<depth) #kg/m^3
127     cprockfunz = lambda bb: 800*(bb<1258)+1693*(bb>=1258)*(bb<1405)+821.111*(bb>=1405)*(bb<5493)+810.484*(bb>=5493)*(bb<depth) #j/kg/K
128     WELL = WELL_VILLAFORTUNA1
129 elif NAME == 'Trecate4':
130     condrockfunz = lambda bb: 1.61*(bb<1632)+2.17*(bb>=1632)*(bb<5106)+2.50*(bb>=5106)*(bb<6189)+2.00*(bb>=6189)*(bb<depth) #W/m/K
131     rhothrockfunz = lambda bb: 1890*(bb<1632)+1801*(bb>=1632)*(bb<5106)+2480*(bb>=5106)*(bb<6189)+2330*(bb>=6189)*(bb<depth) #kg/m^3
132     cprockfunz = lambda bb: 1696*(bb<1632)+830.09*(bb>=1632)*(bb<5106)+810.48*(bb>=5106)*(bb<6189)+821.11*(bb>=6189)*(bb<depth) #j/kg/K
133     WELL = WELL_TREGATE4
134 elif NAME == 'Gela':
135     condrockfunz = lambda bb: 3.16*(bb<2117)+2.17*(bb>=2117)*(bb<2556)+3.12*(bb>=2556)*(bb<2860)+2.17*(bb>=2860)*(bb<depth) #W/m/K
136     rhothrockfunz = lambda bb: 2350*(bb<2117)+1801*(bb>=2117)*(bb<2556)+2480*(bb>=2556)*(bb<2860)+1801*(bb>=2860)*(bb<depth) #kg/m^3
137     cprockfunz = lambda bb: 821.11*(bb<2117)+830.09*(bb>=2117)*(bb<2556)+810.48*(bb>=2556)*(bb<2860)+830.09*(bb>=2860)*(bb<depth) #j/kg/K
138     WELL = WELL_GELA
139 elif NAME == 'Casteggio':
140     condrockfunz = lambda bb: 2.45*(bb<660)+3.28*(bb>=660)*(bb<2212)+2.77*(bb>=2212)*(bb<depth) #W/m/K
141     rhothrockfunz = lambda bb: 1757*(bb<660)+2161*(bb>=660)*(bb<2212)+1787*(bb>=2212)*(bb<depth) #kg/m^3
142     cprockfunz = lambda bb: 1459*(bb<660)+1125*(bb>=660)*(bb<2212)+733.072*(bb>=2212)*(bb<depth) #j/kg/K
143     WELL = WELL_CASTEGGIO
144 elif NAME == 'Comarata':
145     condrockfunz = lambda bb: 3.16*(bb<2362.1)+2.77*(bb>=2362.1)*(bb<2567.1)+3.6*(bb>=2567.1)*(bb<depth) #W/m/K
146     rhothrockfunz = lambda bb: 2399*(bb<2362.1)+2278*(bb>=2362.1)*(bb<2567.1)+2520*(bb>=2567.1)*(bb<depth) #kg/m^3
147     cprockfunz = lambda bb: 821.11*(bb<2362.1)+793.68*(bb>=2362.1)*(bb<2567.1)+807.94*(bb>=2567.1)*(bb<depth) #j/kg/K
148     WELL = WELL_CANVARATA
149
150 #Funzione gradiente geotermico
151 funtzground = lambda z: a*z + b #C
152
153
154
155
    
```

Figure 38 Geological formations' thermal parameters definition section (Python Coaxial.py model structures).

```

35
36 def twat_down_evaluation(zz, step, next, vel, dhydr, portata, cpw, tground, twat_value):
37     twat_down = []
38     for ii in range(len(zz)):
39         condrock:condrockfunz(zz[ii]) #W/m/K
40         rhothrock:rhothrockfunz(zz[ii]) #kg/m^3
41         cprock:cprockfunz(zz[ii]) #j/kg/K
42         alpha = condrock / rhothrock / cprock
43
44         #Il coefficiente totale viene calcolato ogni volta perchè cambia con la profondità.
45         #Il fattore che cambia è la resistenza del terreno poichè i suoi parametri cambiano con la profondità
46         ktot = np.power(next / condrock * np.log(2 * (np.sqrt(alpha * step))/next)) + 1 / funzh(vel, dhydr,-1) #W/m^2/K
47
48         #Scambio termico tra due profondità a distanza dz
49         num1 = dz * 2 * np.pi * next * ktot
50         den1 = portata * cpw
51         aa = (num1 / (2 * den1)) + 1 #st/dz
52
53         #Temperatura acqua dopo scambio termico (vettore di temperatura)
54         twat_value = (num1 / den1 * funtzground(zz[ii]) - dz / 2) - (num1 / (2 * den1)-1) * twat_value) / aa #C°
55         twat_down.append(twat_value)
56     return twat_down
57
58
59 def twat_up_evaluation(zz, twat, step, rint, riso, condiso, portata, cpw):
60
61     #Inverto i vettori perchè ora partiamo dal fondo e risaliamo e quindi quando
62     # noi vogliamo il primo valore di risalita ci dobbiamo riferirci all'ultima
63     # temperatura di discesa
64     zz2 = np.flip(zz) #m
65     twatdalbasso = np.flip(twat)
66     vel2 = portata / (np.pi * np.power(rint,2)) / rhov #m/s
67     hint = funzh(vel2, 2*rint) #W/m^2/K
68     hexttubo = funzh(vel, 2*riso) #W/m^2/K
69
70     #Coeff. di scambio termico comprensivo delle due resistenze convettive e di
71     # quello conduttivo dovuta all'isolante
72     ktotinner = np.power(rint / riso * 1 / hexttubo + rint * np.log(riso / rint) * 1 / condiso + 1 / hint,-1) #W/m^2/K
73     aa1 = (dz * 2 * np.pi * rint * ktotinner / (2 * portata * cpw)) + 1
74
    
```

Figure 37 Developed Python Coaxial.py model general structures.

5.6.3 The Matlab Code

MATLAB is a software for numerical and statistical calculations written in the C programming language. The software work environment consists of six main parts: command prompt where it is possible to insert instructions and define variables; libraries of mathematical functions; graphics system for functions graphs creation; programming language (with intuitive syntax similar to C++); application program interface (for interfacing with other languages and design of graphical interfaces); toolbox (software packages and functions to solve specific problems).

MATLAB R2018b version was used to analyse the WBHEs by implementing the described models (Coaxial and U-tube-WBHE models) in different codes with the general structure illustrated in Figure 39.

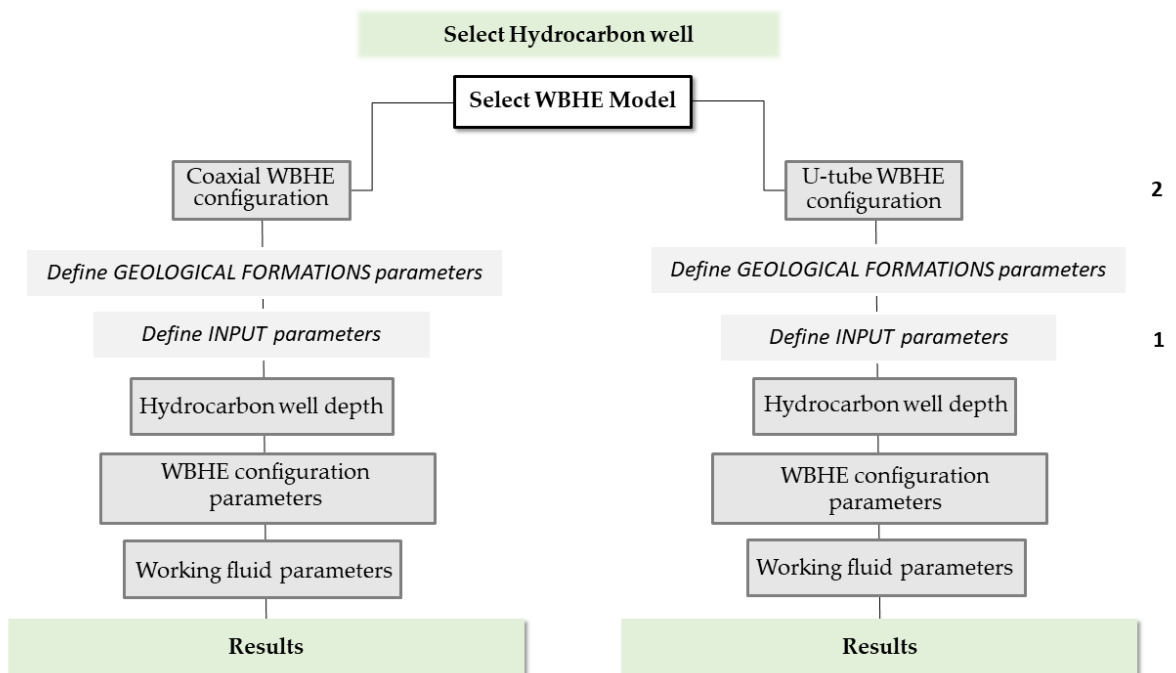


Figure 39 Matlab codes simplified research flowchart.

Unlike the Python codes described above (Chapter 5.6.2), the MATLAB versions are more straightforward in their structure.

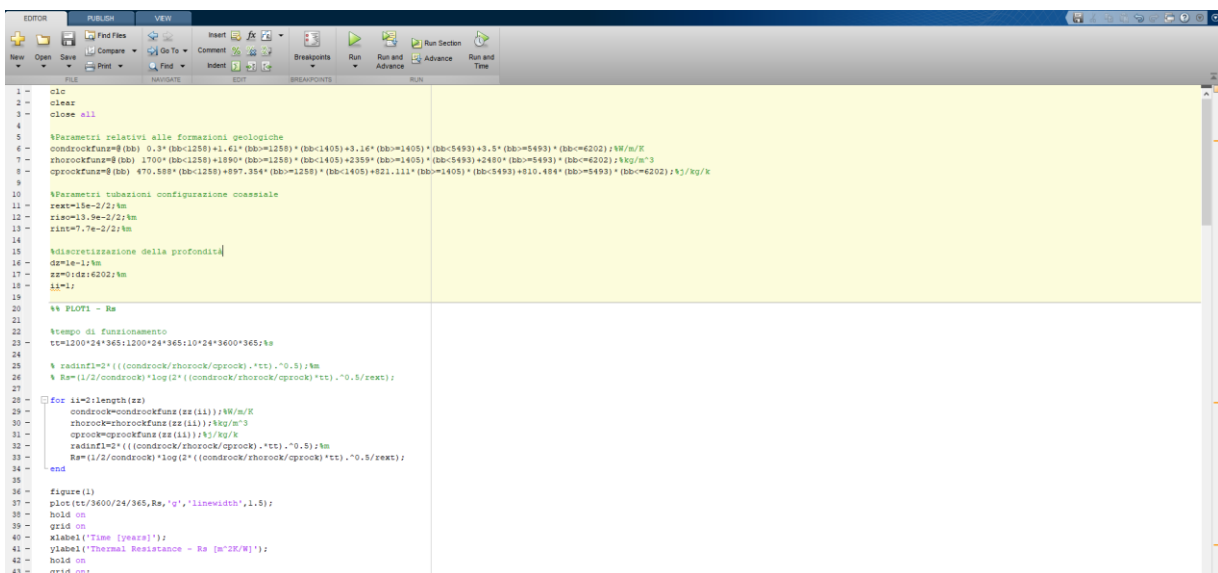
The specific section dedicated to defining the technical input parameters and the one that contains the reconstruction of the geological model with the assignment of the geological formations' thermal parameters are placed within the same main code.

Using the command prompt section of the Matlab software, the information contained in the sections mentioned above can be directly modified and implemented. Therefore, there is no specific external code that collects the input parameters relating to the configuration of the installed well.

As for Python versions, the proposed codes named “Coaxial WBHE configuration” and “U-Tube WBHE configuration” allow the reconstruction of the working fluid temperature profile associated with the selected hydrocarbon well, assessing both the outlet temperature and recoverable thermal energy. The output values and figures can be easily exported in various electronic formats (e.g., PDF, jpeg, png, Tiff files).

In the repository folder provided are made available for their application:

- Coaxial MATLAB model codes, U-tube MATLAB model codes, Pressure losses MATLAB codes (Figs.40 - 41).



```

1 - clc
2 clear
3 close all
4
5 %Parametri relativi alle formazioni geologiche
6 condrockfuns=@(bb) 0.3*(bb-1258)+1.61*(bb-1258)*(bb-1405)+3.16*(bb-1405)*(bb-5493)+3.5*(bb-5493)*(bb-6202);%/m/K
7 zhorockfuns=@(bb) 1700*(bb-1258)+1890*(bb-1258)*(bb-1405)+2359*(bb-1405)*(bb-5493)+2480*(bb-5493)*(bb-6202);%/m^3
8 cprockfuns=@(bb) 470.588*(bb-1258)+897.354*(bb-1258)*(bb-1405)+821.111*(bb-1405)*(bb-5493)+810.484*(bb-5493)*(bb-6202);%/kg/k
9
10 %Parametri tubazioni configurazione coassiale
11 zext=15e-2/2; %m
12 izo=13.5e-2/2; %m
13 rint=7.7e-2/2; %m
14
15 %Iscretizzazione della profondità
16 dz=1e-1; %m
17 zz=@(d):d:6202; %m
18 ii=[];
19
20 %% PLOT1 - Ra
21
22 %tempo di condizionamento
23 ttr=1200*24*365;1200*24*365;10*24*3600*365; %s
24
25 % radinf1=2*((condrock/zhorock/cprock).^tc).^0.5; %K
26 % Ra=(1/2)/condrock*log(2*((condrock/zhorock/cprock).^tc).^0.5/zext);
27
28
29 for ii=2:length(zz)
30     condrock=condrockfuns(zz(ii));%/m/K
31     zhorock=zhorockfuns(zz(ii));%/m^3
32     cprock=cprockfuns(zz(ii));%/kg/k
33     radinf1=2*((condrock/zhorock/cprock).^tc).^0.5; %K
34     Ra=(1/2)/condrock*log(2*((condrock/zhorock/cprock).^tc).^0.5/zext);
35 end
36
37 figure(1)
38 plot(ttr/3600/24/365,Ra,'g','linewidth',1.5);
39 hold on
40 grid on
41 xlabel('Time [years]');
42 ylabel('Thermal Resistance - Ra [m^2K/W]');
43 hold on
44 grid on
  
```

Figure 40 Geological formations' thermal parameters definition section (MATLAB Coaxial model structures).

```

44 %% ANALISI SCAMBIORE
45
46 %water parameters at 100C and 2 bar
47 cpw=4218.46; %/kg/K
48 condw=0.71916; %W/m/K
49 rhow=958.395; %kg/m^3
50 viscw=2.0177e-4; %Pa s
51 %rho=viscw/condw;
52
53 %funz= @(v,drif) rhow*v*drif/viscw;
54 %funzione del calcolo del coeff. convettivo nei tubi. Trovo Russell da
55 %dittus-boelter
56 funz= @(v,drif,raggio) (rho*w*drif/viscw)^0.8*pi^0.4*condw^0.023/(2*raggio);%W/m^2/K
57
58 %coeff. di scambio termico totale comprendendo terreno e parte convettiva nell'anello
59 dhyd= (4*pi*(rext^2-riso^2))/(2*pi*(rext+riso));%m diametro idraulico per il calcolo dei coeff. dimensionali dell'anello
60 areacompi=(rext^2-riso^2);%m^2
61
62 portata=3;%kg/s
63 vel=portata/areaco/rhow;%m/s
64 rext=65;riso=60;%m
65
66 hext=funz(vel,dhyd,dhyd/2);%W/m^2/K
67
68 %profilo temperatura del terreno in relazione alla profondità
69 tground= @(z) 15+0.025*z;%C
70
71 %discretizzazione della profondità
72 dz=1;%m
73 z=0:dz:200;%m
74 il=1;
75
76 %importo la temperatura di entrata dell'acqua nel pozzo
77 twt(il)=50;%C
78 tground(il)=tground(z(il));%C
79
80
81 %loop per profilo temp anello;
82 for il=2:length(z)
83     condrock=condrockfunz(z(il));%W/m/K
84     rhoorock=rhoorockfunz(z(il));%kg/m^3
85     cprock=cprockfunz(z(il));%/kg/K
86
87     %in questo caso il coeff. totale viene calcolato ogni volta perché
88     %cambia con la profondità. Il fattore che cambia è la resistenza del
89     %terreno poiché i suoi parametri cambiano con la profondità
90     ktot=(rext/condrock*log(2*((condrock/rhoorock/cprock)^0.5)/rext)+1/funz(vel,dhyd,dhyd/2))^-1;%W/m^2/K
91     aa=(dz^2*pi*rext*ktot/(2*portata*cpw))+1;

```

```

76 %loop per profilo temp anello;
77 for il=2:length(z)
78     condrock=condrockfunz(z(il));%W/m/K
79     rhoorock=rhoorockfunz(z(il));%kg/m^3
80     cprock=cprockfunz(z(il));%/kg/K
81
82     %in questo caso il coeff. totale viene calcolato ogni volta perché
83     %cambia con la profondità. Il fattore che cambia è la resistenza del
84     %terreno poiché i suoi parametri cambiano con la profondità
85     ktot=(rext/condrock*log(2*((condrock/rhoorock/cprock)^0.5)/rext)+1/funz(vel,dhyd,dhyd/2))^-1;%W/m^2/K
86     aa=(dz^2*pi*rext*ktot/(2*portata*cpw))+1;
87
88     % il=il+1;
89     twt(il)=(dz^2*pi*rext*ktot/(portata*cpw)+tground(z(il)-dz/2)-(dz^2*pi*rext*ktot/(2*portata*cpw)-1)*twt(il-1))/aa;%C
90     tground(il)=tground(z(il));%C
91 end
92
93
94 %inverto i vettori perché ora parliamo dal fondo e risaliamo e quindi quando
95 %noi vogliamo il primo valore di risalita ci dobbiamo riferire all'ultima
96 %temperatura di discesa
97 sz=flip(z);%m
98 twtdalbaso=flip(twt);%C
99 vel=portata/(pi*rint^2)/rhow;%m/s
100 hint=funz(vel,2*rint,rint);%W/m^2/K
101 hextsub=funz(vel,2*riso,riso);%W/m^2/K
102 condiso=0.023; %W/m/K
103
104 %coeff di scambio termico complessivo delle due resistenze convettive e di
105 %quella conduttiva dovuta all'isolante
106 ktotinner=(riso/riso-1)/hextsub+rint*log(rint/riso)^-1/(condiso+1/hint)^-1;%W/m^2/K
107
108 aa1=(dz^2*pi*rint*ktotinner/(2*portata*cpw))+1;
109
110 %loop per l'acqua che torna in superficie il primo valore è uguale
111 %all'ultimo del calcolo per l'acqua che arriva al fondo
112 twt1(il)=twt(il);%C
113
114 for j=2:length(z2)
115     twt1(j)=(dz^2*pi*rint*ktotinner/(portata*cpw)+((twtdalbaso(j)-1)+twtdalbaso(j))/2)-(dz^2*pi*rint*ktotinner/(2*portata*cpw)-1)*twt1(j-1))/aa1;%C
116 end
117
118
119
120 % edito il diagramma del terreno in relazione al profilo di temperatura
121 % dell'acqua (discesa e risalita) riferita al primo ciclo cioè considerando
122 % il tubo interno stabilizzato
123
124

```

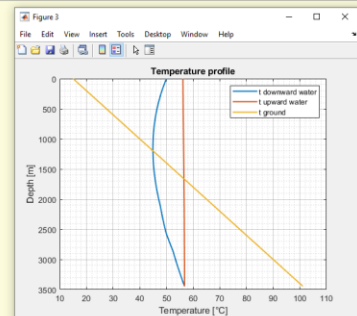


Figure 41 Developed MATLAB Coaxial model general structures (MATLAB Editor).

Chapter 6

Results

The heat exchange models described and implemented in the above-proposed MATLAB and PYTHON software were applied to several Italian hydrocarbon wells. Wells from three main Italian hydrocarbon fields were selected: the Villafortuna–Trecate field (Po Plain, Northwestern Italy), the Val d’Agri-Tempa Rossa field (Southern Apennines), and the Gela field (Southern Sicily). The purpose was to examine heat exchange mechanisms in different Italian hydrocarbon fields, emphasising how the quantity of the potentially extracted thermal energy can change based on:

- Geological and depositional context
- Geothermal closed-loop system selected (Coaxial and/or U-tube WBHEs)

Stratigraphic information and temperature data visualization related to the selected hydrocarbon wells, have been found on the Italian National Geothermal Database (BDNG), the most extensive collection of Italian geothermal data introduced in Chapter 4.2.3. Moreover, technical information regarding productive and dismissed oil and gas wells were also available on the National Mining Office of the Italian Ministry for Economic Development (MISE) and the website of the VIGOR project, promoted by MISE-DGRME (Direzione Generale Risorse Minerarie ed Energetiche) and the Italian Geological Society and the Assomineraria Association.

For properly defining the thermophysical parameters of the associated geological formations, values defined by Pasquale et al., 2011 and Sipio, 2016 and described in Chapter 4.2.2 were used. For both the Coaxial and U-tube models depicted, the assumption that the thermophysical parameters (rock density, volumetric heat capacity and thermal conductivity) are constant values, as described in Kujawa et al. (2005,

2006), Bu et al. (2012, 2014) and Alimonti and Soldo (2016) has been overcome. The stratigraphic data of each case study analysed were considered and implemented in the elaborated models.

The final use of the potentially accumulated thermal energy was considered possible for direct applications through a cascade-type plant system, which can provide specific thermal energy amounts to different production cycles in manufacturing, agricultural and recreational districts. Considering, specifically, the examples of disused Italian hydrocarbon wells selected, as they are located far from inhabited areas, it was therefore not generally possible to hypothesize the use of the extracted thermal energy for building heating purposes. From this consideration derived some of the choices made in defining the input parameters relating to the working fluid features considered (i.e., working fluid inlet flow rate, working fluid inlet temperature).

For the presentation of the below-proposed results, the graphic outputs produced applying the Python code version described in Chapter 5.6.2. were used.

The results contained in the subsequent sections of the Chapter 6 are partially described in the published articles of Gizzi et al., 2021 and Gizzi, 2021 which focused on the analysis of heat exchange mechanisms in different Italian oil fields, emphasizing that the quantity of the potentially extracted thermal energy can change based on depositional context and the selected WBHE technology.

6.1 Influence of ground's thermal properties

During the first phase of work, a preliminary analysis was performed on the thermal properties of the sedimentary geological formations. The purpose was to define the extent of the variation in the thermal outputs as a consequence of the variations in the input data of such ground properties.

Starting from the study of Equation 9, describing the thermal resistance value due to conductive heat transfer, we proceeded to the graphic elaboration of the variation curves of the resistance parameter over time. Figures 42 – 44 describe the variation in R_s parameter when the values of density (ρ), volumetric heat capacity (ρc_s) and the thermal conductivity of rock (λ_s), respectively, change. Moreover, an evaluation of the impact of thermal diffusivity value (α) variation in the R_s parameter was reported in Figure 45. Different input values associated with thermal properties subject to the performed analysis were chosen to adequately cover a significant range for sedimentary geological formations involved.

The ground's thermal properties directly influence ground resistance values (R_s). As a consequence, estimated outlet temperature values can be significantly modified by selected ground properties values. The most significant wellhead temperature variation is caused by changes in thermal conductivity values (λ_s) (Fig.44).

Implementing thermal properties values of geological formations (case studies-specific stratigraphy) is fundamental for improving the performed heat exchange analysis using the proposed models.

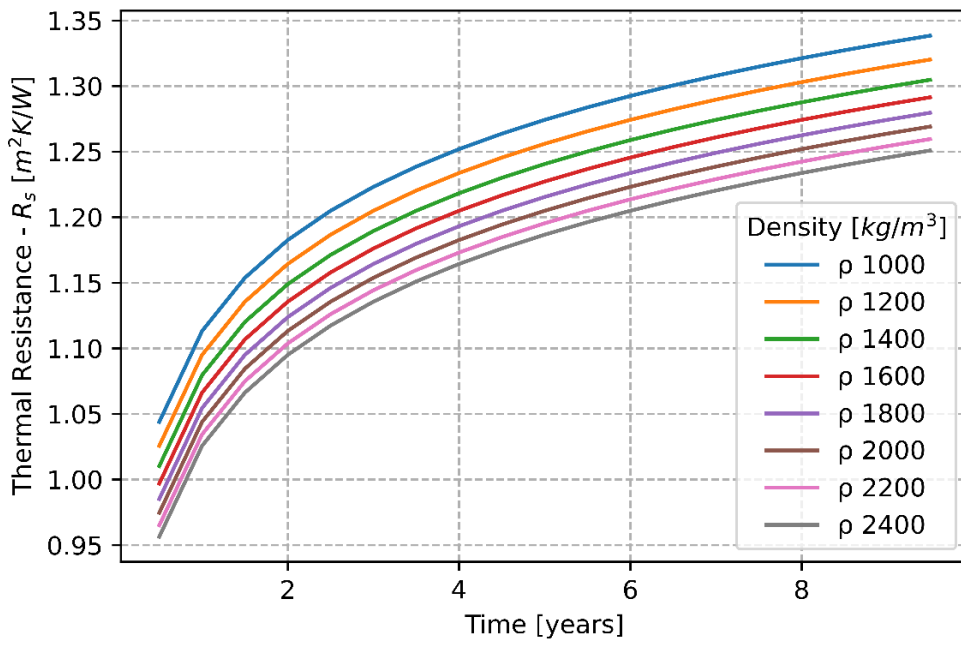


Figure 43 Thermal resistance over time with different ground density values (ρ – kg/m^3).

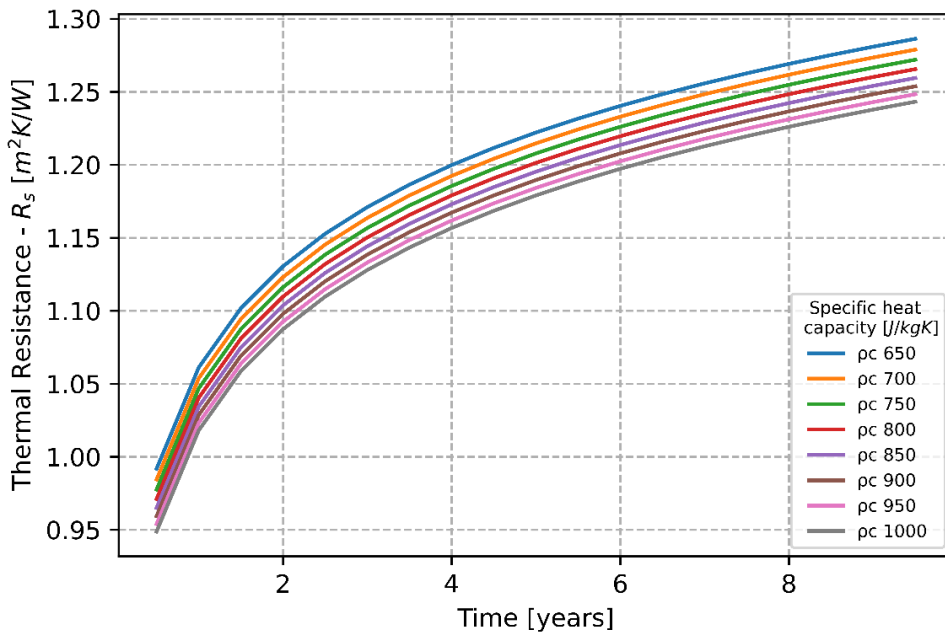


Figure 42 Thermal resistance over time with different specific heat values (ρc rock - J/kgK).

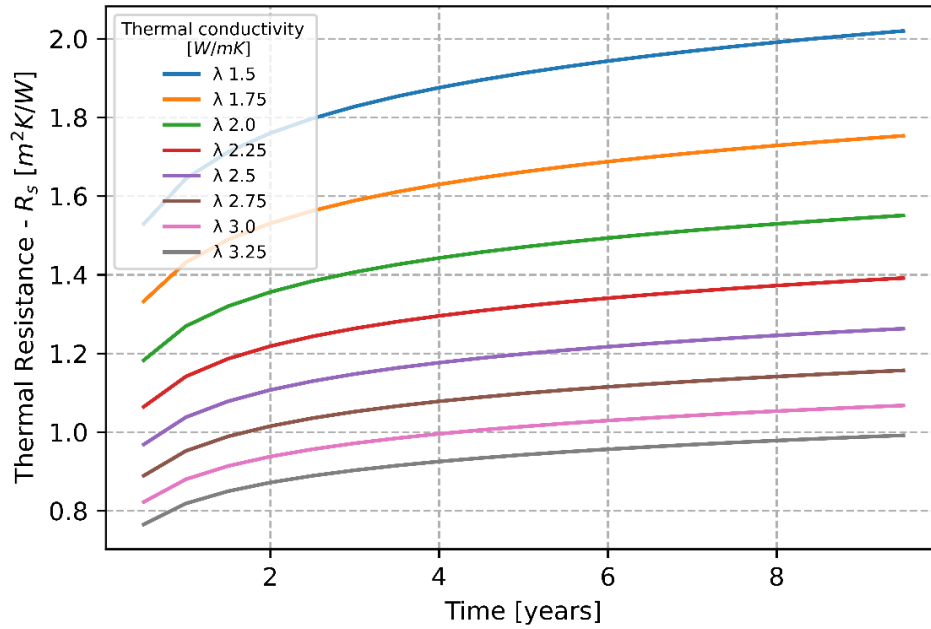


Figure 44 Thermal resistance over time with different conductivity values (λ_s – W/mK).

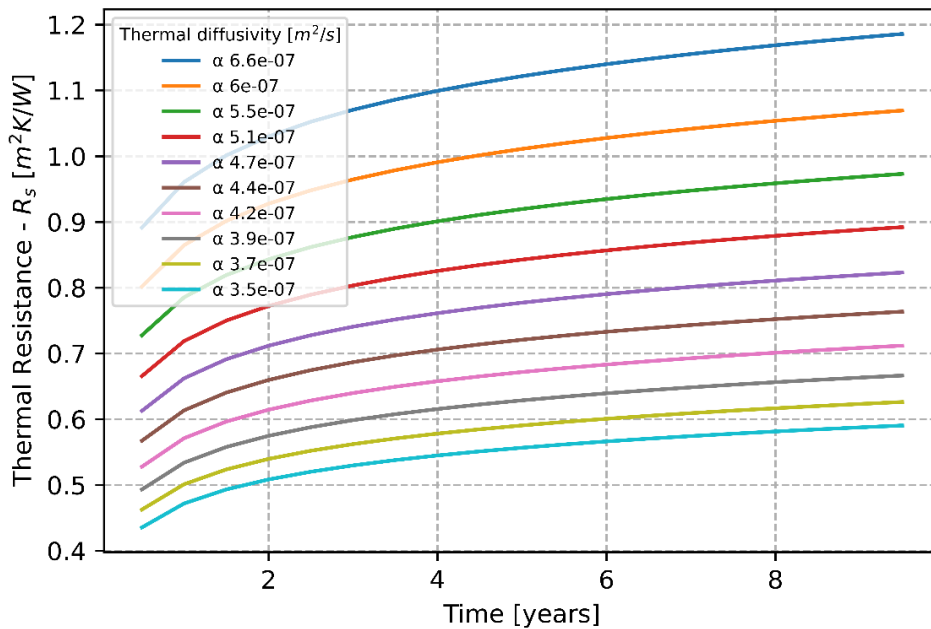


Figure 45 Thermal resistance over time with different thermal diffusivity (α).

6.2 The Villafortuna–Trecate Field

As reported in Chapter 3.1, various petroleum systems have been identified in Italy due to its complex geological and sedimentary history. The Villafortuna–Trecate field is located in the Piedmont Region, between the municipalities of Trecate, Romentino and Galliate. The hydrocarbon system represents one of the most significant oil accumulations of the Italian Middle Triassic carbonate petroleum system (see Chapter 3.1.1). The petroleum system is developed inside the Triassic geological succession. It involves dolomitized platform units of the Late Triassic–Early Jurassic that were charged by Middle Triassic carbonate source rocks deposited in the confined basins created by rifting. Generally, the main reservoir associated with the Villafortuna-Trecate field is identified to be at a depth between 5800 m and 6100 m, with an available temperature of approximately 160–170 °C (Bello & Fantoni, 2002; Gizzi, 2021). Due to its depth can be pursued only in the outer sector of the foredeeps and in foreland regions (the Piedmont area), whereas along the thrust belt it is generally too deep to be reached (the Po Plain).

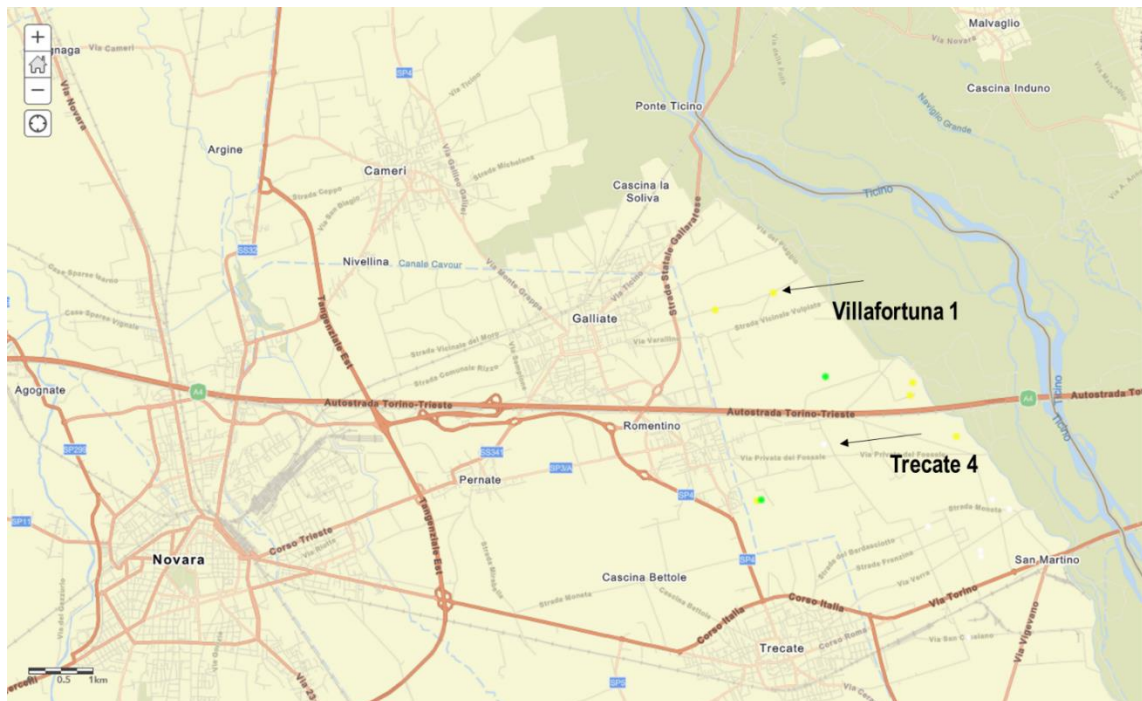


Figure 46 Villafortuna 1 and Trecate 4 hydrocarbon wells location (Villafortuna-Trecate Oilfield, Western Po Plain).

In order to analyse the potential heat exchange performances associated with hydrocarbon wells inside the Villafortuna-Trecate field, the attention was focused on two different disused hydrocarbon wells named Villafortuna 1 and Trecate 4, which are both located in the North-eastern sector of the Piedmont Region, Italy (Fig.46; Tabs.11, 13).

6.2.1 Villafortuna 1 hydrocarbon well

As can be noted by analysing data related to the geological and litho-stratigraphic units and temperature data visualization reported in Tab.12 and Fig.47, the stratigraphic succession associated with the Villafortuna 1 hydrocarbon well is mainly composed of clastic sedimentary and carbonate rocks. The maximum depth reached by the analysed well is equal to 6202 m, with temperatures reaching 165°C.

Table 11 Villafortuna 1 hydrocarbon well (Villafortuna Trecate Oilfield, Western Po Plain) - technical data available on VIDEPI project website

<i>State</i>	<i>Productive, not supplying well</i>
<i>Mineral</i>	<i>OIL</i>
<i>Location</i>	<i>Piemonte Region</i>
<i>Latitude</i>	<i>45,484311</i>
<i>Longitude</i>	<i>8,73465</i>
<i>Field</i>	<i>VILLAFORTUNA</i>
<i>Central</i>	<i>TRECATE CENTRO OLIO</i>
<i>Title</i>	<i>VILLAFORTUNA-TRECATE</i>
<i>Operator</i>	<i>ENI</i>

Table 12 Villafortuna 1 hydrocarbon well - lithostratigraphic profile

<i>Depth</i>	<i>Litho-stratigraphic formation</i>	<i>Age</i>	λ_s	ρc_s	ρ
<i>m</i>			<i>W/mK</i>	<i>J/kg/K</i>	<i>kg/m³</i>
609	<i>Terrigenous sedimentary deposits</i>	<i>Holocene/Upper Pleistocene</i>	0.30	800	1700
1258	<i>Sand (dry)</i>	<i>Pleistocene</i>	0.30	800	1700
1405	<i>Clay Sand</i>	<i>Lower Pliocene</i>	1.61	1696	1890
5493	<i>Clastic sedimentary rocks (Sandstone, Conglomerates and Silty Marl)</i>	<i>Aquitanian - Albian</i>	3.16	821.11	2359
6202	<i>Carbonate rocks - Calcarenite/Dolostone</i>	<i>Lower Cretaceous - Middle Triassic</i>	3.50	810.48	2480

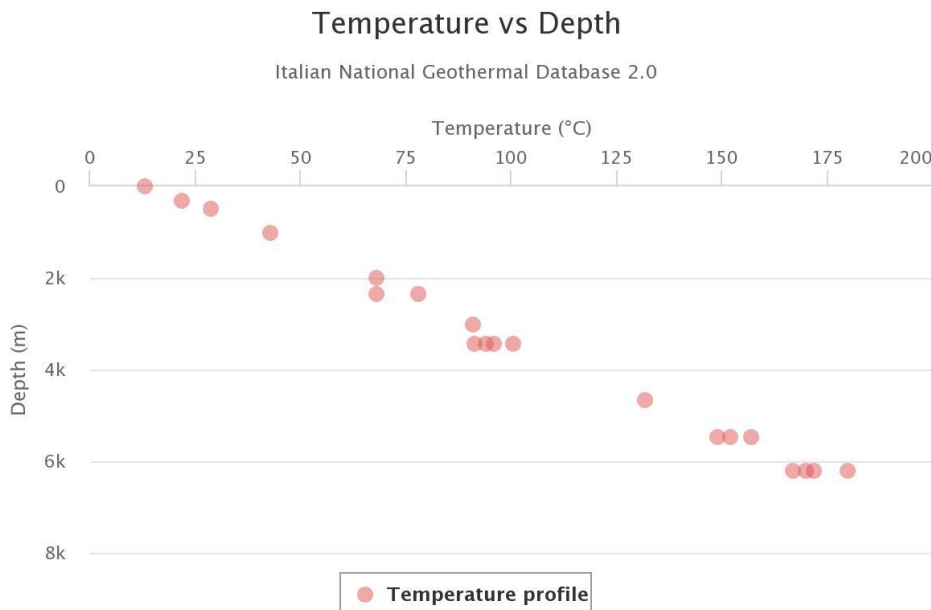


Figure 47 Temperature data visualisation for the Villafortuna 1 hydrocarbon well: Depth (m); Temperature (°C).

Coaxial and U-tube WBHE Configurations

The temperature profiles associated with the described Coaxial and U-tube WBHE system configurations were obtained using the specific ground properties of the selected case study (**Villafortuna 1 hydrocarbon well**) reported in Table 12. Moreover, the

thermal conductivity value of the insulating material was set to 0.025 W/mK. Working fluid inlet flow rate (water) and temperature values were considered 3.0 kg/s and 50°C, respectively. This selected inlet temperature is a typical value for direct applications like production cycles in manufacturing and agricultural districts (Kaczmarczyk et al., 2020). Subsequently, an analysis was conducted on the working fluid temperature's value at the outlet as the inlet flow rate varies.

In the first section of an external pipe of a **Coaxial WBHE system**, the downward fluid is in thermal contact with both the ground on one side and the upward tube on the other. Analysing the temperature profile associated with the coaxial WBHE system configuration considered and implemented within the Villafortuna 1 hydrocarbon well, it is possible to see how, in the first portion of the borehole (1400 m), the selected thermo-vector fluid seems to keep its temperature constant (50°C). The presence of a thick stratigraphic horizon made up of terrigenous sedimentary deposits, characterized by very low conductivity and specific heat values, influences the heat exchange negatively.

As the downward profile line crosses the underground temperature line, the natural heating process begins, and the ground contribution becomes positive. Due to the presence of the insulating material, the heat exchange coefficient between tubes turns out to be minimal, and the increase in working fluid temperature can be associated with the ground's contribution (Fig.48).

Using the fixed inlet working fluid's temperature (50°C), for Coaxial WBHE, the maximum recorded T (°C) outlet temperature is equal to 103.65°C. The thermal power value was evaluated at 678.85 kW.

The inlet flow rate strongly influences the temperature of the wellhead thermal fluid and, consequently, the heat power amount. As observed in Figure 49, considering inlet flow rate values between 0.5 and 1.0 kg/s, the output fluid temperature increases to about 155°C. Consequently, for the specific case study and associated plant configuration, it is possible to identify an inlet flow rate value that potentially optimizes the wellhead fluid's temperature.

Considering the **U-tube WBHE configuration** and its associated temperature profile, it was possible to identify how the ground's contribution was responsible for a sizable temperature variation, both in the downward and upward tube. The fluid was only slightly cooled by the ground over the first borehole section (approximately 1200 m). Subsequently, as the temperature profile line crossed the underground temperature line, the trend was inverted, and the heat carrier fluid temperature began to increase, reaching a maximum temperature value of 94.75°C at a depth of 3000m (upward flow) (Fig.51). As for the considered Coaxial WBHE configuration, the wellhead thermal fluid temperature in the U-tube system changes as the input flow rate parameter varies. For a flow rate value of 1.6 kg/s, the fluid reaches the surface at a maximum temperature of 95.67°C. For higher flow rate values, the recorded wellhead temperatures are progressively lower (Fig.52).

Using the fixed inlet working fluid temperature (50°C) and the estimated fluid temperature at the outlet for the U-tube configuration, the thermal power value was evaluated for 495.43 kW (89.44°C - U-tube WBHE).

Considering a cascading exploitation mode of the heat accumulated by the working fluid in Villafortuna 1 WBHEs, it is possible to hypothesize a multi-variant and comprehensive use of the resource. The outflow temperatures of working fluids at the wellhead for Coaxial and U-tube WBHEs are 103.65°C and 89.44°C, respectively, which allows it to progressively be used for greenhouse heating (100–80°C), food industry (80–70°C), animal breeding (60°C), biomass and agricultural cultures (<50°C).

As mentioned above, the inlet flow rate value strongly influenced the temperature of the wellhead thermal fluid. In both cases, it is possible to identify an inlet flow rate value (kg/s) to obtain a higher fluid temperature at the outlet, optimizing the quantity of extracted thermal power (kW) (Figs.50, 53). However, for the WBHE systems like those analysed, such low inlet flow rates (0.5 – 1.5 kg/s) may not be technically appropriate. The heat-exchange modalities are not the only aspect that must be considered to carry out the correct analysis of the heat transfer mechanisms associated with WBHEs. According to what was reported in Chapter 5.5, pressure loss phenomena need to be analysed as they affect pumping costs and are not negligible in managing a closed-loop geothermal system.

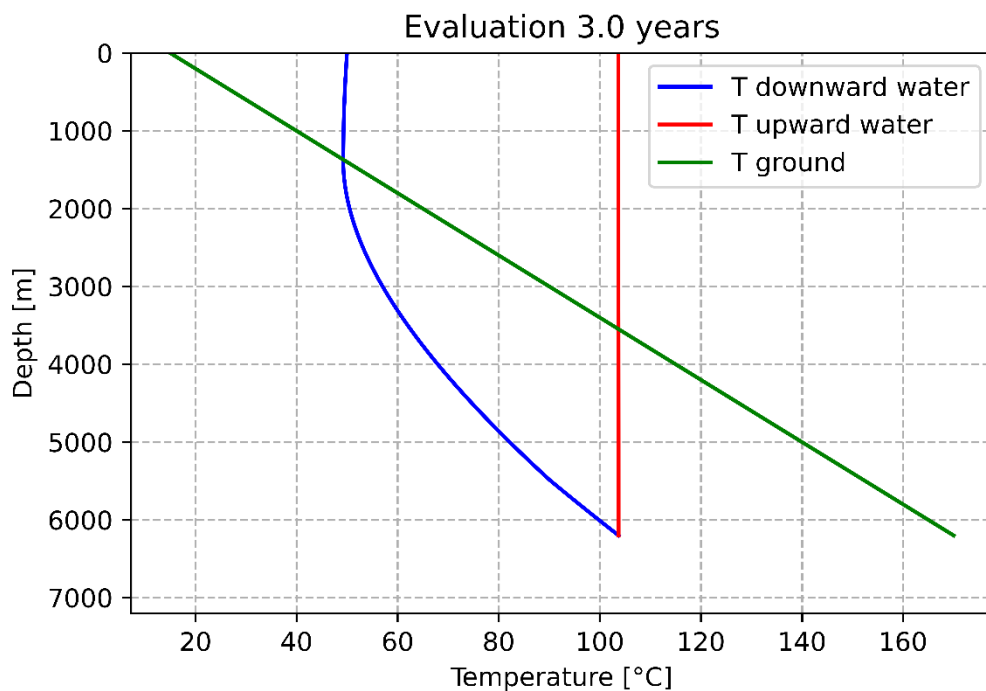


Figure 48 Temperature profile associated with the Coaxial WBHE configuration considering site-specific stratigraphy (Villafortuna 1 hydrocarbon well).

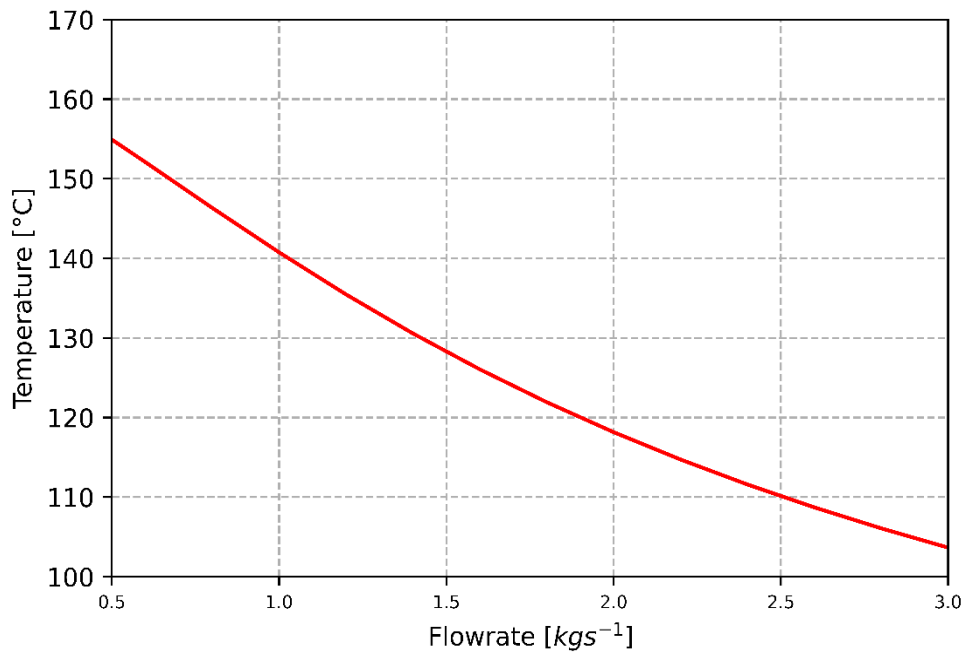


Figure 49 Wellhead temperature as the flow rate value changes: Coaxial WBHE (Villafortuna 1 hydrocarbon well).

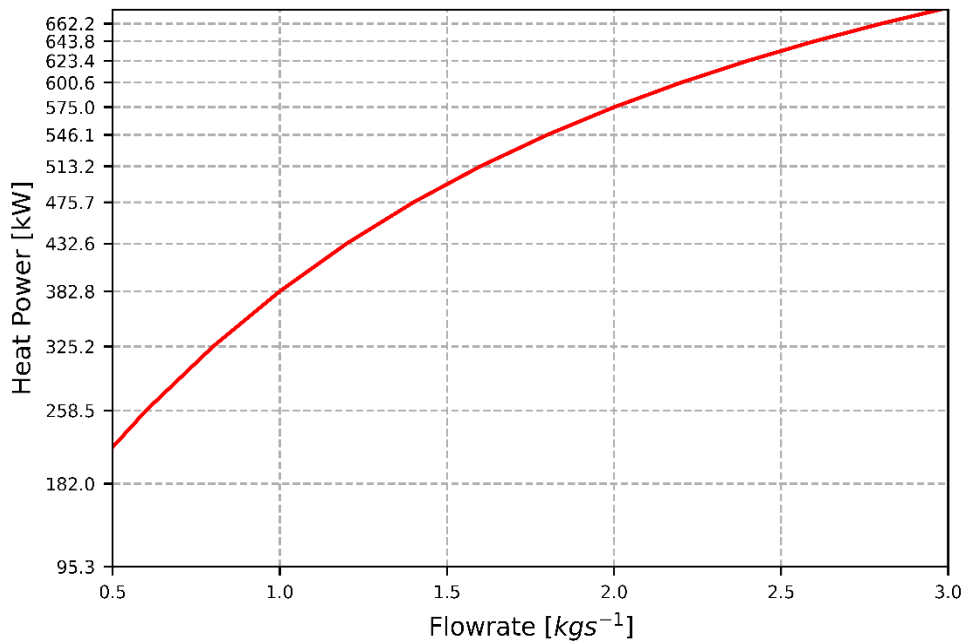


Figure 50 Heat Power as the flow rate value changes: Coaxial WBHE (Villafortuna 1 hydrocarbon well).

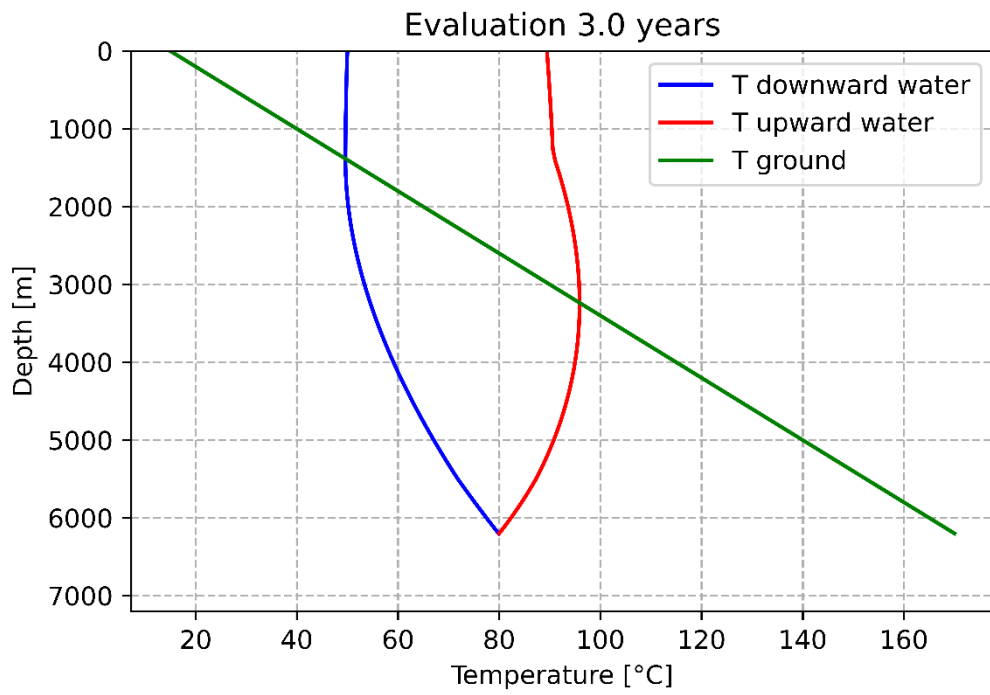


Figure 51 Temperature profile associated with the U-tube WBHE (b) configuration considering site-specific stratigraphy (Villafortuna 1 hydrocarbon well).

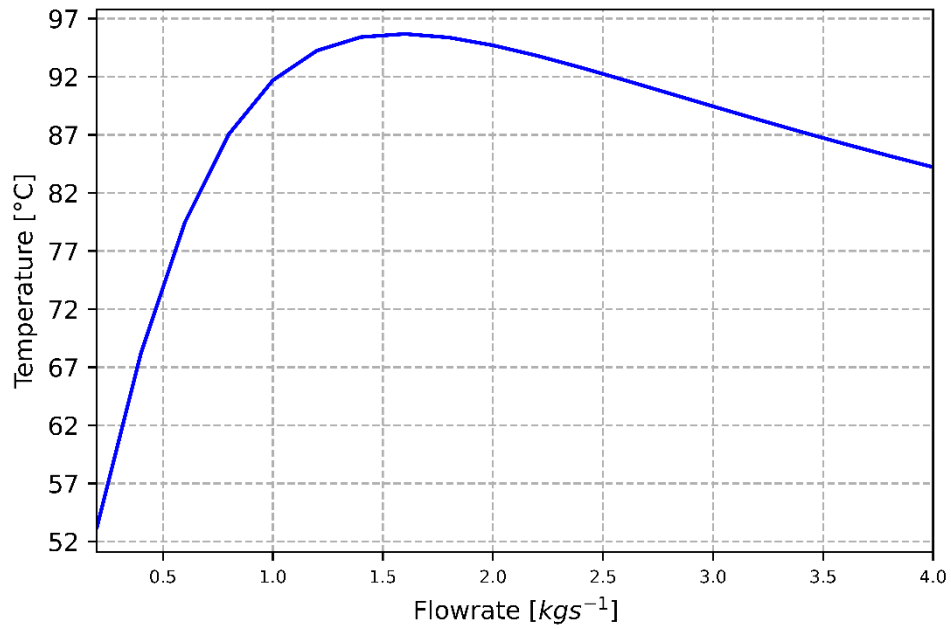


Figure 52 Wellhead temperature as the flow rate value changes: U-tube WBHE (Villafortuna 1 hydrocarbon well).

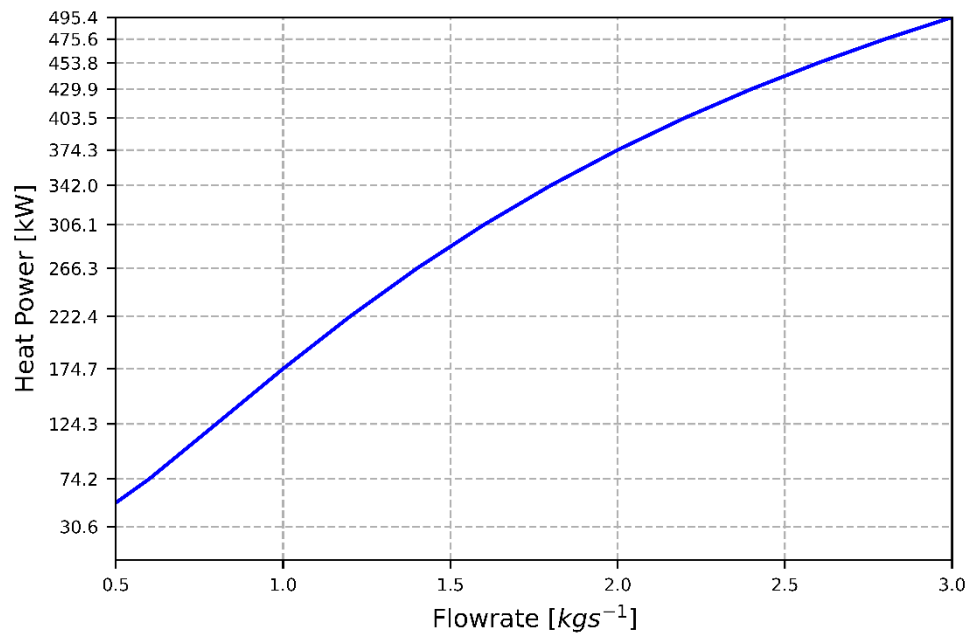


Figure 53 Heat Power as the flow rate value changes: U-tube WBHE (Villafortuna 1).

6.2.2 Trecate 4 hydrocarbon well

The analysis was subsequently carried out on the geothermal performances associated with the Trecate4 hydrocarbon well, located within the Villafortuna-Trecate oilfield as the Villafortuna 1 one.

According to data related to the litho-stratigraphic units reported in Tab.14, the geological formations associated with the Trecate4 well are mainly composed of carbonate platform rocks, except for a surface unit consisting of terrigenous deposits. The analysed well has a maximum depth of 6282 m and bottom-hole temperatures reaching 168 °C (Fig.54).

Table 13 Trecate 4 hydrocarbon well (Villafortuna-Trecate Oilfield, Western Po Plain) - technical data available on VIDEPI project website

<i>State</i>	<i>Monitoring well</i>
<i>Mineral</i>	<i>OIL</i>
<i>Location</i>	<i>Piemonte Region</i>
<i>Latitude</i>	<i>45,462917</i>
<i>Longitude</i>	<i>8,744833</i>
<i>Field</i>	<i>VILLAFORTUNA</i>
<i>Title</i>	<i>VILLAFORTUNA-TRECATE</i>
<i>Operator</i>	<i>ENI</i>

Table 14 Trecate4 hydrocarbon well - lithostratigraphic profile

<i>Depth</i>	<i>Litho-stratigraphic formation</i>	<i>Age</i>	λ_s	ρc_s	ρ
<i>m</i>			<i>W/mK</i>	<i>J/kg/K</i>	<i>kg/m³</i>
1632	<i>Terrigenous sedimentary deposits - Sandy Clay</i>	<i>Holocene/Upper Pleistocene</i>	1.61	1696	1890
5451	<i>Calcareous Marl</i>	<i>Upper Eocene</i>	2.17	830	1801
6189	<i>Carbonate rocks - Calcareenite/Dolostone</i>	<i>Upper Cretaceous - Upper Triassic</i>	3.50	810.48	2480
6282	<i>Clastic sedimentary rocks – Argillaceous Sandstone</i>	<i>Middle Triassic</i>	3.00	821.11	2330

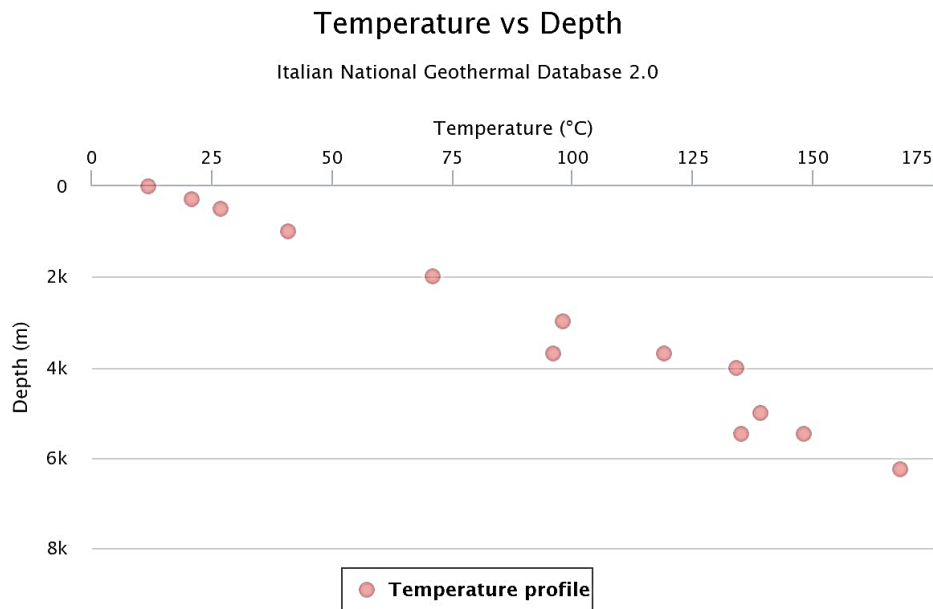


Figure 54 Temperature data visualisation for the Trecate4 hydrocarbon well: Depth (m); Temperature (°C).

Coaxial and U-tube WBHE Configurations

The temperature profiles associated with the described Coaxial and U-tube WBHE system configurations were obtained using the specific ground properties of the selected case study (Trecate4 hydrocarbon well) reported in Table 14. Moreover, the thermal conductivity value of the insulating material was set to 0.025 W/mK. Working fluid inlet flow rate (water) and temperature values were considered 3.0 kg/s and 50°C,

respectively. An analysis was also conducted on the working fluid temperature at the outlet as the inlet flow rate varies.

For the **Coaxial WBHE configuration**, over the first 1200 m downwards, the selected thermo-vector fluid decreases in temperature. As the downward profile line crosses the underground temperature line, the natural heating process begins, and the ground contribution becomes positive. Due to the presence of the insulating material, the heat exchange coefficient between tubes turns out to be lower, and the increase in working fluid temperature can be associated with the ground (Fig.55).

In Coaxial WBHE, the outlet recorded temperature is equal to 98.6°C. The inlet flow rate strongly influences the temperature of the wellhead thermal fluid and, consequently, the heat power amount. As observed in Figure 56, considering inlet flow rate values between 0.5 and 1 kg/s, the output fluid temperature increases to about 155°C. Consequently, for the specific case study and associated plant configuration, it is possible to identify an inlet flow rate value that potentially optimizes the wellhead temperature.

Considering the **U-tube WBHE configuration** and its associated temperature profile, it was possible to identify how the ground's contribution was responsible for a sizable temperature variation, both in the downward and upward tube. The fluid was slightly cooled by the ground over the first borehole section (approximately 1200 m). Subsequently, as the temperature profile line crossed the underground temperature line, the trend was inverted, and the heat carrier fluid temperature began to increase, reaching an outlet temperature value of 84°C (Fig.58). As for the considered Coaxial WBHE configuration, the wellhead thermal fluid temperature in U-tube WBHE changes as the input flow rate parameter varies. For a flow rate value of 1.6 kg/s, the fluid reaches the surface at a maximum temperature of 89°C. For higher flow rate values, the wellhead temperatures recorded are progressively lower (Fig.59).

Using the fixed inlet working fluid temperature (50°C) and the estimated maximum fluid temperature at the outlet for the different configurations, thermal power values were evaluated for 616.7 kW (98.6 °C - Coaxial WBHE) and 427.9 kW (84 °C - U-tube WBHE) (Figs. 57, 60). Considering a cascading exploitation mode of the heat accumulated, also for Trecate 4 WBHEs, it is possible to hypothesize a multi-variant and extensive resource use. The outflow temperatures of working fluids at the wellhead for Coaxial and U-tube WBHEs are 98.6 °C and 84 °C, respectively, which allows it to progressively be used for greenhouse heating (100–80°C), food industry (80–70°C), animal breeding (60°C), biomass and agricultural cultures (<50°C).

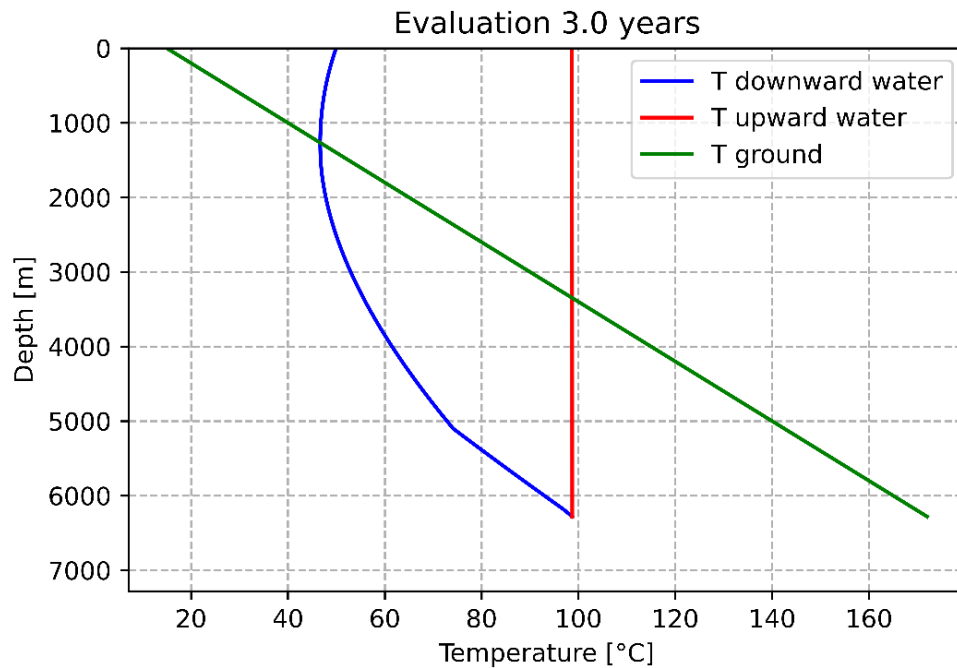


Figure 55 Temperature profile associated with the coaxial WBHE configuration considering site-specific stratigraphy (Trecate4 hydrocarbon well).

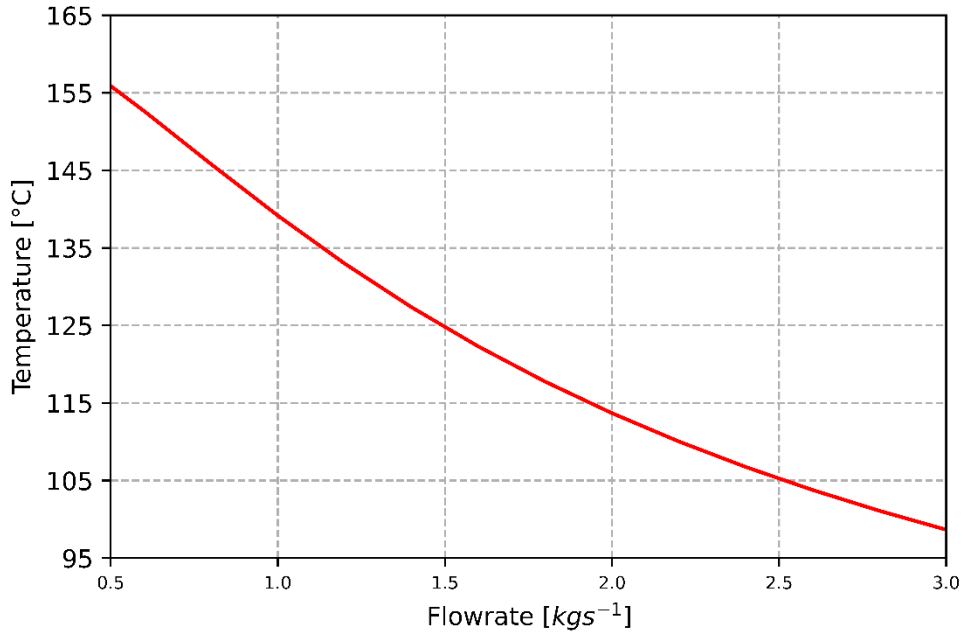


Figure 56 Wellhead temperature as the flow rate value changes: Coaxial WBHE (Trecate4 hydrocarbon well).

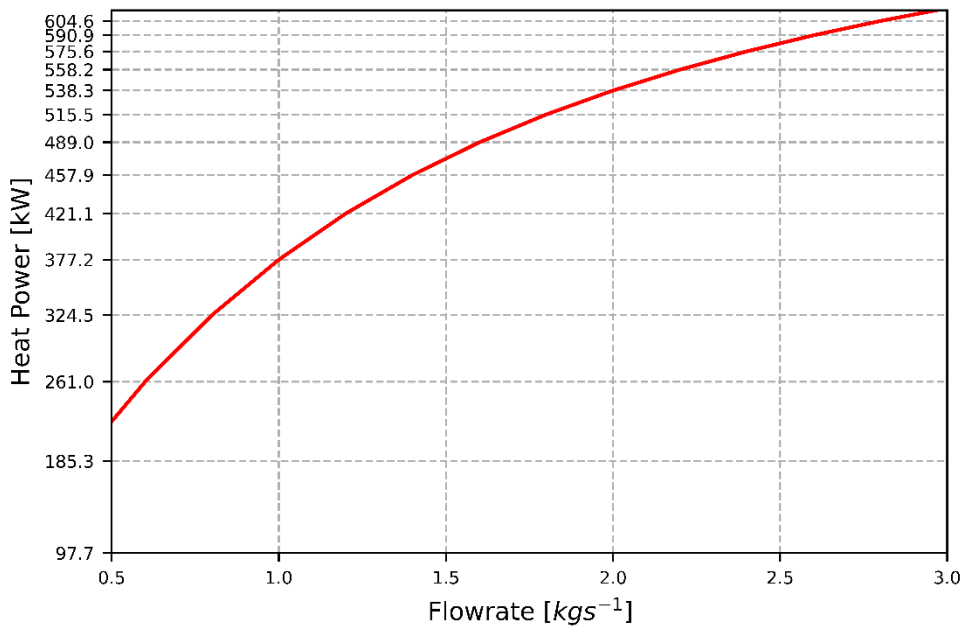


Figure 57 Heat Power as the flow rate value changes: Coaxial WBHE (Trecate4 hydrocarbon well).

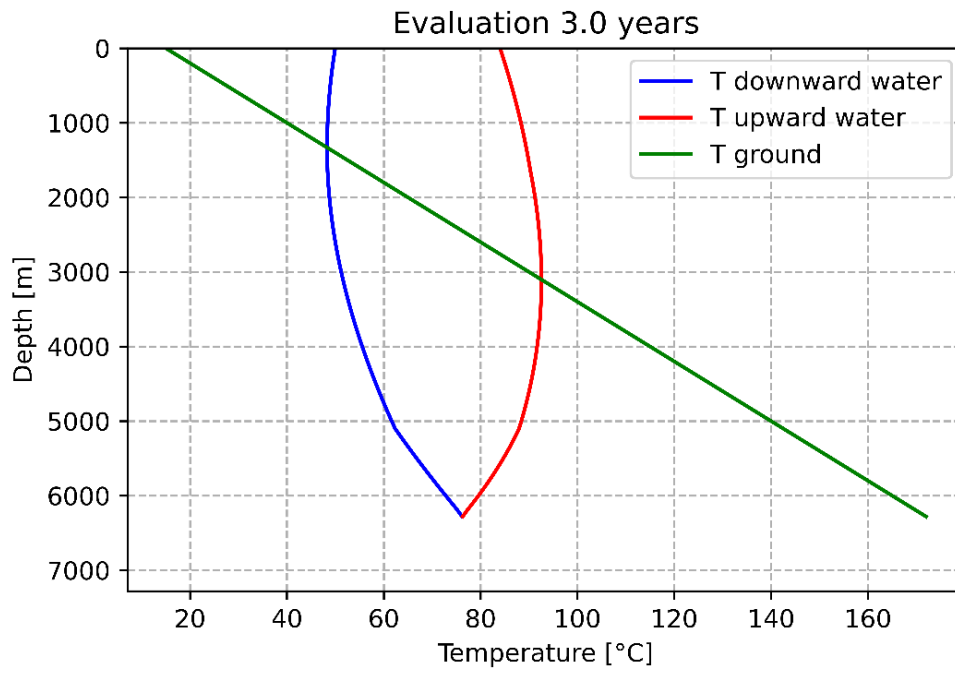


Figure 58 Temperature profile associated with the U-tube WBHE (b) configuration considering site-specific stratigraphy (Trecate4 hydrocarbon well).

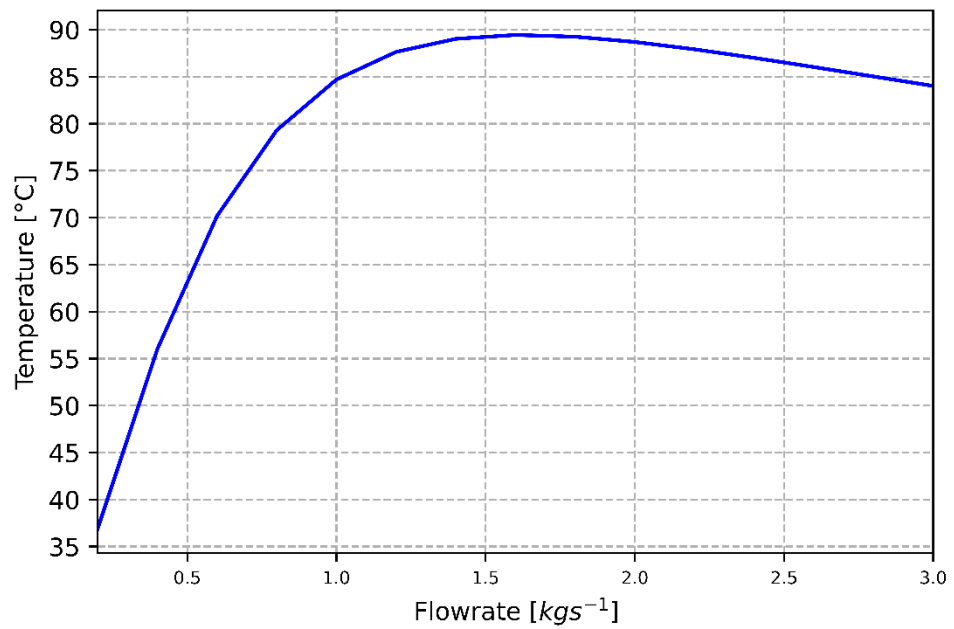


Figure 59 Wellhead temperature as the flow rate value changes: U-tube WBHE (Trecate4 hydrocarbon well).

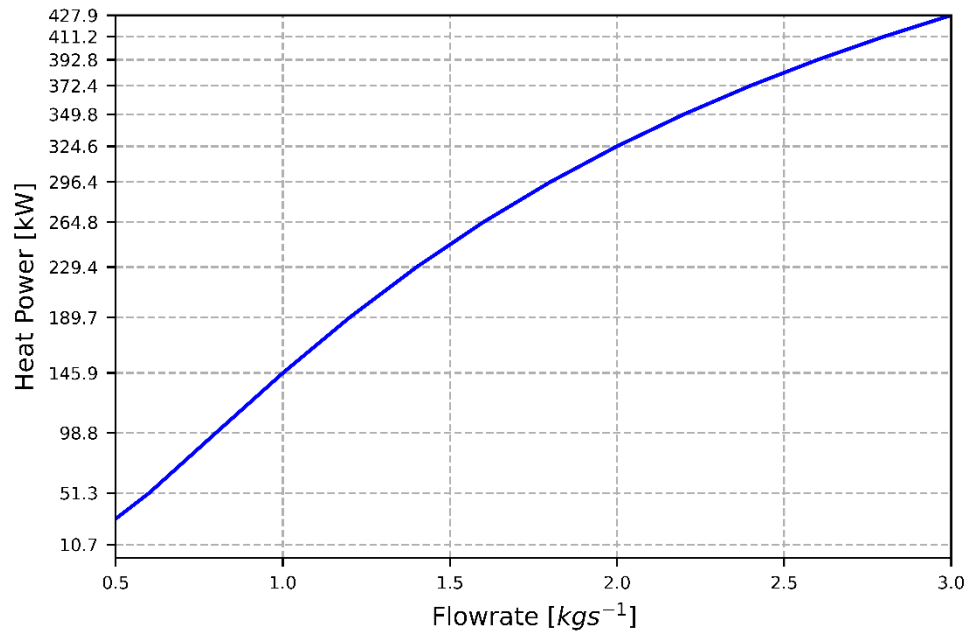


Figure 60 Heat Power as the flow rate value changes: U-tube WBHE (Trecate4 hydrocarbon well).

6.3 The Val d'Agri-Tempa Rossa Field

6.3.1 Tempa Rossa 1D hydrocarbon well

The third selected case study was represented by the Tempa Rossa 1D hydrocarbon well, located within the Tempa Rossa oilfield (Fig.61; Tab.15). The system lies in the Mesozoic carbonate substratum of the foredeep/foreland area and the southern Apennines' external thrust belt. It bears Italy's most significant oil and gas accumulations, namely the Val d'Agri and Tempa Rossa Oilfield (See Chapter 3.1.1). The reservoirs are represented by fractured limestones of the buried Apulia Platform, extending in time from the Cretaceous to the Miocene. The oil column exceeds 1000 m, sometimes reaching more than 2000 m. Lower Pliocene shales represent the seal. The source rocks, identified in a few deep wells of the area, are mainly Albian–Cenomanian in age and marine anoxic carbonates containing Sulphur (Cazzini, 2018).

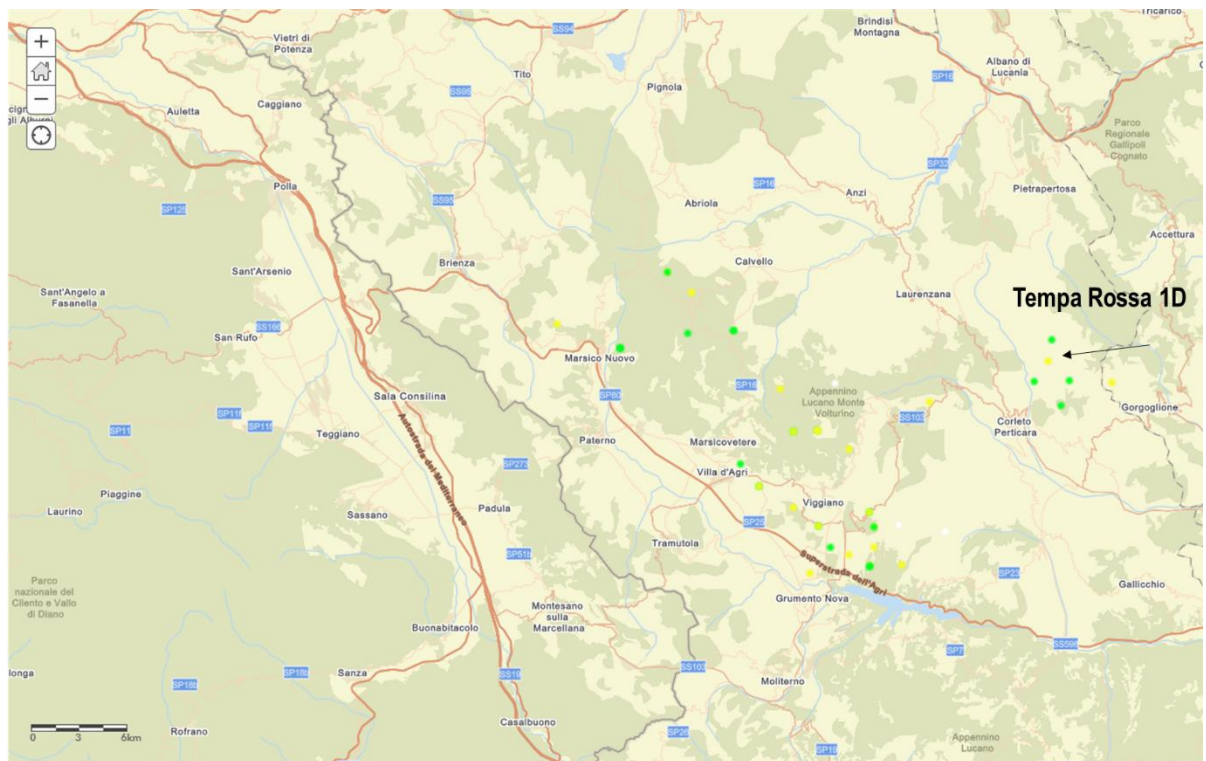


Figure 61 Tempa Rossa 1D hydrocarbon well location (Tempa Rossa Field, Basilicata Region)

Unlike Villafortuna 1 and Trecate 4 hydrocarbon well, litho-stratigraphic units of the Tema Rossa 1d are mainly composed of sandstone with associated shales (Tab.16). The maximum depth reached by the analysed well turns out to be equal to 5042 m, with temperatures reaching 107°C (Fig.62).

Table 15 Tempa Rossa 1D hydrocarbon well (Tempa Rossa Field, Basilicata Region) - technical data available on VIDEPI project website

State	<i>Productive, not supplying well</i>
Mineral	<i>OIL</i>
Location	<i>Basilicata Region</i>
Latitude	<i>40,4206</i>
Longitude	<i>16,06593</i>
Field	<i>GORGOGNONE</i>
Central	<i>CENTO OLIO TEMPA ROSSA</i>
Title	<i>GORGOGNONE</i>
Operator	<i>TOTAL E&P ITALIA</i>

Table 16 Tempa Rossa 1D hydrocarbon well - lithostratigraphic profile

Depth	Litho-stratigraphic formation	λ_s	ρc_s	ρ
<i>m</i>		<i>W/mK</i>	<i>J/kg/K</i>	<i>kg/m³</i>
23	<i>Superficial sedimentary deposits</i>	0.30	800	1700
2912	<i>Sandstones interspersed with shale and clays</i>	3.00	808.6	2330
5042	<i>Clays, argillites and calcarenites</i>	2.34	829.4	1917

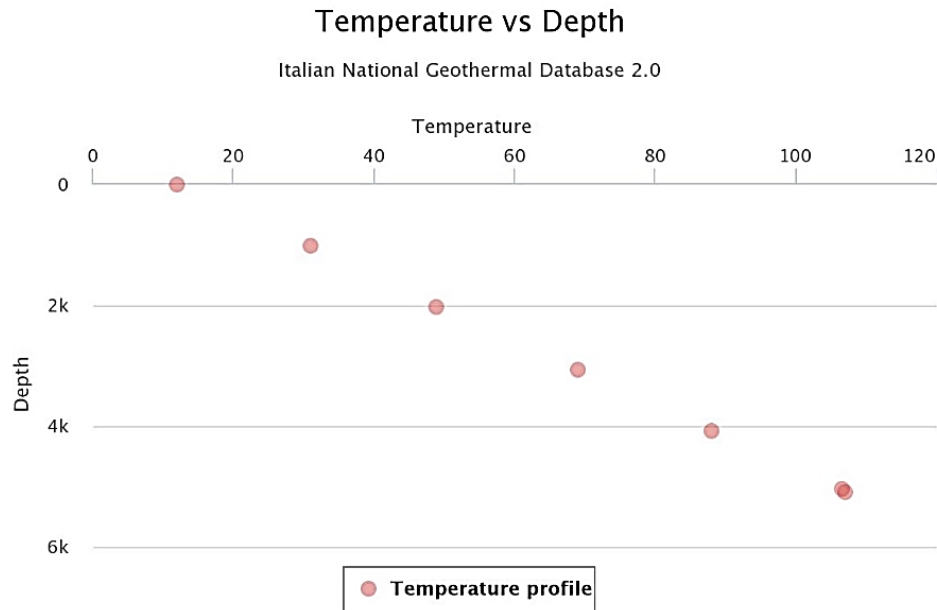


Figure 62 Temperature data visualization for the Tempa Rossa 1D hydrocarbon well: Depth (m); Temperature (°C)

Coaxial and U-tube WBHE Configurations

As for Villafortuna 1 and Trecate 4 hydrocarbon wells, the Tempa Rossa 1D temperature profiles associated with the described Coaxial and U-tube WBHE systems were obtained using the specific ground properties of the selected case study reported in Table 16. Moreover, the thermal conductivity value of the insulating material was set to 0.025 W/mK. Working fluid inlet flow rate (water) and temperature values were considered 3.0 kg/s and 50 °C, respectively.

In the first section of an external pipe of a **Coaxial WBHE system**, the downward fluid is in thermal contact with both the ground on one side and the upward tube on the other. Because of its thermal properties, the ground provides a negative heat contribution. In contrast, the inner tube of the Coaxial WBHE provides a positive one. As the negative contribution is more significant, the water temperature (working fluid temperature) decreases: the thermovector fluid was cooled at depths of up to 1800 m (Fig.63). As soon as the downward profile line crosses the underground temperature line, the natural

heating process begins, and the ground contribution becomes positive. Due to the presence of the insulating material, the heat exchange coefficient between tubes turns out to be minimal, and the increase in working fluid temperature can be associated with the ground.

Using the fixed inlet working fluid temperature (50°C), in the Coaxial WBHE, the outlet recorded temperature is equal to 55.38°C . The thermal power value was evaluated at 70.33 kW. The inlet flow rate strongly influences the temperature of the wellhead thermal fluid and, consequently, the heat power amount. As observed in Figure 64, considering inlet flow rate values between 0.5 and 1 kg/s, the output fluid temperature increases to about 78°C . The output fluid temperature progressively decreases for flow rates higher than 3.0 kg/s. Consequently, for this specific case study and associated plant configuration, it is possible to identify an inlet flow rate value that potentially optimizes the wellhead temperature.

Over the first borehole section of the **U-tube WBHE configuration** (approximately 2000 m), the fluid was cooled by the ground. Subsequently, as the temperature profile line crossed the underground temperature line, the trend was inverted, and the heat carrier fluid temperature began to increase, reaching a maximum temperature value of 55.60°C at a depth of 2700m (upward flow). However, the fluid temperature leaving the U-tube WBHE results in a temperature equal to the inlet fluid (48.8°C) (Figure 65). As observed in Figure 66, considering lower inlet flow rate values, the output fluid temperature decreases.

Unlike Villafortuna 1 and Trecate 4 hydrocarbon wells, outlet working fluid temperatures (55.38°C and 48.8°C for Coaxial and U-tube WBHE, respectively) and thermal loads accumulated in correspondence with Tempa Rossa 1D turns out to be sufficient neither to justify the costs of plant retrofitting nor to plan a cascading exploitation of the geothermal fluid produced.

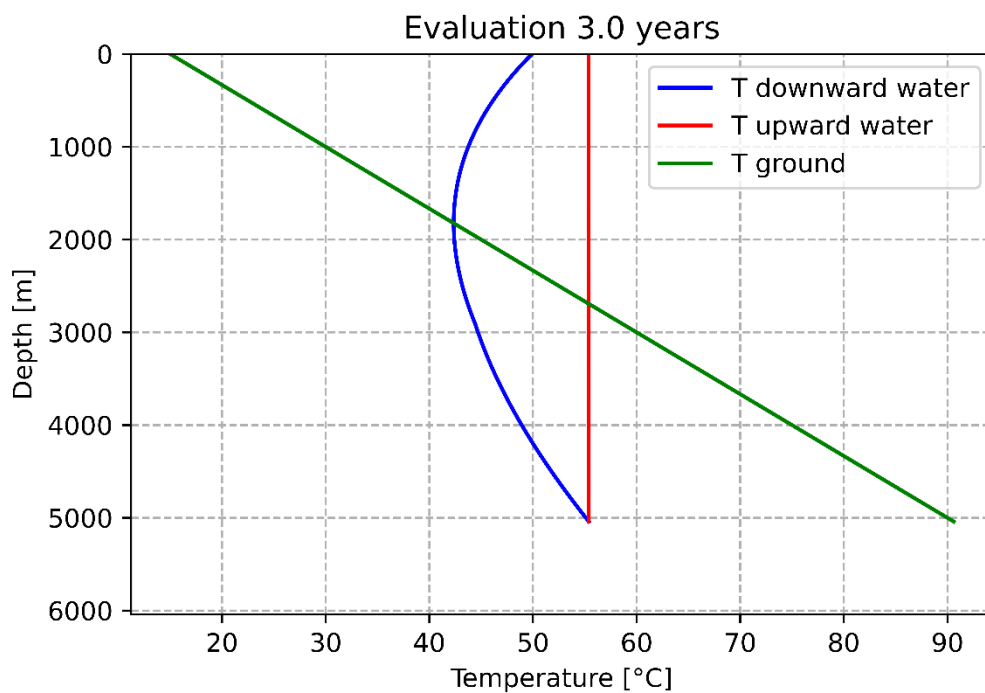


Figure 63 Temperature profile associated with the coaxial WBHE configuration considering site-specific stratigraphy (Tempa Rossa 1D hydrocarbon well).

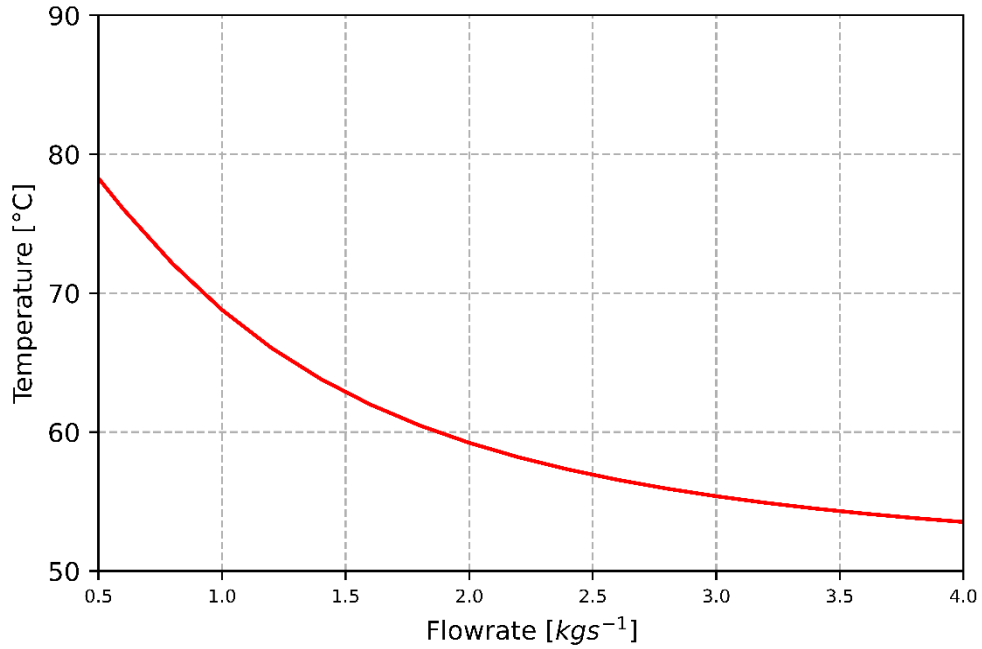


Figure 64 Wellhead temperature as the flow rate value changes: Coaxial WBHE (Tempa Rossa 1D hydrocarbon well).

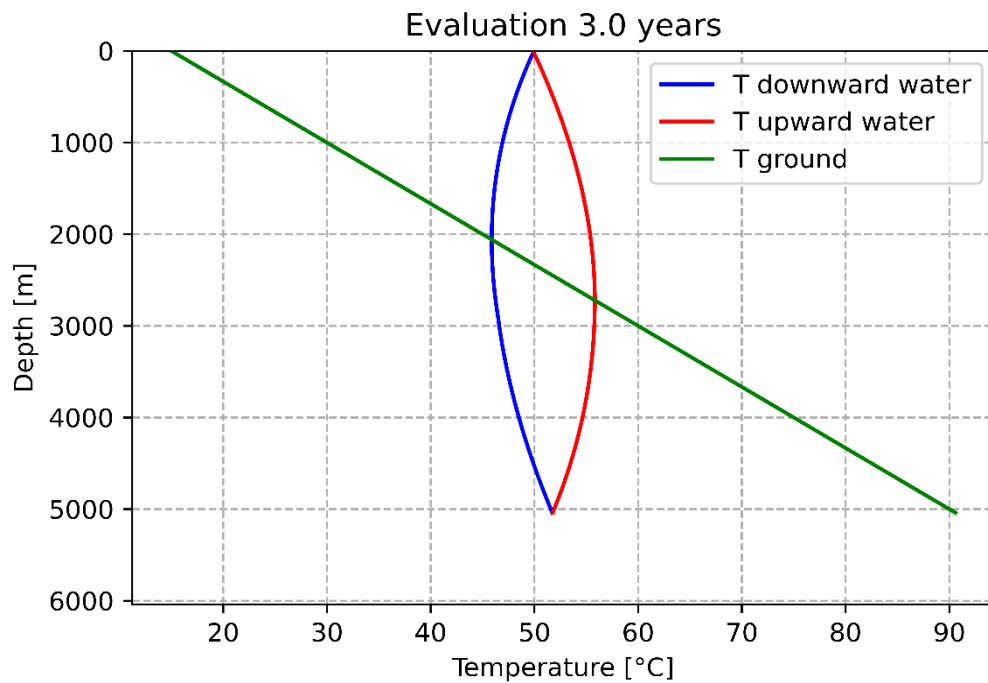


Figure 65 Temperature profile associated with the U-tube WBHE (b) configuration considering site-specific stratigraphy (Tempa Rossa 1D hydrocarbon well).

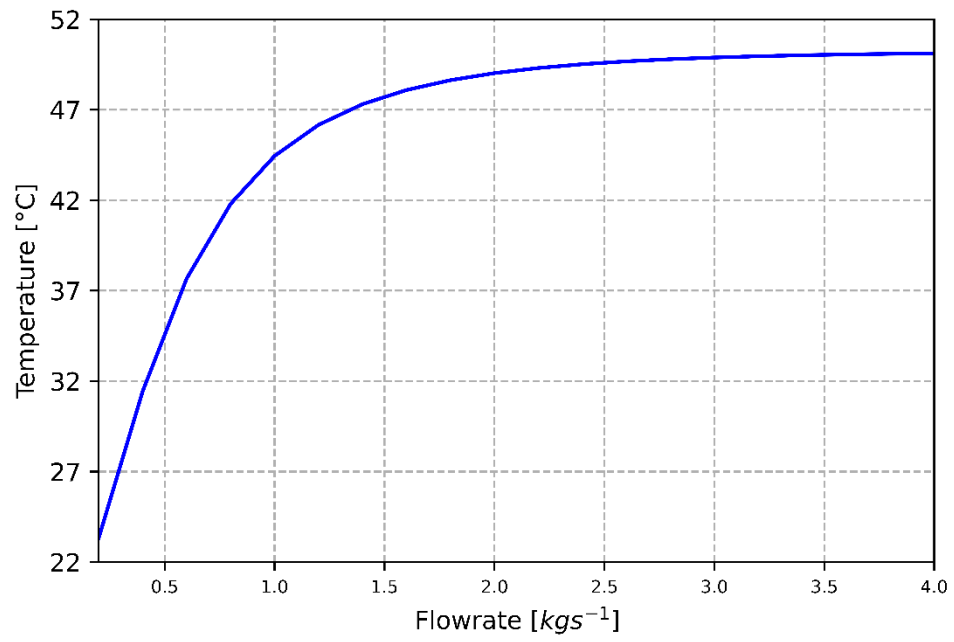


Figure 66 Wellhead temperature as the flow rate value changes: U-tube WBHE (Tempa Rossa 1D hydrocarbon well).

6.4 The Gela Field

6.4.1 Gela 38 hydrocarbon well

The fourth considered case study is represented by the Gela 38 hydrocarbon well (Gela oilfield, Sicily) (Fig.67; Tab.17). The Gela field pertains to the Late Triassic–Early Jurassic petroleum system, linked to the main phase of the Tethyan rifting and explored the three systems, both in the foreland and in the thrust belt from Lombardy to Sicily. The source rocks are terrigenous or mixed carbonate/terrigenous and were deposited during the anoxic stage that preceded the extension of the Jurassic basins. The Ragusa-Gela fields, discovered in the 1950s, have been the most significant Italian oil production for a long time. The reservoir is provided by fractured, massive dolomites of the Upper Triassic Gela Formation. The traps are large-scale anticlines, probably of polyphased age, bounded by high angle normal faults (Granath & Casero, 2004).

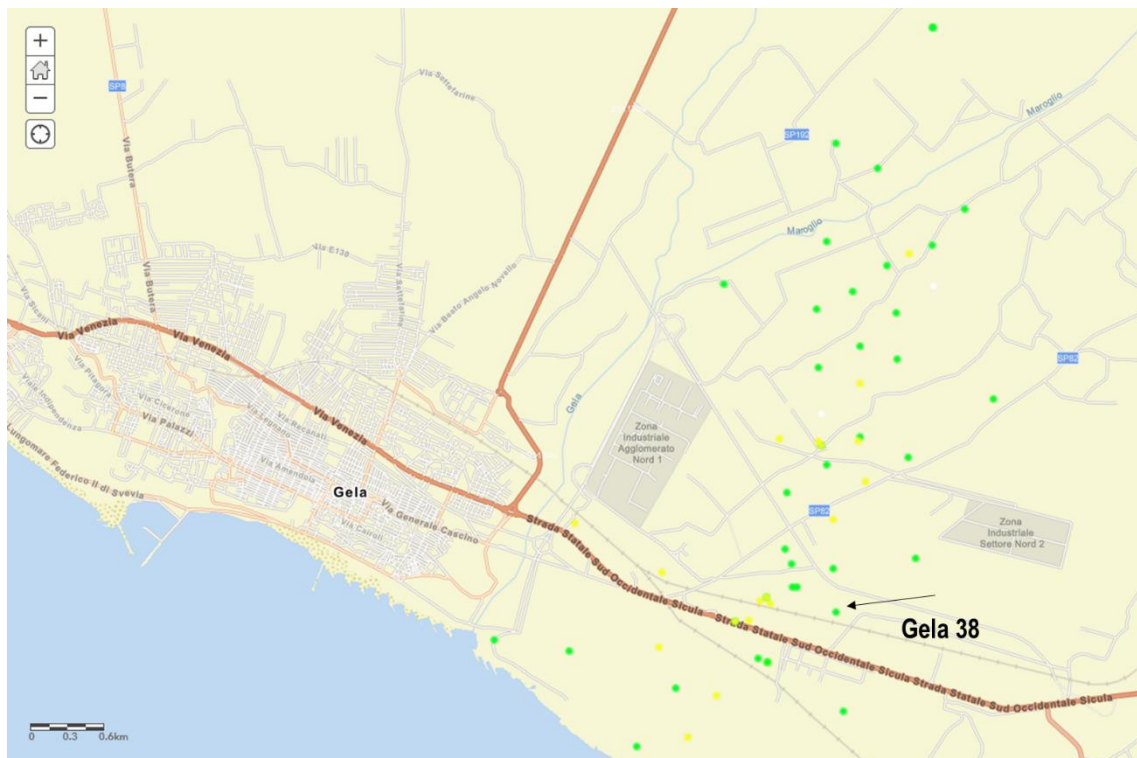


Figure 67 Gela 38 hydrocarbon well location (Gela Field, Sicily Region).

Considering the available information related to the lithological and temperature data, reported in Tab.18 and Fig.68, the stratigraphic succession of the area turns to be composed of marl, calcareous marl and clays. The maximum depth reached by the analysed well is equal to 3446 m, with temperatures reaching 85°C.

Table 17 Gela 38 hydrocarbon well (Gela Field, Sicily Region) - technical data available on VIDEPI project website

State	<i>Productive well</i>
Mineral	<i>OIL</i>
Location	<i>Sicilia Region</i>
Latitude	<i>37,0555</i>
Longitude	<i>14,1834</i>
Field	<i>GELA TERRA</i>
Central	<i>NUOVO CENTRO OLIO GELA</i>
Title	<i>GELA-AGIP</i>
Operator	<i>ENI MEDITERRANEA IDROCARBURI</i>

Table 18 Gela 38 hydrocarbon well - lithostratigraphic profile

Depth	Litho-stratigraphic formation	λ_s	ρc_s	ρ
<i>m</i>		<i>W/mK</i>	<i>J/Kg/K</i>	<i>kg/m³</i>
1772	<i>Marls, clays and gypsum</i>	3.16	1937	2359
2117	<i>Marl, calcareous marl and clays</i>			
2556	<i>Limestone and marl</i>	2.17	1495	1801
2582	<i>Limestone</i>			
2860	<i>Limestone, dolomitic limestone and marl</i>	3.12	810.48	2480
3156	<i>Limestone, marl and dolomite</i>	2.17	830.09	1801
3446	<i>Marls, clays and gypsum</i>			

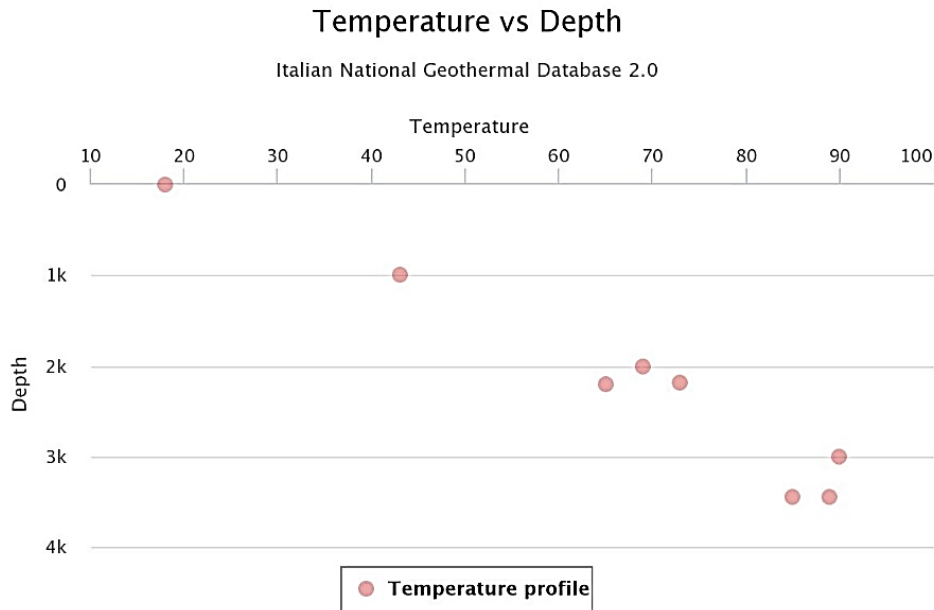


Figure 68 Temperature data visualization for the Gela 38 hydrocarbon well: Depth (m); Temperature (°C)

Coaxial and U-tube WBHE Configurations

As for the TempaRossa 1D hydrocarbon well, the temperature profiles associated with the Coaxial and U-tube WBHE systems were obtained by making use of the specific ground properties of the selected case study reported in Table 18. Moreover, the thermal conductivity value of the insulating material was set to 0.025 W/mK. Working fluid inlet flow rate (water) and temperature values were considered as 3.0 kg/s and 50 °C, respectively.

Using the fixed inlet working fluid temperature (50°C), in the **Coaxial WBHE system**, the outlet recorded temperature is equal to 56.28°C (Fig.69). Thermal power value was evaluated for 81.91 kW. The inlet flow rate strongly influences the temperature of the wellhead thermal fluid and, consequently, the heat power amount. As observed in Figure 70, by considering inlet flow rate values between 0.5 and 1 kg/s, the output fluid temperature increases up to about 78°C. Consequently, also for this specific case study and associated plant configuration, it is possible to identify an inlet flow rate value that potentially allows an optimization of the wellhead temperature.

Considering the **U-tube WBHE configuration** and its associated temperature profile, it was possible to identify how the ground's contribution was responsible for a sizable temperature variation, both in the downward and upward tube. Over the first borehole section of the U-tube WBHE configuration (approximately 1200 m), the fluid was cooled by the ground. Subsequently, as the temperature profile line crossed the underground temperature line, the trend was inverted, and the heat carrier fluid temperature began to increase, reaching a maximum temperature value of 56.41°C at a depth of 1700m (upward flow) (Fig.71). As for the considered Coaxial WBHE configuration, the wellhead thermal fluid temperature in the U-tube system changes as the input flow rate parameter varies. For a flow rate value of 1.6 kg/s, the fluid reaches the surface at a maximum temperature of 52.74°C (Fig.72).

Using the fixed inlet working fluid temperature (50°C) and the estimated fluid temperature at the outlet for the U-tube configuration, the thermal power value was evaluated for 33.79 kW (52.60°C - U-tube WBHE).

As for TempaRossa 1D hydrocarbon well, outlet working fluid temperatures (56.28°C and 52.74°C for Coaxial and U-tube WBHE, respectively) and thermal loads accumulated in correspondence with Gela 38 turns out to be sufficient neither to justify the costs of plant retrofitting nor to plan a cascading exploitation of the geothermal fluid produced.

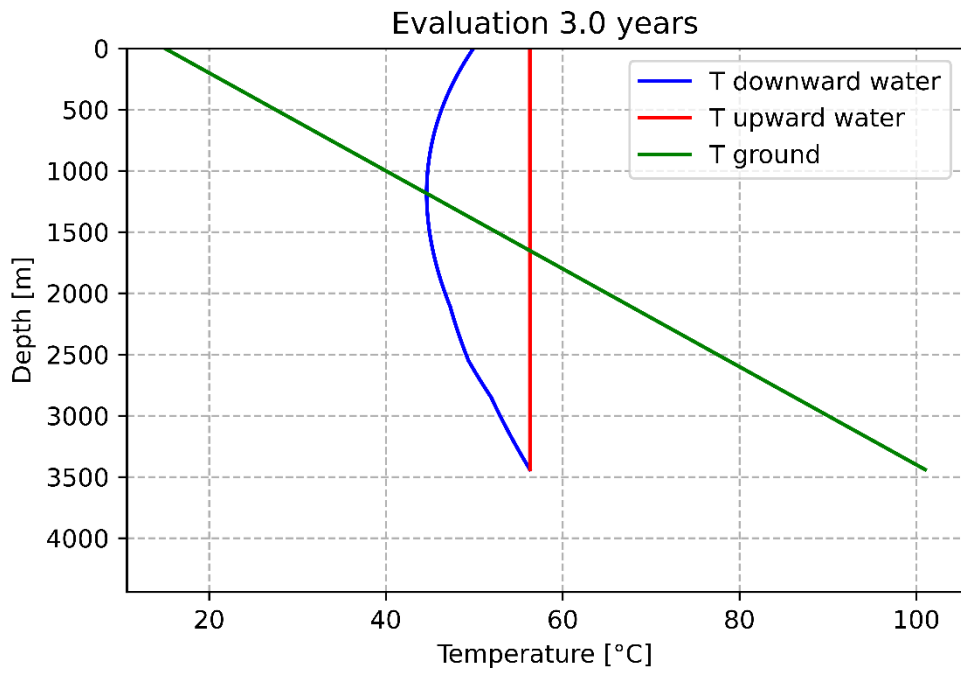


Figure 69 Temperature profile associated with the coaxial WBHE configuration considering site-specific stratigraphy (Gela 38 hydrocarbon well).

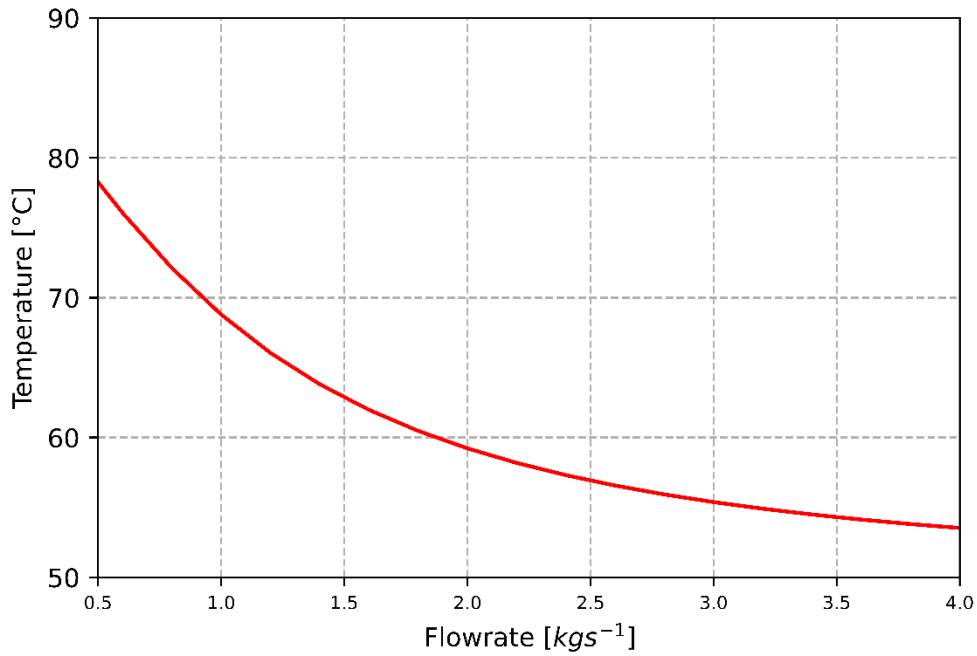


Figure 70 Wellhead temperature as the flow rate value changes: Coaxial WBHE (Gela 38 hydrocarbon well).

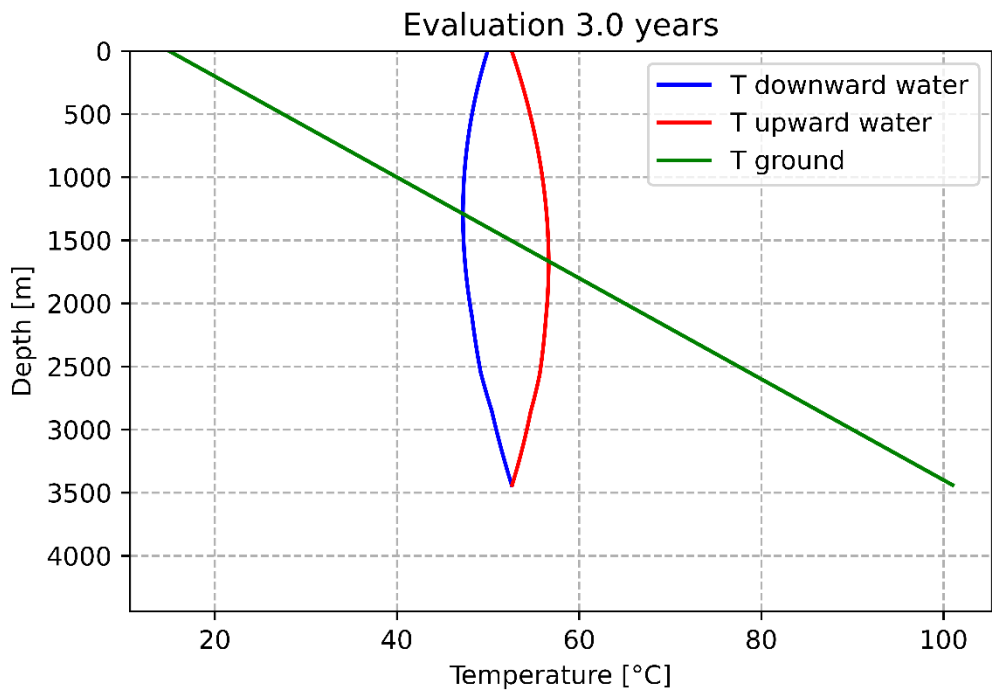


Figure 71 Temperature profile associated with the U-tube WBHE (b) configuration considering site-specific stratigraphy (Gela 38 hydrocarbon well).

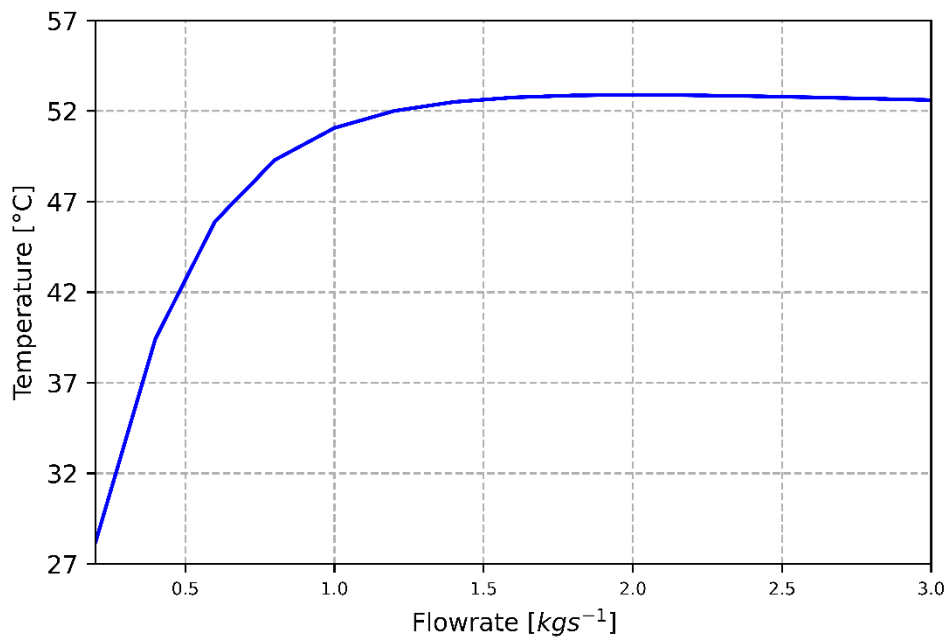


Figure 72 Wellhead temperature as the flow rate value changes: U-tube WBHE (Gela 38 hydrocarbon well).

Chapter 7

Discussion

Geothermal energy represents an independent form of sustainable energy sources, exploitable for both generating electricity and direct uses, while producing very low GHG emissions levels. Depending on their temperature ranges, geothermal resources can be used in a broadly defined field of direct applications. According to Buonasorte et al., 2011, within accessible depths, Italy is endowed with geothermal resources of different nature and temperatures. Hence, it has a substantial geothermal potential, which could be tapped much more intensively. These are renewable on the human timescale, eco-friendly, and cost-effective at several temperature levels.

For sedimentary basin contexts, it is required to comprehensively know the recorded temperature gradient values, the existing geological formations, considering their thickness and rocks' thermal properties values to define geothermal energy extraction conditions. As an ever-increasing number of wells are eventually depleted and abandoned in sedimentary basins that host oilfields, we are faced with an extensive availability of disused hydrocarbon facilities. Recognized problems due to the additional financial burden of decommissioning and cleaning up pollution emerge as consequences of the plants' disposal phases.

Oil companies could potentially take advantage of the opportunity to sell non-economically productive facilities to geothermal energy-specialized companies, along with all relevant reservoir data that have been collected. Therefore, valuable time and money could be saved, avoiding well plugging and disposal operations. Besides, many geological and geophysical reservoir data such as permeability and bottomhole temperature were also gathered for wells that failed to show economic viability during the first exploration phases. Existing data can be applied to define whether a well's

repurposing project for geothermal energy extraction purposes is economically feasible or not.

The conversion process of an already drilled hydrocarbon well into a geothermal one has several shared advantages:

1. Due to the availability of a wellbore structure, the repurposing project does not require any other drilling activities, which makes it from 42–95% cost-effective. Besides, this condition plays a crucial role in avoiding constructional risks, declining completion costs, and payback period. Existing surface facilities such as service roads, pipes will eliminate part of the further initial investment costs (Tester et al., 1994).

2. Boundary conditions are already known. Also, geological properties of rocks, reservoir features, wells' completion data, and oilfields' production history are available. This initial condition can represent an essential convenience in starting to evaluate geothermal energy potentially exploitable from a selected hydrocarbon well.

3. The external casing, the wellbore's structure with equipping inner pipe can be used in planning the most advantageous geothermal energy system's configuration.

Petroleum systems in Italian sedimentary basins have been widely explored for both oil and gas extraction. Following the data provided by MISE (2021) and progressively collected within the ViDEPI Project, at the end of September 2021, 8110 hydrocarbon wells are registered and located on the Italian territory: less than 10% of these are currently productive - supplying wells.

In the deepest regions of such sedimentary contexts geological and geophysical exploration campaigns have ascertained the coexistence of hydrocarbons and potentially exploitable geothermal energy resources. Abandoned oil wells in mentioned mature oilfields represent suitable candidate structures for geothermal heat exploitation, thus providing useful access to subsurface resources.

Due to the physicochemical properties being unsuitable for terrestrial ecosystems, extracted geothermal fluids via open-loop geothermal systems must be treated before

the re-injection into the underground. Since these operations require the drilling and maintenance of additional wells, the treatment and pumping of fluids often entailed higher economic costs related to potential geothermal projects. Closed-loop technologies represent an adequate alternative to conventional open-loop geothermal systems as a heat carrier fluid circulates inside a closed wellbore heat exchanger (WBHEs), while no ground fluids are extracted from the surrounding rocks.

From an engineering perspective, the most influential parameters on the heat amount that can be exchanged in WBHEs configurations are represented by the inlet flow rate (q), inlet fluid temperature (T), physico-chemical features of the selected heat carrier fluid (λ_f), thermal conductivity values of the WBHE pipes' insulating material, thermal conductivity values of WBHE pipes' material. Simultaneously, due to the continuous spatial variability of geological formations associated with hydrocarbon wells in oilfields, the thermophysical parameters of geological strata surrounding the well, as well as values of depth of strata and volume thickness, must be appropriately considered to achieve accurate and realistic estimates of heat exchange performances.

Heat exchange mechanisms in three different Italian oilfields (the Villafortuna-Trecate, Val d'Agri - Tempa Rossa and Gela fields) were reconstructed, employing simplified analytical models. Differences in potentially extracted thermal energy were emphasized, both considering the peculiar geological context and the selected WBHE system configuration (Coaxial or U-Tube WBHE).

With a fixed inlet working fluid flow rate of 3 kg/s and a set inlet temperature of 50°C, instantaneous thermal power values exploitable considering a **Coaxial WBHE** were evaluated in 678.85 kW for Villafortuna 1 and 616.7 kW for Trecate 4 (Villafortuna-Trecate Field, Po Plain). Tempa Rossa 1D well (Southern Apennines, Basilicata region) and Gela 38 hydrocarbon well (Sicily) recorded values equal to 70.33 kW and 81.91 kW, respectively.

The maximum extracted fluid temperatures from a Coaxial WBHE in Villafortuna 1 and Trecate 4 hydrocarbon wells are 103.65°C and 98.6°C. Unlike Villafortuna 1 and Trecate 4, Tempa Rossa 1D and Gela 38 wells are characterized by lower values of

outlet fluid temperatures: 55.38°C and 56.28°C, respectively. As such, implementing a Coaxial WBHE in such a hydrocarbon well may not be energetically or economically worthwhile.

Similar considerations reported above can be made by analysing thermal power values obtained from a **U-tube WBHE**. With a fixed inlet working fluid flow rate of 3 kg/s and a temperature of 50°C, thermal power values were estimated at 495.43 kW for Villafortuna 1, 427.9 kW for Trecate 4, 33.79 kW for the Gela 38 hydrocarbon well. Villafortuna 1, Trecate 4, Gela 38 U-tube WBHE recorded a maximum extracted fluid temperature of 89.44°C, 84.0°C, 52.60°C, respectively. Unlike Trecate 4, Villafortuna 1 and Gela 38, for Tempa Rossa 1D hydrocarbon well it was observed an outlet temperature of the working fluid (48.8°C) was lower than the fixed fluid set inlet temperature (50°C). Therefore, geothermal energy recovery is less than the dissipation phenomena (Tab.19).

As for the Coaxial WBHEs, Tempa Rossa 1D and Gela 38 hydrocarbon wells' thermal load values would not be helpful for any direct geothermal applications: the implementation of a U-tube WBHE system in such hydrocarbon wells turns out to not be energetically convenient.

The above-reported discussions are specific to the four selected case studies (the Villafortuna-Trecate, Val d'Agri - Tempa Rossa and Gela fields). The same analysis approach can be performed for that onshore not supplying hydrocarbon wells within the different Italian hydrocarbon fields.

Ground's temperature profile (local geothermal gradient) guides the identification of suitable candidate sites. Unlike what happens for the case studies placed within the Villafortuna-Trecate field and despite their considerable depths, the moderate values of geothermal gradient (30°C/km) limit the possibilities for a geothermal reconversion project of existing boreholes drilled in Val d'Agri - Tempa Rossa field.

Table 19 Recorded working fluid temperatures in Villafortuna 1, Trecate 4, Tempa Rossa 1D, Gela 38 hydrocarbon wells

	<i>Depth</i>	<i>Coaxial WBHE</i>	<i>U-tube WBHE</i>
	<i>m</i>	<i>°C</i>	<i>°C</i>
<i>Villafortuna 1</i>	<i>6202</i>	<i>103.65</i>	<i>89.44</i>
<i>Trecate 4</i>	<i>6282</i>	<i>98.6</i>	<i>84.0</i>
<i>Temparossa 1D</i>	<i>5042</i>	<i>55.38</i>	<i>48.8</i>
<i>Gela 38</i>	<i>3446</i>	<i>56.28</i>	<i>52.60</i>

As described in Chapter 4.1.1, depending on their temperature ranges, geothermal energy resources can have several types of direct uses (i.e., district heating, domestic heating and/or cooling of small and medium buildings, agricultural, zootechnical, industrial applications). The various possible applications of geothermal resources, together with the corresponding temperature demand, are schematically illustrated by the Lindal diagram (Kaczmarczyk et al., 2020) (Fig.17).

According to Carella & Sommaruga, 2000 non-electric uses of geothermal energy in Italy are mainly associated with the spa business. Still, a large share is also related to agricultural applications (greenhouses and fish farming) followed by space heating, including district heating (DH). The main existing applications in space heating are in the Abano area, Ferrara and Vicenza (Northern Italy) and Larderello area (Tuscany). Agribusiness facilities include greenhouses at Amiata and Pantani (in central Italy) as well as the fish farms of Orbetello (Tuscany), Brindisi and Sannicandro (Apulia).

Direct use of geothermal heat in the Abano area consists of the individual heating of a large number of spa hotels and of a spa center. Geothermal fluids with temperature ranges of about 65°C to 87°C are used directly, after filtering, for health treatments and to supply the swimming pools. Geothermal plants associated with a spa town are also located in Acqui Terme (NW Italy) and Bagno di Romagna (North-eastern Apennines), with fluids' temperatures of 70°C and 45°C, respectively.

Considering the use of heat in agriculture, it is generally limited to high revenue products, whose sales can recoup the relatively high costs of the process. One of the main applications is flower-growing: the Italian geothermal greenhouses are dedicated to flower and potted plant growing, with minor horticultural applications. Temperature in the utilisation network of the Piancastagnaio municipality (Tuscany) greenhouse complex is about to 40°C. In addition, following the discovery by ENEL of shallow hot water in a 500 m deep well near Civitavecchia (Latium, North of Rome) in 1960, a private flower growing firm has developed glass greenhouses where exploited fluid's temperature is around 50°C (Carella, 1992; Carella & Sommaruga, 1999).

Galzignano plant (Veneto) was the first geothermal agricultural structure of commercial size installed in Italy (Martino, 1989). Greenhouses use the heat from three shallow (200-300 m deep) wells drilled between 1966 and 1984. The non-saline fluid has a temperature of 63°C. After circulating in steel plate heat exchangers, the geothermal water is discharged at a temperature of 30-35°C.

The Rodigo plant (Lombardy), which started operations in 1990, uses geothermal heat for integrated and cascaded heating of greenhouses and a fish farm. A temperature drop from 59°C to 38°C, is used in the greenhouses to grow potted flowers and plants and nursery vegetables from November to April. Besides, a geothermal aquaculture operation consisting of several plants (Cosima, Vigneto, Ittima) is located on the Tuscany Tyrrhenian seashore, in a lagoonal area where several conventional fish farms are active (Carella, 1992; Facchini et al., 1993). Some 45 wells, less than 100 m deep in karstified Mesozoic limestones tap generally saline (up to 36 g/l) water at a temperature of 19 to 25°C (average 21°C).

Eventually, several large privately owned fish farms are installed in the Apulia coast of SE Italy. The average temperature of the fluids used is 25°C.

The temperature values mentioned above, referring to applications inherent within the agriculture, greenhouse heating and fish farming sectors refer to fluids extracted through drilled producing wells that reach deep geothermal reservoirs. Considering the potentially extracted temperature values obtained from a single-well Coaxial and U-tube WBHE (Tab.19), they can potentially be applied for the same direct uses. Specifically,

the outflow working fluids' temperatures of at the wellhead for Villafortuna 1 and Trecate 4 analysed wells, could be progressively used for some of direct applications: greenhouse heating (100°C - 40°C), soil heating (60°C - 30°C), animal breeding, aquaculture and agricultural cultures (<30 °C). Further analyses based on ISTAT data could be useful to bring out quantitative estimates on potential end-users of heat existing at local and regional scales.

To date, only a few deep WBHE installations have been implemented worldwide, but within 2500 m only, with mixed success, primarily in Europe (Falcone et al., 2018):

- The 2300 m deep BHE of Weggis, Switzerland, with a bottomhole temperature of 78 °C, has been operational since 1994 (Rybach and Hopkirk, 1995). Conceived as a deep geothermal borehole, it was completed as a BHE due to the low water yield encountered. From 1995 to 2000, the BHE delivered 220 MWh/yr (thermal) for both direct heating and as a source for the heat pumps, at an average temperature out of the deep BHE of 40.5°C and average return temperature of 33.3°C. Three additional multi-family dwellings were subsequently connected and the amount of delivered heat nearly doubled, inducing a reduction of the return temperature to 29.9 °C.
- The deep BHE in Weissbad, Switzerland, used an existing drillhole of 1600 m depth, which was subsequently deepened in 1993 with the aim of finding a porous/fractured aquifer at depth and supplying an adjacent spa and hotel complex (Kohl and Rybach, 2004). The well was cemented down to 1213.3 m, at a downhole temperature of 45°C (geothermal gradient of 37.5°C/km) and a centralized steel pipe was inserted. It was anticipated that the design would achieve an average delivery temperature of about 15°C, but BHE operation revealed a yield of just 10.6°C, at a water circulation rate of 10.5 m³/h.
- A concentric injection/production, 2500 m deep geothermal well, adjacent to the futuristic C-shaped, 6-storey building in Aachen, Germany, was planned to provide heating and cooling. Several technical issues arose with the glass fiber reinforced plastic pipe used as an internal tube in the cased wellbore. After, a new

type of plastic for the inner tube was developed and patented at RWTH Aachen University, but was unable to be deployed at depths greater than 1.965 km. As a result, a maximum temperature of just 35°C (instead of the planned 60°C) was attained at the wellhead. The well's costs were funded with support from the state of North Rhine- Westphalia (€2.49 million), the EU (€1.45 million) and a net share from RWTH of €1.69 million.

The limitations that emerged from the pilot installations described above suggest the need to deepen the research on single-well engineered closed-loop solutions, to increasingly optimize the exploitation of the geothermal resource's potential identified, avoiding technical issues, and limiting economic losses.

Simplified tools for a reuse strategies analysis, such as those presented in the proposed research work, guide the identification of case studies potentially suitable for an energy reconversion project. However, developing a more rigorous understanding of the thermal sustainability and economic feasibility of proposed closed-loop projects is required, through specific case-by-case approaches. Besides, preliminary results produced through the use of simplified models must be validated through numerical simulations methods. Computational intelligence-based techniques can also be applied to optimize the design of a WBHE from both economic and energy points of view.

Finally, R&D efforts are needed along with the directions of defining multi-criteria analysis approaches that allow understanding where a closed-loop geothermal solution may be worthwhile, according to the existing social local and regional contexts.

Chapter 8

Conclusions and future research perspectives

Clean energy production using affordable, sustainable, and reliable energy resources has become one of the central topics of European and National development policy visions. Besides, the Italian Piano Nazionale Integrato per l'Energia e il Clima establishes the new national targets for 2030 on energy efficiency, renewable sources, and the reduction of CO₂ emissions. It also fixes the targets for energy security, interconnections, the single energy market and competitiveness, sustainable development, and mobility. The primary aims of national energy companies have become to provide energy solutions that are increasingly sustainable and distant from those based on fossil fuels through technological development and environmental protection values.

Geothermal energy resources can ensure new renewable potentiality, establishing its importance for a new national production model for the forthcoming future. In some Italian sedimentary contexts, it was demonstrated that geothermal energy resources have the potential to make a significant contribution to the increasing demand for power consumption and environmental sustainability.

The use of geothermal energy resources to support anthropogenic activities has been a long-lasting tradition in Italy, renewed in recent decades with the increasing use of low enthalpy geothermal energy (LEG) with combined systems of heat pumps and geothermal exchange. However, for medium to high enthalpy geothermal energy solutions, the expensive capital costs of drilling geothermal wells still represent one of the main challenges to implementing this resource in new energy systems: from 42–

95% of the total geothermal project cost can be mitigated by repurposing an abandoned hydrocarbon well in sedimentary basins.

In the proposed research work, with the primary aim to develop simplified investigation tools that can guide the comprehension of the possibility of converting existing hydrocarbon fields into geothermal ones, two different simplified heat exchange models (U-tube and coaxial WBHE) have been described and implemented in both Python and Matlab programming languages. Considering each selected study's site-specific geological and thermophysical properties in the performed models was fundamental as it contributed to improving the amount of heat exchange phenomena. The results obtained from the developed models (U-tube and Coaxial) demonstrated how the Coaxial WBHE technology performs better for each hydrocarbon well analysed. Even for variable inlet flow rate values, ever-higher output temperatures for the Coaxial configuration are recorded; obtained thermal powers were consequently higher. The differences in the quantity of potentially extracted thermal energy in the three different Italian fields (the Villafortuna-Trecate, Val d'Agri – Tempa Rossa and Gela fields) were significant. As described in Chapter 5, the outflow temperatures of working fluid at the wellhead for both Coaxial and U-tube WBHEs in Villafortuna 1 and Trecate 4 hydrocarbon wells (Northwestern Italy) could be progressively used for some of several direct applications: greenhouse heating (100°C - 40°C), soil heating (60°C - 30°C), animal breeding, aquaculture and agricultural cultures (<30 °C). Coaxial or U-tube wellhole heat exchangers' implementation in Tempa Rossa 1D and Gela 38 hydrocarbon wells is not energetically or economically worthwhile.

It is necessary to emphasize that a geothermal converting project like the one described can be achieved without emissions of CO₂ into the atmosphere. Besides, oil companies have a definite possibility of reducing abandonment costs. This last point can be a driving force to make available the primary data required to conduct more detailed analyses on several hydrocarbon wells' sites located on the Italian territory, identifying the most suitable candidates.

Improving the accuracy of the proposed simplified tools (Coaxial and U-tube WBHE models) through future analysis is still required. The basic assumption related to the

constancy of the properties of the water as a working fluid must be overcome by correctly analysing the possibility of having different working fluids or phase change (evaporation) in the well that would change the proposed models. The role in heat transfer and performance of extracting heat from abandoned wells of intraformational flows also needs to be appropriately considered. Hydrocarbon wells are drilled with a series of casings which are metal tubes. They are cemented with the primary purpose of providing strength to the well and creating a barrier between the well and fluids. Each casing is built into the previous one, and the diameter decreases with the increasing number of the casings. In the final definition of the configuration of the geothermal exchanger to be implemented inside an oil reservoir, it is necessary to consider this complex configuration. A further modification of the proposed simplified models will be required: it will be needed to overcome the assumption that considers the diameters of the well's casings as fixed, improving the model by inserting a function that describes how their diameter varies with the depth of the well.

Future research to improve the performance and the technical and economic applicability of the WBHEs is necessary. The aspects to be also deepened are the pipes materials, the design, and the conversion systems. There is a lack of specific studies on materials that are made up of the pipes of the WBHEs and their unit costs.

In order to improve the heat recovery, the research should focus on the possibility to use for the internal pipe a material able to isolate it, reducing the heat losses during the recovery of heated fluid. Instead, the grouting material mainly affects the heat exchange with the formation. Therefore, more improvements are needed on the grouting materials than on materials constituting the external casing.

The more critical weakness point of the WBHE is the few real case applications.

Despite the above considerations, the proposed tools with their associated simplified models allow for a preliminary definition of the possibility of a selected Italian hydrocarbon well to be converted into a geothermal one, by using WBHE technologies. The identification of case studies potentially suitable for an energy reconversion project can be easily made by making use of such instruments.

After a preliminary analysis of the presence of industries, agricultural districts, it will be required to produce detailed evaluations of the industrial plants available in the area near the selected wells. Identifying multi-criteria analysis approaches for technical feasibility and cost-benefit analyses of the configuration specified could represent the object of future research works. Considering the advantage of avoiding risks, the WBHEs may encourage a positive social response to geothermal plants. It could be a new opportunity for deep geothermal resources exploitation.

Considering that only a limited number of wells have a productive or potentially productive operational state (898 onshore wells), a national project aimed at evaluating the potential associated with the geothermal reuse of wells through WBHEs can represent an excellent contribution to the energy transition. The further potential increase of geothermal energy use through the mentioned system's implementations could significantly contribute to reaching 2030 national targets on energy efficiency, renewable sources, and the reduction of CO₂ emissions.

Table 20 Additional abbreviation of parameters

Additional abbreviations		
Parameter	Symbol	Unit of measure
Volumetric heat capacity of the fluid	ρc_f	[J m ⁻³ K ⁻¹]
Volumetric heat capacity of the rock	ρc_s	[J m ⁻³ K ⁻¹]
Density	ρ	[Kg m ⁻³]
Thermal conductivity of the fluid	λ_f	[W m ⁻¹ K ⁻¹]
Thermal conductivity of the rock	λ_s	[W m ⁻¹ K ⁻¹]
Heat conductivity of the porous media	λ_m	[W m ⁻¹ K ⁻¹]
Heat conductivity of the pipe material	λ_i	[W m ⁻¹ K ⁻¹]
Viscosity	μ	[kg m ⁻¹ s ⁻¹]
Thermal diffusivity of the rock	α_s	[ms ⁻¹]
Radius of thermal influence	r_s	[m]
Temperature of the rock	T	[°C]
Temperature at the interface of wellbore/formation	T_w	[°C]
Fluid temperature in the outer pipe	T_{fo}	[°C]
Fluid temperature in the inner pipe	T_{fi}	[°C]
Temperature of the environment at the inlet	T_{ei}	[°C]
Temperature of the environment at the surface	T_{es}	[°C]
Time	t	[h]
Flow rate	q	[m ³ h ⁻¹]
Fluid velocity	v_f	[ms ⁻¹]
Heat transfer coefficient – outer pipe fluid and wellbore outside	k_w	[Wm ⁻² K ⁻¹]
Heat transfer coefficient – the outer pipe and inner pipe	k_{i0}	[Wm ⁻² K ⁻¹]
Convective heat transfer coefficient	h_f	[m ⁻² K ⁻¹]
Coefficient of convective heat transfer to the inner wall	h_0	[Wm ⁻² K ⁻¹]
Standard gravity	g	[ms ⁻²]

References

AGIP (1977). Temperature Sotterranee (Subterranean Temperatures) - Inventario dei Dati Raccolti Dall'AGIP Durante La Ricerca Di Idrocarburi in Italia. AGIP, Milano, 1390 pp.

AGIP (1986). Aggiornamenti temperature sotterranee - Pozzi a terra - Esplorazione Geotermica

AGIP (1994). Acque dolci sotterranee - Inventario dei dati raccolti dall'AGIP durante la ricerca di idrocarburi in Italia (dal 1971 al 1990), 515 pp.

Albanese, C., Allansdottir, A., Amato, L., Ardizzone, F., Bellani, S., Bertini, G., Botteghi, S., Bruno, D., Caielli, G., Caiozzi, F., Caputi, A., Catalano, R., Chiesa, S., Contino, A., D'Arpa, S., De Alteriis, G., De Franco, R., Dello Buono, D., Destro, E., Di Sipio, E., Donato, A., Doveri, M., Dragone, V., Ellero, A., Fedi, M., Ferranti, L., Florio, G., Folino, M., Galgaro, A., Gennaro, C., Gianelli, G., Giaretta, A., Gola, G., Greco, G., Iaquina, P., Inversi, B., Iorio, M., Iovine, G., Izzi, F., La Manna, M., Livani, M., Lombardo, G., Lopez, N., Magnelli, D., Maio, D., Manzella, A., Marchesini, I., Martini, G., Masetti, G., Mercadante, A., Minissale, A., Montanari, D., Montegrossi, G., Monteleone, S., Muto, F., Muttoni, G., Norini, G., Pellizzone, A., Perotta, P., Petracchini, L., Pierini, S., Polemio, M., Rizzo, E., Russo, L., Sabatino, M., Santaloia, F., Santilano, A., Scrocca, S., Soleri, S., Tansi, C., Terranova, O., Teza, G., Tranchida, G., Trumpy, E., Uricchio, V & Valenti, V. (2014). VIGOR: Sviluppo geotermico nelle Regioni della Convergenza. Progetto VIGOR – Valutazione del Potenziale Geotermico delle Regioni della Convergenza, POI Energie Rinnovabili e Risparmio Energetico 2007-2013, CNR-IGG, ISBN: 9788879580113

Alimonti, C., Berardi, D., Bocchetti, D., & Soldo, E. (2016). Coupling of energy conversion systems and wellbore heat exchanger in a depleted oil well. *Geothermal Energy*, 4(1). <https://doi.org/10.1186/s40517-016-0053-9>

Alimonti, C., & Soldo, E. (2016). Study of geothermal power generation from a very deep oil well with a wellbore heat exchanger. *Renewable Energy*, 86, 292–301. <https://doi.org/10.1016/j.renene.2015.08.031>

Alimonti, C., Soldo, E., Bocchetti, D., & Berardi, D. (2018). The wellbore heat exchangers: A technical review. *Renewable Energy*, 123, 353–381. <https://doi.org/10.1016/j.renene.2018.02.055>

Alimonti, C., & Gnoni, A. A. (2015). Harnessing the fluids heat to improve mature oil field: The Villafortuna-Trecate case study. *Journal of Petroleum Science and Engineering*, 125, 256–262. <https://doi.org/10.1016/j.petrol.2014.11.029>

Alimonti, C., Soldo, E., & Scrocca, D. (2021). Looking forward to a decarbonized era: Geothermal potential assessment for oil & gas fields in Italy. *Geothermics*, 93 (June 2020), 102070. <https://doi.org/10.1016/j.geothermics.2021.102070>

Alishaev, M. G., Abdulagatov, I., & Abdulagatova, Z. Z. (2012). Effective thermal conductivity of fluid-saturated rocks: Experiment and modeling. *Engineering Geology*, 135–136, 24–39. <https://doi.org/10.1016/j.enggeo.2012.03.001>

Allahvirdizadeh, P. (2020). A review on geothermal wells: Well integrity issues. *Journal of Cleaner Production*, 275 (September), 124009. <https://doi.org/10.1016/j.jclepro.2020.124009>

Allansdottir, A., Pellizzone, A., & Manzella, A. (2019). Geothermal Energy and Society. In *Lecture Notes in Energy* (Vol. 67), Springer Cham. <https://doi.org/10.1007/978-3-319-78286-7>

Armstead, H.C. (1983). *Geothermal Energy, Its Past, Present and Future Contributions to Energy Needs of Man*. 2nd Edition, London, New York, 289 p.

Arndt, D., Baer, K., Fritsche, J.-G., & Sass, I. (2011). 3D structural model of the Federal State of Hesse (Germany) for geopotential evaluation [Geologisches 3D-Modell von Hessen zur Bestimmung von Geo-Potenzialen.]. *Zeitschrift Der Deutschen Gesellschaft Für Geowissenschaften*, 162, 353–369. <https://doi.org/10.1127/1860-1804/2011/0162-0353>

Axelsson, G., & Stefansson, V. (2003). Sustainable Management of Geothermal Resources. *International Geothermal Conference, Reykjavík, January 2002*, 40–48

Bär, K., Rühaak, W., Schulte, D., Welsch, B., & Chauhan, S. (2015). Medium Deep High Temperature Heat Storage. European Geothermal Congress 2013 Pisa, Italy, 3-7 June 2013, 17 (October), 6305. <http://meetingorganizer.copernicus.org/EGU2015/EGU2015-6305-1.pdf>

Barbacki, A. P. (2000). The use of abandoned oil and gas wells in Poland for recovering geothermal heat. Proceedings World Geothermal Congress 2000, 3361–3365

Barbier, E., & Fanelli, M. (1977). Non-electrical uses of Geothermal energy. Progress in Energy and Combustion Science, 3(2), 73–103. [https://doi.org/https://doi.org/10.1016/0360-1285\(77\)90009-0](https://doi.org/https://doi.org/10.1016/0360-1285(77)90009-0)

Baria, R., & Beardsmore, G. R. (2012). Encyclopedia of Sustainability Science and Technology. Encyclopedia of Sustainability Science and Technology, April 2017. <https://doi.org/10.1007/978-1-4419-0851-3>

Bauer, S., Pfeiffer, T., Boockmeyer, A., Dahmke, A., & Beyer, C. (2015). Quantifying Induced Effects of Subsurface Renewable Energy Storage. Energy Procedia, 76, 633–641. <https://doi.org/10.1016/j.egypro.2015.07.885>

Beall, S. E., & Samuels, G. (1971). The use of warm water for heating and cooling plant and animal enclosures. Oak Ridge National Laboratory, ORNL-TM-3381, 56 pp.

Bello, M., & Fantoni, R. (2002). Deep oil play in Po Valley. Deformation and hydrocarbon generation in a deformed foreland. AAPG Hedberg Conference: Deformation History, Fluid Flow Reconstruction and Reservoir Appraisal in Foreland Fold and Thrust Belts, 14–18 May 2002, Palermo, Abstracts book, 1–4

Bergman T. L., Lavine A. S., Incropera F. P. & Dewitt D. P. (2011). Introduction To Heat Transfer. Sixth Edition. John Wiley & Sons (January 1, 2013). United States of America

Bertello, F., Fantoni, R., & Franciosi, R. (2008). Overview of the Italy's petroleum systems and related oil and gas occurrences. 70th European Association of Geoscientists and Engineers Conference and Exhibition 2008: Leveraging Technology. Incorporating SPE EUROPEC 2008, 1 (June), 74–78. <https://doi.org/10.3997/2214-4609.20147556>

Bertello, F., Fantoni, R., Franciosi, R., Gatti, V., Ghielmi, M., & Pugliese, A. (2010). From thrust-and-fold belt to foreland: hydrocarbon occurrences in Italy. Geological Society, London, Petroleum Geology Conference Series, 7(1), 113 LP – 126. <https://doi.org/10.1144/0070113>

Bertello, F., Fantoni, R., Franciosi, R., Gatti, V., Ghielmi, M., & Puglise, A. (2010). From thrust-and-fold belt to foreland: Hydrocarbon occurrences in Italy. *Petroleum Geology Conference Proceedings*, 7(0), 113–126. <https://doi.org/10.1144/0070113>

Bertini, G., Cappetti, G., Fiordelisi, A. (2005). *Giornale di Geologia Applicata* 1, 247–254, doi: 10.1474/GGA.2005-01.0-24.0024

Bertotti, G., Picotti, V., Bernoulli, D., & Castellarin, A. (1993). From rifting to drifting: tectonic evolution of the South-Alpine upper crust from the Triassic to the Early Cretaceous. *Sedimentary Geology*, 86(1–2), 53–76. [https://doi.org/10.1016/0037-0738\(93\)90133-P](https://doi.org/10.1016/0037-0738(93)90133-P)

Bethke, C. M., Harrison, W. J., Upson, C., & Altaner, S. P. (1988). Supercomputer Analysis of Sedimentary Basins. *Science*, 239(4837), 261–267. <http://www.jstor.org/stable/1700720>

Blackwell D., & Steele John. (1989). Heat flow and geothermal potential of Kansas. In *Biul. Kans. Geol. Surv.* (Vol. 226, pp. 267–295)

Blank, L., Meneses Rioseco, E., Caiazza, A., & Wilbrandt, U. (2021). Modeling, simulation, and optimization of geothermal energy production from hot sedimentary aquifers. In *Computational Geosciences* (Vol. 25, Issue 1). *Computational Geosciences*. <https://doi.org/10.1007/s10596-020-09989-8>

Bu, X., Ma, W., & Gong, Y. (2014). Electricity generation from abandoned oil and gas wells. *Energy Sources, Part A: Recovery, Utilization and Environmental Effects*, 36(9), 999–1006. <https://doi.org/10.1080/15567036.2010.551255>

Bu, X., Ma, W., & Li, H. (2012). Geothermal energy production utilizing abandoned oil and gas wells. *Renewable Energy*, 41, 80–85. <https://doi.org/10.1016/j.renene.2011.10.009>

Buonasorte, G., Cataldi, R., Franci, T., Grassi, W., Manzella, A., Meccheri, M., & Passaleva, G. (2011). Previsioni di crescita della geotermia in Italia fino al 2030 - Per un nuovo manifesto della geotermia italiana. *Unione Geotermica Italiana*.

Busby, J. (2014). Geothermal energy in sedimentary basins in the UK. *Hydrogeology Journal*, 22(1), 129–141. <https://doi.org/10.1007/s10040-013-1054-4>

Caracciolo, V., & Milano, I. (2000). *Unione Geotermica Italiana*. Geothermal space and agribusiness heating in Italy 1. *World Geothermal Congress 2000*, 117–122

Carannante, G., Pugliese, A., Ruberti, D., Simone, L., Vigliotti, M., & Vigorito, M. (2009). The Cretaceous evolution of a sector of the Apulia Platform from subsurface and outcrop data (Campania-Molise Apennines). *Bollettino della Societa Geologica Italiana*, 128(1), 3–31

Carella R. (1992). The several uses of low temperature geothermal energy for heating. CEC, DG XVII, Thermie maxibrochure, 23 pp.

Carella, R., & Sommaruga, C. (1999). Italian agricultural uses of geothermal energy. *Bulletin d'Hydrogéologie*, 17(17). <http://www.geothermal-energy.org/pdf/IGAstandard/EGC/1999/Carella.pdf>

Cataldi, R., Mongelli, F., Squarci, P., Taffi, L., Zito, G., & Calore, C. (1995). Geothermal ranking of Italian territory. *Geothermics*, 24(1), 115–129. [https://doi.org/10.1016/0375-6505\(94\)00026-9](https://doi.org/10.1016/0375-6505(94)00026-9)

Caulk, R. A., & Tomac, I. (2017). Reuse of abandoned oil and gas wells for geothermal energy production. *Renewable Energy*, 112, 388–397. <https://doi.org/10.1016/j.renene.2017.05.042>

Cazzini, F. F. (2018). The history of the upstream oil and gas industry in Italy. *Geological Society Special Publication*, 465(1), 243–274. <https://doi.org/10.1144/SP465.2>

Cazzola, A., Fantoni, R., Franciosi, R., Gatti, V., & Ghielmi, M. (2011). From thrust and fold belt to foreland basins: hydrocarbon exploration in Italy. *AAPG, International Conference 2011*, 10374(Mi), 2–5

Charnyi, I. A. (1948). Movement of the boundary of change in aggregate state with body cooling or heating, *Izv. OTN AN SSSR*, No. 2

Charnyi, I. A. (1953). Heating of a critical area of formation in pumping of hot water into a well, *Neft. Khoz.*, No. 3

Cheng, W. L., Huang, Y. H., Lu, D. T., & Yin, H. R. (2011). A novel analytical transient heat-conduction time function for heat transfer in steam injection wells considering the wellbore heat capacity. *Energy*, 36(7), 4080–4088. <https://doi.org/10.1016/j.energy.2011.04.039>

Cheng, W. L., Li, T. T., Nian, Y. Le, & Wang, C. L. (2013). Studies on geothermal power generation using abandoned oil wells. *Energy*, 59, 248–254. <https://doi.org/10.1016/j.energy.2013.07.008>

Cheng, W. L., Li, T. T., Nian, Y. Le, & Xie, K. (2014a). An analysis of insulation of abandoned oil wells reused for geothermal power generation. *Energy Procedia*, 61, 607–610. <https://doi.org/10.1016/j.egypro.2014.11.1181>

Cheng, W. L., Li, T. T., Nian, Y. Le, & Xie, K. (2014b). Evaluation of working fluids for geothermal power generation from abandoned oil wells. *Applied Energy*, 118, 238–245. <https://doi.org/10.1016/j.apenergy.2013.12.039>

Davies, J. H. (2013). Global map of solid Earth surface heat flow. *Geochemistry, Geophysics, Geosystems*, 14(10), 4608–4622. <https://doi.org/10.1002/ggge.20271>

Davis, A. P., & Michaelides, E. E. (2009). Geothermal power production from abandoned oil wells. *Energy*, 34(7), 866–872. <https://doi.org/10.1016/j.energy.2009.03.017>

Davis, M. G., Chapman, D. S., Van Wagoner, T. M., & Armstrong, P. A. (2007). Thermal conductivity anisotropy of metasedimentary and igneous rocks. *Journal of Geophysical Research: Solid Earth*, 112(5), 1–7. <https://doi.org/10.1029/2006JB004755>

Delbeke, J., Runge-Metzger, A., Slingenberg, Y., & Werksman, J. (2019). The paris agreement. *Towards a Climate-Neutral Europe: Curbing the Trend*, 24–45. <https://doi.org/10.4324/9789276082569-2>

Dickson, M. H., & Fanelli, M. (2020). What is Geothermal Energy? *Renewable Energy*, 302–328. <https://doi.org/10.4324/9781315793245-25>

Di Sipio, E., Galgaro, A., Destro, E., Giaretta, A., Chiesa, S., Manzella, A. & VIGOR Team. (2016). VIGOR Team. Thermal conductivity of rocks and regional mapping JO - Proceedings of European Geothermal Congress 2013, Pisa, Italy, 3-7 June 2013

Dyad'kin, Yu. D., Gendler, S.G., (1985). *Heat and Mass Transfer Processes in Extraction of Geothermal Energy*, Izd. LGI, Leningrad.

ENEL, ENI-AGIP, CNR, ENEA (1988). *Inventario delle risorse geotermiche nazionali e indagine d'insieme sul territorio nazionale*. Ministero dell'Industria, del Commercio e dell'Artigianato (Ministero dello Sviluppo Economico)

ENI (1972). *Acque dolci sotterranee - Inventario dei dati raccolti dall'AGIP durante la ricerca di idrocarburi in Italia*. 914 pp. ISBN-10: A000097736

European Commission (2016). *Urban Agenda for the EU*. Amsterdam, NL. Available online: https://ec.europa.eu/regional_policy/fr/ (accessed on 17 October 2021)

European Commission (2019). *Urban agenda for the EU Multi-level governance in action*. Available online: https://ec.europa.eu/regional_policy/sources/docgener/brochure/urban_agenda_eu_en.pdf (accessed on 17 October 2021)

Falcone, G., Liu, X., Okech, R. R., Seyidov, F., & Teodoriu, C. (2018). Assessment of deep geothermal energy exploitation methods: The need for novel single-well solutions. *Energy*, 160, 54–63. <https://doi.org/10.1016/j.energy.2018.06.144>

Fantoni, R., Bersezio, R. & Forcella, F. (2004). Alpine structure and deformation chronology at the Southern Alps-Po Plain border in Lombardy *Boll. Soc. Geol. It.*, 123 (2004), 463-476, 9 ff

Fantoni, R. & Scotti, P. (2009). Time of hydrocarbon generation vs trap forming age in Mesozoic oil play in Po Plain. *Rendiconti Società Geologica Italiana*, 5, Convegno Annuale Gruppo di Geologia Strutturale, 25–28 February 2009, Udine, 89–92

Fantoni, R., Galimberti, R., Ronchi, P., & Scotti, P. (2011). Po Plain Petroleum Systems: Insights from Southern Alps Outcrops (Northern Italy). *Search and Discovery Article*, 20120, 7 pp

Gascuel, V., Bédard, K., Comeau, F. A., Raymond, J., & Malo, M. (2020). Geothermal resource assessment of remote sedimentary basins with sparse data: lessons learned from Anticosti Island, Canada. *Geothermal Energy*, 8(1), 1–32. <https://doi.org/10.1186/s40517-020-0156-1>

Gehlin, S. E. A., Hellström, G., & Nordell, B. (2003). The influence of the thermosiphon effect on the thermal response test. *Renewable Energy*, 28(14), 2239–2254. [https://doi.org/https://doi.org/10.1016/S0960-1481\(03\)00129-0](https://doi.org/https://doi.org/10.1016/S0960-1481(03)00129-0)

Gestore dei Servizi Energetici S.p.A. (2018). *RAPPORTO STATISTICO 2018: Energia da fonti rinnovabili in Italia*. www.gse.it, 168. <https://www.europeanbiogas.eu/eba-statistical-report-2019/>

Ghielmi, M., Amore, M. R., Bolla, E. M., Carubelli, P., Knezaurek, G., & Serraino, C. (2012). The Pliocene to Pleistocene Succession of the Hyblean Foredeep (Sicily , Italy)*. Search and Discovery Article, 30221, 30220

Giovanni, B., Guido, C., & Adolfo, F. (2005). Characteristics of Geothermal Fields in Italy. *Giornale Di Geologia Applicata*, 1, 247–254. <https://doi.org/10.1474/GGA.2005-01.0-24.0024>

Gizzi, M. (2021). Closed-loop systems for geothermal energy exploitation from hydrocarbon wells: An Italian case study. *Applied Sciences (Switzerland)*, 11(22). <https://doi.org/10.3390/app112210551>

Gizzi, M., Taddia, G., & Lo Russo, S. (2021). Reuse of decommissioned hydrocarbon wells in Italian oilfields by means of a closed-loop geothermal system. *Applied Sciences (Switzerland)*, 11(5). <https://doi.org/10.3390/app11052411>

Granath, J., & Casero, P. (2004). Tectonic setting of the petroleum systems of Sicily. *AAPG Hedberg Series*, 391–411.

Gruescu, C., Giraud, A., Homand, F., Kondo, D., & Do, D. P. (2007). Effective thermal conductivity of partially saturated porous rocks. *International Journal of Solids and Structures*, 44(3), 811–833. <https://doi.org/https://doi.org/10.1016/j.ijsolstr.2006.05.023>

Gudmundsson, J., Freeston, D., Lienau, P. (1985). The lindal diagram. *GRC Trans.*, 9, 15–17

Haaland, S.E. (1983). Simple and Explicit Formulas for the Friction Factor in Turbulent Flow. *Trans. ASIVIE, J. of Fluids Engineering*, 103: 89-9

IEA (2020). Special Report on Clean Energy Innovation: Accelerating technology progress for a sustainable future. *Energy Technology Perspective*, 185. https://webstore.iea.org/download/direct/4022?fileName=Energy_Technology_Perspectives_2020_-_Special_Report_on_Clean_Energy_Innovation.pdf

IEA (2021). Net Zero by 2050: A Roadmap for the Global Energy Sector. International Energy Agency, 224

IPCC (2021). Climate Change 2021. The Physical Science Basis. Contribution of Working Group 1 to Sixth Assessment Report of the Intergovernmental Panel on Climate Change. <https://www.ipcc.ch/report/ar6/wg1/>

IRENA (2019). Global Energy Transformation: A Roadmap to 2050. In Global Energy Transformation. A Roadmap to 2050

IRENA (2021). Renewable capacity statistics 2021 International Renewable Energy Agency, Abu Dhabi

Kaczmarczyk, M., Tomaszewska, B., & Operacz, A. (2020). Sustainable utilization of low enthalpy geothermal resources to electricity generation through a cascade system. *Energies*, 13(10). <https://doi.org/10.3390/en13102495>

Kaiser, O., & Scheck-wenderoth, M. (2010). Chemie der Erde Geothermal energy in sedimentary basins : What we can learn from regional numerical models. 70, 33–46. <https://doi.org/10.1016/j.chemer.2010.05.017>

Kamila, Z., Kaya, E., & Zarrouk, S. J. (2021). Reinjection in geothermal fields: An updated worldwide review 2020. *Geothermics*, 89 (January), 101970. <https://doi.org/10.1016/j.geothermics.2020.101970>

Kharseh, M., Al-Khawaja, M., & Hassani, F. (2019). Optimal utilization of geothermal heat from abandoned oil wells for power generation. *Applied Thermal Engineering*, 153. <https://doi.org/10.1016/j.applthermaleng.2019.03.047>

Kujawa, T., Nowak, W., & Stachel, A. A. (2005). Analysis of the exploitation of existing deep production wells for acquiring geothermal energy. *Journal of Engineering Physics and Thermophysics*, 78(1), 127–135. <https://doi.org/10.1007/s10891-005-0038-1>

Kujawa, Tomasz, Nowak, W., & Stachel, A. A. (2006). Utilization of existing deep geological wells for acquisitions of geothermal energy. *Energy*, 31(5), 650–664. <https://doi.org/10.1016/j.energy.2005.05.002>

Kohl, T. and Rybach, L. (2004). Projekt Statistik Geothermische Nutzung der Schweiz für die Jahre 2002 und. http://www.ub.unibas.ch/digi/a125/sachdok/2009/IBB_1_004629691.pdf, 2004

Kukkonen, I. T., Jokinen, J., & Seipold, U. (1999). Temperature and pressure dependencies of thermal transport properties of rocks: Implications for uncertainties in thermal lithosphere models and new laboratory measurements of high-grade rocks in the central Fennoscandian Shield. *Surveys in Geophysics*, 20(1), 33–59. <https://doi.org/10.1023/A:1006655023894>

Labus, M., & Labus, K. (2018). Thermal conductivity and diffusivity of fine-grained sedimentary rocks. *Journal of Thermal Analysis and Calorimetry*, 132(3), 1669–1676. <https://doi.org/10.1007/s10973-018-7090-5>

Lee, Y., & Deming, D. (1998). Evaluation of thermal conductivity temperature corrections applied in terrestrial heat flow studies. *Journal of Geophysical Research*, 103, 2447–2454. <https://doi.org/10.1029/97JB03104>

Levenspiel, O. (1984). *The Three Mechanisms of Heat Transfer: Conduction, Convection, and Radiation* BT - *Engineering Flow and Heat Exchange* (O. Levenspiel (Ed.); pp. 161–188). Springer US. https://doi.org/10.1007/978-1-4615-6907-7_9

Liebel, H. T., Huber, K., Frengstad, B., Ramstad, R., & Brattli, B. (2010). Rock core samples cannot replace thermal response tests—a statistical comparison based on thermal conductivity data from the Oslo Region (Norway). *Proceedings of Renewable Energy Research Conference, 2010*

Limpasurat, A., Falcone, G., Teodoriu, C., Barrufet, M. A., & Bello, O. O. (2011). Artificial geothermal energy potential of steam-flooded heavy oil reservoirs. *International Journal of Oil, Gas and Coal Technology*, 4(1), 31–46. <https://doi.org/10.1504/IJOGCT.2011.037743>

Liu, X., Falcone, G., & Alimonti, C. (2018). A systematic study of harnessing low-temperature geothermal energy from oil and gas reservoirs. *Energy*, 142, 346–355. <https://doi.org/10.1016/j.energy.2017.10.058>

Lo Russo, S., Gizzi, M., & Taddia, G. (2020). Abandoned oil and gas wells exploitation by means of closed-loop geothermal systems: A review. *Geingegneria Ambientale e Mineraria*, 160, 3–11. <https://doi.org/10.19199/2020.2.1121-9041.03>

Lucchi, F. R. (1990). Turbidites in foreland and on-thrust basins of the northern Apennines. *Palaeogeography, Palaeoclimatology, Palaeoecology*, 77(1), 51–66. [https://doi.org/https://doi.org/10.1016/0031-0182\(90\)90098-R](https://doi.org/https://doi.org/10.1016/0031-0182(90)90098-R)

Lund, J. W. (2010). Direct utilization of geothermal energy. *Energies*, 3(8), 1443–1471. <https://doi.org/10.3390/en3081443>

Lund, J. W., & Boyd, T. L. (2016). Direct utilization of geothermal energy 2015 worldwide review. *Geothermics*, 60, 66–93. <https://doi.org/10.1016/j.geothermics.2015.11.004>

Lund, J. W., & Toth, A. N. (2021). Direct utilization of geothermal energy 2020 worldwide review. *Geothermics*, 90 (November 2020), 101915. <https://doi.org/10.1016/j.geothermics.2020.101915>

Lyubimova, E. A. (1968). Component parts of the World Heat Flow Data Collection. PANGAEA. <https://doi.org/10.1594/PANGAEA.809800>

Manzella, A., Serra, D., Cesari, G., Bargiacchi, E., Cei, M., Cerutti, P., Conti, P., Giudetti, G., Lupi, M., & Vaccaro, M. (2019). Geothermal Energy Use, Country Update for Italy. European Geothermal Congress 2019. Den Haag, The Netherlands, 11-14 June 2019

Martinelli, G., Cremonini, S., & Samonati, E. (2012). Geological and Geochemical Setting of Natural Hydrocarbon Emissions in Italy. *Advances in Natural Gas Technology*, 1969. <https://doi.org/10.5772/37446>

Martino, L. (1989). Il calore geotermico nelle colture protette. Tavola Rotonda, Ente Fiere Padova, 5 pp

Mehmood, A., Yao, J., Fan, D., Bongole, K., Liu, J., & Zhang, X. (2019). Potential for heat production by retrofitting abandoned gas wells into geothermal wells. *PLoS ONE*, 14(8). <https://doi.org/10.1371/journal.pone.0220128>

Minervini, M., Ghielmi, M., Rogledi, S., & Rossi, M. (2008). Tectono-stratigraphic framework of the Messinian-to-Pleistocene succession in the Western Po Plain Foredeep. *Rendiconti Online Societa Geologica Italiana*, 3(2), 562–563.

Ministero dello Sviluppo Economico; Ministero dell’Ambiente e della Tutela del Territorio e del Mare; Ministero delle Infrastrutture e dei Trasporti. (2019). Piano Nazionale Integrato per l’Energia e il Clima (National Energy and Climate Plan). https://www.mise.gov.it/images/stories/documenti/it_final_necp_main_en.pdf%0Ahttps://www.mise.gov.it/index.php/it/198-notizie-stampa/2040668-pniec2030

Ministero dello Sviluppo Economico; Ministero dell’Ambiente e della Tutela del Territorio e del Mare; Ministero delle Infrastrutture e dei Trasporti. (2021). Strategia Italiana Di Lungo Termine Sulla Riduzione Delle Emissioni Dei Gas a Effetto Serra. 1–100.

Miuccio, G., Frixia, A., & Bertamoni, M. (2000). The Trapanese structural domain in the Termini Imerese Mountain area (Sicily). *Memoria Della Societa Geologica Italiana*, 55, 227–234. G. Digital Library

Moeck, I. S. (2014). Catalog of geothermal play types based on geologic controls. *Renewable and Sustainable Energy Reviews*, 37, 867–882. <https://doi.org/10.1016/j.rser.2014.05.032>

Montanari, D., Minissale, A., Doveri, M., Gola, G., Trumpy, E., Santilano, A., & Manzella, A. (2017a). Geothermal resources within carbonate reservoirs in western Sicily (Italy): A review. *Earth-Science Reviews*, 169(March), 180–201. <https://doi.org/10.1016/j.earscirev.2017.04.016>

Montanari, D., Minissale, A., Doveri, M., Gola, G., Trumpy, E., Santilano, A., & Manzella, A. (2017b). Geothermal resources within carbonate reservoirs in western Sicily (Italy): A review. *Earth-Science Reviews*, 169(March), 180–201. <https://doi.org/10.1016/j.earscirev.2017.04.016>

Moon, H., Kim, H. & Nam, Y. (2019) Study on the Optimum Design of a Ground Heat Pump System Using Optimization Algorithms. *Energies*, 12, 4033; doi:10.3390/en12214033

Muffler, P., & Cataldi, R. (1978). Methods for regional assessment of geothermal resources. *Geothermics*, 7(2), 53–89. [https://doi.org/https://doi.org/10.1016/0375-6505\(78\)90002-0](https://doi.org/https://doi.org/10.1016/0375-6505(78)90002-0)

Nasr, M., Raymond, J., Malo, M., & Gloaguen, E. (2018). Geothermal potential of the St. Lawrence Lowlands sedimentary basin from well log analysis. *Geothermics*, 75(July 2017), 68–80. <https://doi.org/10.1016/j.geothermics.2018.04.004>

Nathenson, M., & Muffler, L. J. P. (1975). Geothermal resources in hydrothermal convection systems and conduction-dominated areas. In: *Assessment of geothermal resources of the United States - 1975*. Geological Survey Circular 726 (White, D. E. and Williams, D. L.). 104–121. <https://pubs.usgs.gov/circ/1975/0726/report.pdf>

Nian, Y. Le, & Cheng, W. L. (2018a). Insights into geothermal utilization of abandoned oil and gas wells. *Renewable and Sustainable Energy Reviews*, 87(June 2017), 44–60. <https://doi.org/10.1016/j.rser.2018.02.004>

Nian, Y. Le, & Cheng, W. L. (2018b). Evaluation of geothermal heating from abandoned oil wells. *Energy*, 142, 592–607. <https://doi.org/10.1016/j.energy.2017.10.062>

North, F. K. (1971). Characteristics of Oil Provinces : a Study for Students. *Bulletin of Canadian Petroleum Geology*, 19(3), 601–658. <https://doi.org/10.35767/gscpgbull.19.3.601>

Onajite, E. (2014). *Seismic Data Analysis Techniques in Hydrocarbon Exploration*. Elsevier. <https://doi.org/10.1016/C2013-0-09969-0>

Operacz, A.; Chowaniec, J. (2018). Prospective of geothermal water use in the Podhale Basin according to geothermal step distribution. *Geol. Geophys. Environ.*, 44, 379–389.

Pasquale, V., Gola, G., Chiozzi, P., & Verdoya, M. (2011). Thermophysical properties of the Po Basin rocks. *Geophysical Journal International*, 186(1), 69–81. <https://doi.org/10.1111/j.1365-246X.2011.05040.x>

Pasquier, P., & Marcotte, D. (2012). Short-term simulation of ground heat exchanger with an improved TRCM. *Renewable Energy*, 46, 92–99. <https://doi.org/10.1016/j.renene.2012.03.014>

Pellizzone, A., Allansdottir, A., Manzella, A. (2019). Geothermal Resources in Italy: Tracing a Path Towards Public Engagement. In: Manzella, A., Allansdottir, A., Pellizzone, A. (eds) *Geothermal Energy and Society. Lecture Notes in Energy*, vol 67. Springer, Cham. https://doi.org/10.1007/978-3-319-78286-7_11

Perez Donoso, P. I., Rojas, A. E. O., & Meneses Rioseco, E. (2020). Bilinear pressure diffusion and termination of bilinear flow in a vertically fractured well injecting at constant pressure. *Solid Earth*, 11(4), 1423–1440. <https://doi.org/10.5194/se-11-1423-2020>

Pouloupatis, P., Florides, G., & Tassou, S. (2011). Measurements of ground temperatures in Cyprus for ground thermal applications. *Renewable Energy*, 36, 804–814. <https://doi.org/10.1016/j.renene.2010.07.029>

Raffensperger, J. P., & Vlassopoulos, D. (1999). The potential for free and mixed convection in sedimentary basins. *Hydrogeology Journal*, 7(6), 505–520. <https://doi.org/10.1007/s100400050224>

Raos, S., Ilak, P., Rajšl, I., Bilić, T., & Trullenque, G. (2019). Multiple-Criteria Decision-Making for Assessing the Enhanced Geothermal Systems. *Energies*, 12(9). <https://doi.org/10.3390/en12091597>

Rybach, L. & Hopkirk, R. (1995). Shallow and Deep Borehole Heat Exchangers - Achievements and Prospects. *Pro. World Geothermal Congress 1995*: 2133-2139

Reyes, A. G. (2007). Abandoned oil and gas wells: a reconnaissance study of an unconventional geothermal resource. In *GNS Science Report 2007/23* (Issue July).

Riney, T. D. (1991). Pleasant Bayou Geopressured - Geothermal Reservoir. 114, 315–322. <https://www.osti.gov/servlets/purl/893428>

Ruiz-calvo, F., Rosa, M. De, Acuña, J., Corberán, J. M., & Montagud, C. (2015). Experimental validation of a short-term Borehole-to-Ground (B2G) dynamic model. *Applied Energy*, 140, 210–223. <https://doi.org/10.1016/j.apenergy.2014.12.002>

Sanyal, S. K., & Butler, S. J. (2010). Geothermal Power Capacity from Petroleum Wells – Some Case Histories of Assessment. *World Geothermal Congress*, April, 25–29. https://pangea.stanford.edu/ERE/db/IGAstandard/record_detail.php?id=6797

Sarbu, I., & Sebarchievici, C. (2014). General review of ground-source heat pump systems for heating and cooling of buildings. *Energy and Buildings*, 70, 441–454. <https://doi.org/10.1016/j.enbuild.2013.11.068>

Soldo, E., & Alimonti, C. (2015). From an Oilfield to a Geothermal One : Use of a Selection Matrix to Choose Between Two Extraction Technologies. *World Geothermal Congress 2015*, April, 19–25.

Stephenson, M. H., Ringrose, P., Geiger, S., Bridden, M., & Schofield, D. (2019). Geoscience and decarbonization: Current status and future directions. *Petroleum Geoscience*, 25(4), 501–508. <https://doi.org/10.1144/petgeo2019-084>

Sui, D., Wiktorski, E., Røksland, M., & Basmoen, T. A. (2019). Review and investigations on geothermal energy extraction from abandoned petroleum wells. *Journal of Petroleum Exploration and Production Technology*, 9(2), 1135–1147. <https://doi.org/10.1007/s13202-018-0535-3>

Tao, W.Q. (2001). *Numerical Heat Transfer*, 2nd ed.; Xi'an Jiaotong University Press: Xi'an, China. pp. 195–203.

Templeton, J. D., Ghoreishi-Madiseh, S. A., Hassani, F., & Al-Khawaja, M. J. (2014). Abandoned petroleum wells as sustainable sources of geothermal energy. *Energy*, 70, 366–373. <https://doi.org/10.1016/j.energy.2014.04.006>

Tester, J. W., Herzog, H. J., Chen, Z., Potter, R. M., & Frank, M. G. (1994). Prospects for universal geothermal energy from heat mining. *Science & Global Security*, 5(1), 99–121. <https://doi.org/10.1080/08929889408426418>

Trumpy, E., Botteghi, S., Caiozzi, F., Donato, A., Gola, G., Montanari, D., Pluymaekers, M. P. D., Santilano, A., Van Wees, J. D., & Manzella, A. (2016). Geothermal potential assessment for a low carbon strategy: A new systematic approach applied in southern Italy. *Energy*, 103, 167–181. <https://doi.org/10.1016/j.energy.2016.02.144>

Trumpy, Eugenio, & Manzella, A. (2017). Geothopica and the interactive analysis and visualization of the updated Italian National Geothermal Database. *International Journal of Applied Earth Observation and Geoinformation*, 54, 28–37. <https://doi.org/10.1016/j.jag.2016.09.004>

Unione Energie per la mobilità (2021, dicembre 2021) <https://www.unem.it/>

United Nations. (2018). Energy Transition UN Report - Towards the achievement of SDG 7 Net-zero emissions. 157–166.

Van Rossum, G. (1995). Python tutorial, Technical Report CS-R9526. Centrum Voor Wiskunde En Informatica (CWI).

Vedova, B., Bellani, S., Pellis, G., & Squarci, P. (2001). Anatomy of an Orogen: the Apennines and Adjacent Mediterranean Basins. *Anatomy of an Orogen: The Apennines and Adjacent Mediterranean Basins*, May 2014. <https://doi.org/10.1007/978-94-015-9829-3>

Violante, A C, & Guidi, G. (2020). *Geotermia a bassa entalpia e decarbonizzazione*. 141–143. <https://doi.org/10.12910/EAI2020-052>

Vosteen, H.-D., Rath, V., Clauser, C., & Lammerer, B. (2003). The thermal regime of the Eastern Alps from inversion analyses along the TRANSALP profile. *Physics and Chemistry of The Earth - PHYS CHEM EARTH*, 28, 393–405. [https://doi.org/10.1016/S1474-7065\(03\)00060-3](https://doi.org/10.1016/S1474-7065(03)00060-3)

Wang, K., Yuan, B., Ji, G., & Wu, X. (2018). A comprehensive review of geothermal energy extraction and utilization in oilfields. *Journal of Petroleum Science and Engineering*, 168, 465–477. <https://doi.org/https://doi.org/10.1016/j.petrol.2018.05.012>

Wang, S., Yan, J., Li, F., Hu, J., & Li, K. (2016). Exploitation and utilization of oilfield geothermal resources in China. *Energies*, 9(10), 1–13. <https://doi.org/10.3390/en9100798>

Waples, D., & Waples, J. (2004). A Review and Evaluation of Specific Heat Capacities of Rocks, Minerals, and Subsurface Fluids. Part 1: Minerals and Nonporous Rocks. *Natural Resources Research*, 13, 97–122. <https://doi.org/10.1023/B%3ANARR.0000032647.41046.e7>

Wight, N. M., & Bennett, N. S. (2015). Geothermal energy from abandoned oil and gas wells using water in combination with a closed wellbore. *Applied Thermal Engineering*, 89, 908–915. <https://doi.org/10.1016/j.applthermaleng.2015.06.030>

Yang, H., Cui, P., & Fang, Z. (2010). Vertical-borehole ground-coupled heat pumps: A review of models and systems. *Applied Energy*, 87(1), 16–27. <https://doi.org/https://doi.org/10.1016/j.apenergy.2009.04.038>

Yasar, E., Erdogan, Y., & Güneçli, H. (2008). Determination of the thermal conductivity from physico-mechanical properties. *Bulletin of Engineering Geology and the Environment*, 67, 219–225. <https://doi.org/10.1007/s10064-008-0126-5>

Zarrouk, S. J., & Moon, H. (2014). Efficiency of geothermal power plants: A worldwide review. *Geothermics*, 51, 142–153. <https://doi.org/10.1016/j.geothermics.2013.11.001>